

Aus der Abteilung für Experimentelle Pharmakologie, European Center for
Angioscience der Medizinischen Fakultät Mannheim
(Direktor: Prof. Dr. rer. nat. Thomas Wieland)

**The role of vascular endothelial cadherin and the
therapeutic potential of intravitreally administrated
mesenchymal stem cells in retinal vasoregression**

Inauguraldissertation
zur Erlangung des Doctor scientiarum humanarum (Dr. sc. hum.)
der
Medizinischen Fakultät Mannheim
der Ruprecht-Karls-Universität
zu
Heidelberg

vorgelegt von
Hongpeng Huang

aus
Heilongjiang, China
2020

Dekan: Prof. Dr. med. Sergij Goerd

Referent: PD Dr. Yuxi Feng

Abbreviations	1
Units.....	3
1 Introduction	4
1.1 Diabetes	4
1.2 Diabetic retinopathy	4
1.3 Retinal vasoregression	5
1.4 Retinal neurovascular unit	6
1.4.1 Pericyte morphology and characterization.....	7
1.4.2 Pericyte function.....	8
1.4.3 Pericyte-endothelial signal transduction	8
1.4.4 Endothelial cell-cell junctions.....	11
1.4.4.1 VE-cadherin structure.....	12
1.4.4.2 VE-cadherin endocytosis and degradation.....	13
1.4.4.3 VE-cadherin phosphorylation	14
1.5 The potential mechanism of pericyte loss in retinopathy	16
1.6 Rodent retinopathy models.....	17
1.6.1 Ins2 ^{Akita} mouse.....	17
1.6.2 Rats with polycystic kidney disease.....	18
1.6.3 Nucleoside diphosphate kinase B knockout mouse	18
1.6.3.1 The NDPK family.....	18
1.6.3.2 NDPKs and G-protein activation	19
1.6.3.3 NDPKs and endocytosis.....	20
1.6.3.4 NDPKs and diabetes.....	21
1.7 Mesenchymal stem cells.....	21
1.8 Therapeutic effects of MSCs in retinal degenerative diseases	23
1.8.1 MSC plasticity.....	23
1.8.2 Paracrine signaling.....	24
1.9 Aims of this study.....	25
2 Materials and Methods.....	27
2.1 Materials	27
2.1.1 Animals.....	27
2.1.2 Cells	27
2.1.3 Chemical materials.....	27
2.1.4 Cell culture medium and substances.....	28
2.1.5 siRNA	29
2.1.6 Buffers	29
2.1.7 Antibody.....	30
2.1.8 Primers	32
2.1.9 Kits	32
2.1.10 Consumable materials.....	33
2.1.11 Apparatuses.....	33
2.1.12 Software	34
2.2 Methods.....	35
2.2.1 Isolation of HUVECs.....	35

2.2.2 HUVEC and pericyte culturing.....	35
2.2.3 HUVEC-pericyte co-culture	35
2.2.4 RNA interference	36
2.2.5 VE-cadherin internalization assay	36
2.2.6 Membrane protein extraction.....	37
2.2.7 Isolation of human ASCs	37
2.2.8 Isolation of rat BMSCs.....	37
2.2.9 Human ASC, rat BMSC, and RFPEC culturing.....	38
2.2.10 Concentration of human ASC supernatant	38
2.2.11 Cell labeling	38
2.2.12 Intravitreal injection.....	39
2.2.13 Retinal digestion and quantitative retinal morphometry	39
2.2.14 Immunofluorescence staining	40
2.2.15 Microglia quantification	41
2.2.16 Multifocal electroretinography.....	41
2.2.17 Cryosectioning.....	42
2.2.18 Immunoblotting.....	42
2.2.19 Dot blot.....	42
2.2.20 Ex vivo experiments	43
2.2.21 Retinal RNA isolation.....	43
2.2.22 Real-time polymerase chain reaction (PCR)	43
2.2.23 Retinal perfusion	44
2.2.24 Statistical analysis	44
3 Results.....	45
3.1 The role of VE-cadherin in retinal vasoregression	45
3.1.1 VE-cadherin expression is reduced in NDPK B deficient retinas before pericyte loss	45
3.1.2 VE-cadherin expression is reduced in the retinas of PKD rats before pericyte loss	48
3.1.3 VE-cadherin expression is reduced in the retinas of <i>Ins2^{Akita}</i> mice before pericyte loss	48
3.1.4 VE-cadherin expression is reduced in deep retinal capillaries of NDPK B ^{-/-} mice.....	49
3.1.5 Reduced expression of VE-cadherin in endothelial cells is associated with pericyte loss.....	50
3.1.6 NDPK B ^{-/-} mice display increased permeability of retinal vasculature.....	52
3.1.7 NDPK B loss or HG reduces plasma membrane VE-cadherin levels in endothelial cells.....	52
3.1.8 NDPK B loss or HG promotes VE-cadherin internalization and VE-cadherin Tyr 685 phosphorylation in endothelial cells	57
3.1.9 NDPK B loss or HG induces lysosome-mediated VE-cadherin degradation in endothelial cells	59
3.1.10 NDPK B deficiency or HG induces phosphorylation of VE-	

cadherin at Tyr 685 via Src kinase activation	61
3.2 Intravitreal injection of MSCs as a therapeutic intervention in vasoregressive retina.....	62
3.2.1 Characterization of MSCs.....	62
3.2.2 Intravitreally injected MSCs are unable to migrate into the retina of the rat eye	62
3.2.3 Intravitreally injected BMSCs induce cataract and retinal vasoregression in SD rats	64
3.2.4 Intravitreally injected BMSCs aggravate retinal vasoregression in PKD rats.....	65
3.2.5 Intravitreally injected human ASCs lead to retinal vasoregression in SD rats and aggravate retinal vasoregression in PKD rats.....	67
3.2.6 Intravitreal injection of HUVECs, RFPECs, and concentrated supernatant dose not cause retinal vasoregression in SD rats.....	72
3.2.7 Intravitreally injected BMSCs do not affect the neuronal function in SD and PKD rats	72
3.2.8 Intravitreally injected BMSCs activate retinal glial cells in SD rats	76
3.2.9 BMSC injection-induced retinal vasoregression is associated with immune response.....	77
3.2.10 Intravitreally injected BMSCs increase retinal HSP90 expression in SD rats.....	79
4 Discussion	83
4.1 Adequate expression of VE-cadherin stabilizes pericytes.....	83
4.2 Endothelial cells with NDPK B deficiency or treated with HG show similarities in Src kinase activation, and VE-cadherin phosphorylation, internalization, and degradation.....	84
4.3 Evaluation of intravitreally injected MSCs in pre-clinical and clinical studies	86
4.4 Intravitreally injected MSCs induce inflammatory responses.....	88
4.5 Further studies.....	90
5 Summary	92
6 References	94
7 Publications	111
8 Curriculum vitae	112
9 Acknowledgments	113

Abbreviations

Ang1/2	Angiopoietin-1/2
AGEs	Advanced glycation end products
AQP	Aquaporin
AR	Aldose reductase
ASCs	Adipose-derived stem cells
Arg1	Arginase 1
FGF2	Basic fibroblast growth factor
Bax	Bcl-2-associated X protein
BDNF	Brain-derived neurotrophic factor
BMSCs	Bone marrow-derived stem cells
BRB	Blood-retina barrier
CNTF	Ciliary neurotrophic factor
C3	Complement component 3
Cfb	Complement factor b
Cx43	Connexin 43
DAPI	4, 6-diamidino-2-phenylindole
DME	Diabetic macular edema
ddH ₂ O	Double distilled water
DR	Diabetic retinopathy
EGF	Epidermal growth factor
ERG	Electroretinography
FACs	Fluorescence-activated cell sorter
FCS	Fetal calf serum
FGF2	Basic fibroblast growth factor
FITC	Fluorescein isothiocyanate
GAPDH	Glyceraldehyde 3-phosphate dehydrogenase
GCL	Ganglion cell layer
GDNF	Glial cell-derived neurotrophic factor
GDP	Guanosine diphosphate
GFAP	Glial fibrillary acid protein
GS	Glutamine synthetase
GTP	Guanosine triphosphate
HG	High glucose
HSCs	Hematopoietic stem cells
HSPs	Heat shock proteins
HUVECs	Human umbilical cord endothelial cells

ICAM-1	Intercellular adhesion molecule 1
ILM	Inner limiting membrane
INL	Inner nuclear layer
IL	Interleukin
Iba1	Ionized calcium-binding adaptor molecule 1
MCP	Monocyte chemoattractant protein
MSCs	Mesenchymal stem cells
MMP	Matrix metalloproteinase
NADPH	Nicotinamide adenine dinucleotide phosphate
NDPKs	Nucleoside-diphosphate kinases
NG	Normal glucose
NG2	Neural/glial antigen 2
NGF	Nerve growth factor
ONL	Outer nuclear layer
PAS	Periodic acid Schiff
PBS	Phosphate-buffered saline
PDGFR	Platelet-derived growth factor receptor
PDR	Proliferative diabetic retinopathy
PKD	Polycystic kidney disease
QPCR	Quantitative polymerase chain reaction
RD	Retinal degeneration
RFPECs	Rat fat pad endothelial cells
RNV	Retinal neurovascular unit
ROS	Reactive oxygen species
RPE	Retinal pigment epithelium
SDS	Sodium dodecyl sulfate
SD	Sprague Dawley
SMA	Smooth muscle actin
TBS	Tris-buffered saline
TBST	Tris-buffered saline with Tween 20
TGF	Transforming growth factor
TNF	Tumor necrosis factor
VEC	VE-cadherin
VEGF	Vascular endothelial growth factor
VEGFR2	Vascular endothelial growth factor receptor 2
VE-PTP	Receptor-type tyrosine-protein phosphatase
WB	Western blot

Units

g	Gram
mg	Milligram
µg	Microgram
µL	Microliter
mL	Milliliter
L	Liter
M	Molar
mM	Millimolar
mol	Mole
µmol	Micromole
pmol	Picomole
mm	Millimeter
µm	Micrometer
m ²	Square meter
cm ²	Square centimeter
mm ²	Square millimeter
h	Hour
min	Minute
s	Second
v	Volt
U	Unit
KDa	KiloDalton
rpm	Round per minute

1 Introduction

1.1 Diabetes

Diabetes is a metabolic disorder caused by hyperglycemia resulting from defects in insulin secretion and function. Long-term exposure to hyperglycemia leads to the dysfunction, failure, and damage of multiple organs, particularly kidneys, nerves, eyes, heart, and blood vessels (Association, 2010). Currently, the incidence of diabetes is growing at alarming rates worldwide. According to the 2013 report of the International Diabetes Federation (IDF), approximately 382 million people had diabetes, and this number will reach 592 million by 2035 based on investigations in 130 countries. This indicates that the number of people with diabetes will increase by 55% by 2035. As shown in **Fig. 1**, China contributes the most to the world population of patients with diabetes, which is approximately 98.4 million. India is in second place, with approximately 65.1 million diabetic people. The prevalence of diabetes increases, especially in developing countries. Therefore, diabetes has already become a leading public health challenge and a significant economic burden worldwide (Guariguata et al., 2014a).

2013		2035	
Country/territory	Millions	Country/territory	Millions
<i>Top 10 countries/territories of number of people with diabetes (20–79 years), 2013 and 2035</i>			
China	98.4	China	142.7
India	65.1	India	109.0
United States of America	24.4	United States of America	29.7
Brazil	11.9	Brazil	19.2
Russian Federation	10.9	Mexico	15.7
Mexico	8.7	Indonesia	14.1
Indonesia	8.5	Egypt	13.1
Germany	7.6	Pakistan	12.8
Egypt	7.5	Turkey	11.8
Japan	7.2	Russian Federation	11.1

Figure 1: Top ten countries showing the number of people with diabetes in 2013 and 2035. Permission obtained from copyright © 2014 Elsevier Ireland Ltd (Guariguata et al., 2014b).

1.2 Diabetic retinopathy

Diabetic retinopathy (DR) is a diabetic complication that impairs the vision of

patients with diabetes, and is associated with vascular and neuronal damage, retinal edema, hemorrhage, and abnormal growth of new blood vessels (Abcouwer and Gardner, 2014). Clinical evidence reveals that DR affects nearly 93 million people worldwide, approximately 28 million of whom are at the risk of developing vision loss (Pascolini and Mariotti, 2012; Sivaprasad et al., 2012; Yau et al., 2012). The World Health Organization (WHO) has predicted that approximately 15–17% cases of total blindness in Europe and the USA are due to DR (Resnikoff et al., 2004). Statistically, the data from epidemiological studies indicate that almost all patients with type 1 diabetes (T1D) will develop at least retinopathy after 20 years of diabetes. More importantly, retinopathy will occur in approximately 80% patients with insulin-dependent type 2 diabetes (T2D) and in 50% patients with insulin-independent T2D after 20 years of diabetes (Klein et al., 1989). Among patients with diabetes worldwide, 33% show overall prevalence of DR. Longer disease duration, higher hemoglobin A1C (HbA1c) level, and hypertension will increase the risk of DR (Yau et al., 2012). Thus, DR is becoming an ever-increasing health burden and global problem.

1.3 Retinal vasoregression

DR has been consistently considered a microvascular disease. It is primarily classified into the early stage, which is non-proliferative DR, and the late stage, which is proliferative DR. Retinal vasoregression is a hallmark of early DR, which is characterized by initial retinal pericyte loss and subsequent formation of acellular capillaries (**Fig. 2**). Without the protection of pericytes, retinal endothelial cells are susceptible to ischemia, angiogenic factors, and inflammatory factor attack, which lead to endothelial cell death. Acellular capillary with no blood flow is formed after pericyte and endothelial disappearance. Retinal capillary occlusion induced by pericyte loss and subsequent endothelial cell death aggravates ischemia. In response to progressive capillary loss, vascular endothelial growth factor (VEGF) level is elevated, which results in the formation of newly abnormal vessels. The breakage of retinal vessel effortlessly induces retinal vascular leakage and bleeding, which impairs vision.

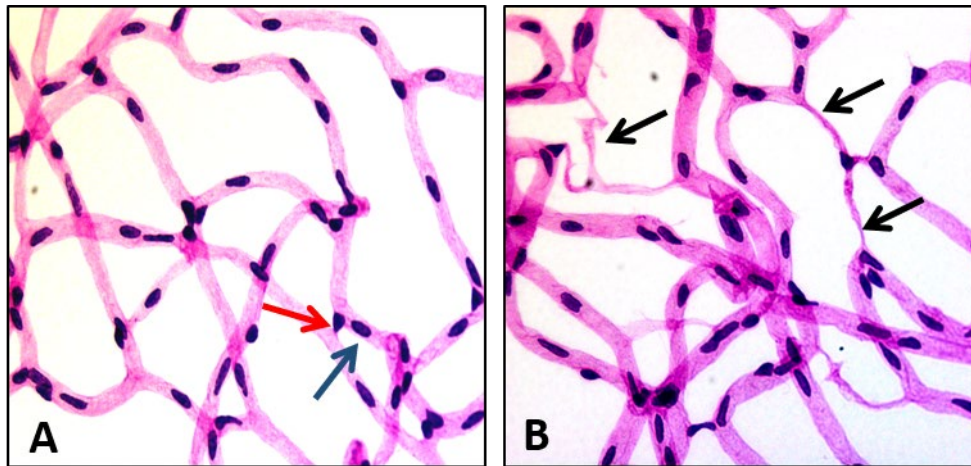


Figure 2: Retinal vasoregression in rats. (A) Normal retinal vasculature in rats. The red arrow indicates pericytes. The dark blue arrow indicates endothelial cells. (B) Rats with retinal vasoregression. Black arrow indicates acellular capillaries.

1.4 Retinal neurovascular unit

Pericytes belong to vascular mural cells that are located at the abluminal surface of the capillary. They closely communicate with endothelial cells and are embedded in the vascular basement membrane (Armulik et al., 2011; Shepro and Morel, 1993a). Pericytes are the major components of the retinal neurovascular unit (RNV). In the normal RNV, they combine with endothelial cells, microglial cells, astrocytes, Muller cells, and neuronal cells, and are crucial for blood-retina barrier (BRB) permeability, angiogenesis, cellular metabolism and neuroinflammation (**Fig. 3**) (Sweeney et al., 2016). The impairment of the RNV is involved in DR pathogenesis. Under diabetic conditions, all the components of RNV are disrupted by long-term exposure to hyperglycemia. Hyperglycemia causes retinal endothelial cell dysfunction by affecting mitochondria function, which increases oxidative stress and accelerates endothelial cell death (Davidson and Duchon, 2007). Retinal endothelial cells are the crucial elements for BRB, which is disrupted by chronic hyperglycemia exposure. The main contributors to BRB destruction are VEGF, proinflammatory cytokines, such as IL-1 β , TNF- α , and IL-6, and monocyte chemoattractant protein-1 (MCP-1) (Tang and Kern, 2011). The reduced thickness of the nerve fiber layer and increased expression of Bax, caspase-3, and caspase-9 shows that the retinal ganglion cells are dead (Kern and Barber, 2008). Retinal glial cells, such as Muller cells, are activated due to the upregulation of GFAP (Qiu et al., 2018). Microglial cells have immunological cell

functions. After exposure to hyperglycemic conditions, microglial cells are activated and can release several immunological cytokines and chemokines to aggravate retinal damage (Joussen et al., 2004). Chronic HG exposure disrupts the signaling pathway among retinal cells. As a result, increase in VEGF and Ang-2 expression are observed. The elevated Ang-2 level leads to pericyte loss and endothelial cell dysfunction, which ultimately induces vascular leakage. Severe retinal and vitreous bleeding can cause vision loss (Gardner and Davila, 2017).

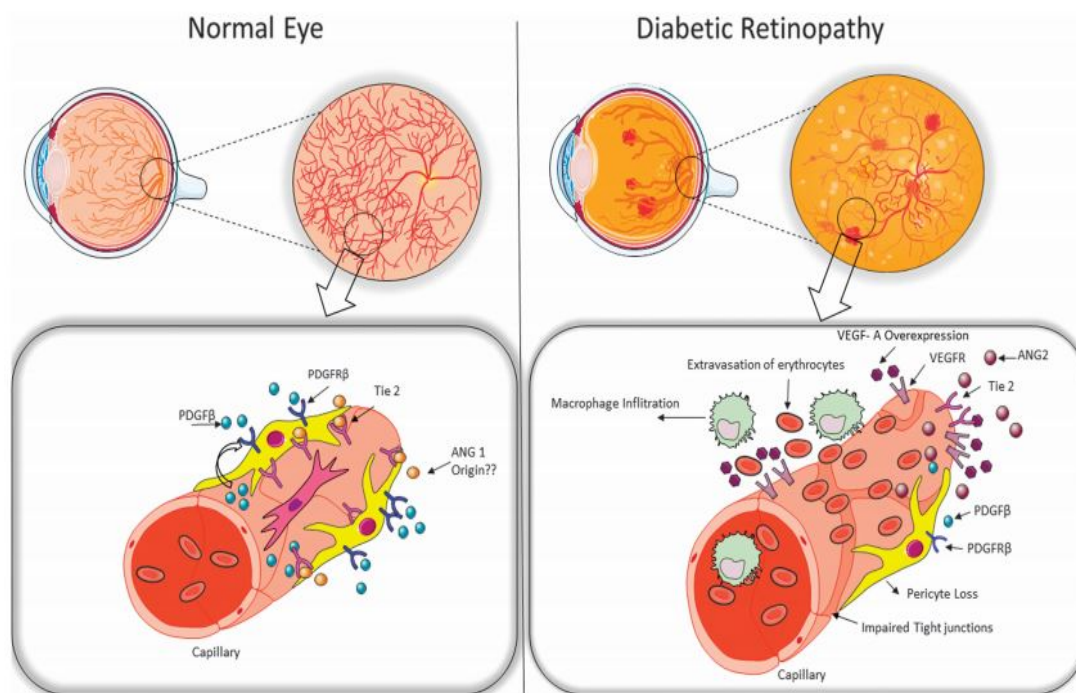


Figure 3: Retinal neurovascular unit is composed of retinal endothelial cells, pericytes, astrocytes, Muller cells, and neuronal cells. Permission obtained from copyright © 2018 Macmillan Publishers Limited, part of Springer Nature (Santos et al., 2018)

1.4.1 Pericyte morphology and characterization

Pericytes are specialized cells mainly present in the capillaries, which are derived from the neural crest during embryonic development (Etchevers et al., 2001). French scientist Charles Rouget initially proposed the existence of pericytes in 1873 (Rouget, 1873), and they were named “pericytes” by Zimmermann in 1923 (Zimmermann, 1923). Similar to smooth muscle cells, pericytes possess contractile properties and regulate vascular tone (Hamilton

et al., 2010). In mature rodents, retinal capillary pericytes are associated with endothelial cells and astrocytes, and wrap around the capillary. In contrast to the elongated shape of the endothelial cell nucleus, pericytes have prominent round nuclei. Pericytes exhibit extended processes that cover the wall of blood vessels (Dore-Duffy and Cleary, 2011). The retina has the most abundant pericyte coverage. The ratio of pericyte to endothelial cells in the retina ranges from 1:1 to 1:3. In other tissues, such as the brain, lung, and skeletal muscle, this ratio is 1:5, 1:10, and 1:100, respectively (Frank et al., 1987; Frank et al., 1990; Kuwabara and Cogan, 1963; Laties et al., 1979; Shepro and Morel, 1993b). Pericytes can express several cell surface markers, including NG2, PDGFR β , CD13, and CD146 (Gerhardt and Betsholtz, 2003; Murfee et al., 2005; Xu et al., 2013). In addition, pericytes also express contractile and cytoskeletal proteins such as α SMA, vimentin, desmin and nestin (Fujimoto and Singer, 1987; Lardon et al., 2002; Morikawa et al., 2002).

1.4.2 Pericyte function

Retinal pericytes contribute to blood-retina barrier integrity, and are responsible for vessel maturation and stabilization, angiogenesis, and vascular remodeling. Dysfunction or loss of pericyte is linked to many diseases such as DR (Zlokovic, 2011). Hammes et al. have demonstrated that pericyte loss is the first sign of early DR by quantifying pericyte coverage in a retinal capillary using retinal digestion preparation from rodent models. Pericyte loss subsequently induces retinal endothelial cell dysfunction, which further promotes acellular capillary formation and capillary occlusion, aggravating retinal ischemia and enhancing VEGF production (Hammes et al., 2011). Therefore, pericyte coverage is crucial for the stabilization of retinal vasculature. In addition to retinal disease, pericytes also play a critical role in Alzheimer-like neurodegeneration, as pericyte loss promotes the progressive pathology of Alzheimer's disease, such as increase in amyloid β -peptide content, tau pathology, and neuronal cell loss (Halliday et al., 2016; Sagare et al., 2013). Decreased pericyte coverage has also been observed in diseases, such as stroke, multiple sclerosis, brain tumor, and aging (Duz et al., 2007; Feng et al., 2008; Ho, 1985). Thus, pericyte can be a therapeutic target for retinal and neuronal degenerative disease.

1.4.3 Pericyte-endothelial signal transduction

Pericytes connect to endothelial cells via adhesion junctions (AJs), tight junctions (TJs), and gap junctions (GJs). The signal pathways and molecules between endothelial cells and pericytes, including Ang/Tie-2, TGF- β signaling pathway, and PDGF-B/PDGFR- β play crucial roles in protecting vascular integrity (**Fig. 4**).

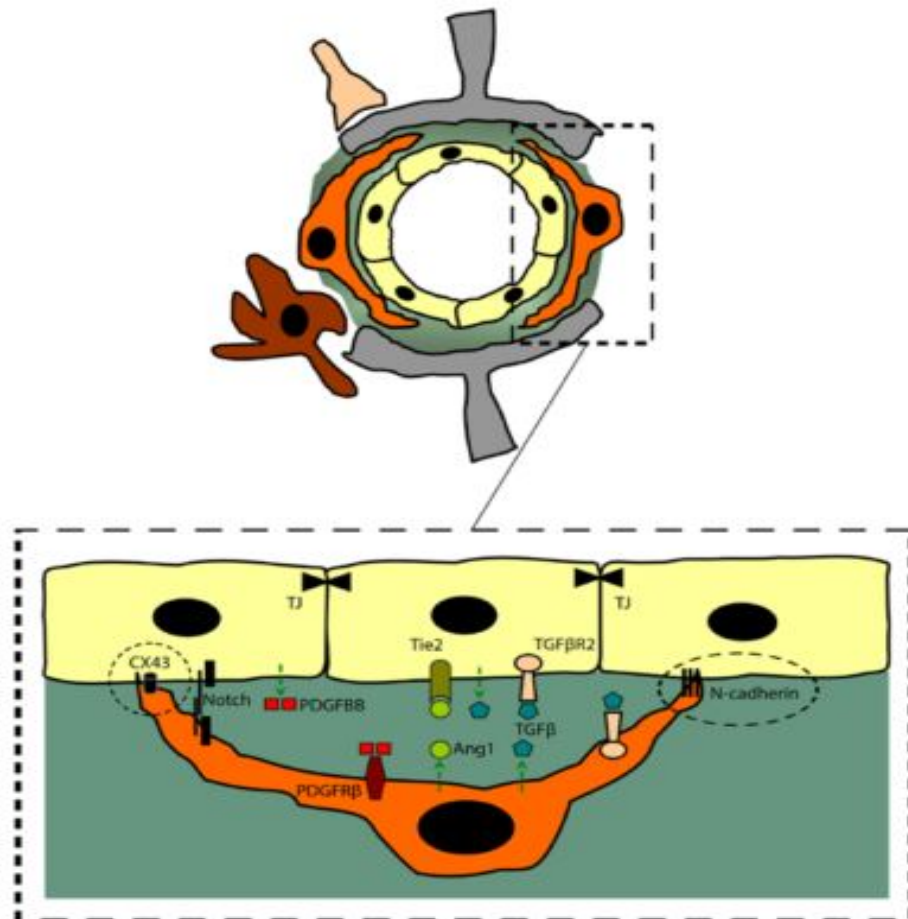


Figure 4: Signaling pathway and junctional molecules between endothelial cells and pericytes in retinal capillary. Reprinted from an open access article distributed under the Creative Common Attribution License (ElAli et al., 2014).

(1) Angiopoietin-Tie-2 signaling

The Tie-2 receptor, a transmembrane tyrosine kinase highly expressed in the endothelium, is essential for the regulation of vascular barrier function in healthy and diseased states. It has two ligands Ang-1 and -2, which exert opposing effects on this receptor. Ang-1, mainly secreted by pericytes, preserves

vascular integrity, whereas Ang-2, an antagonist of Tie-2 expressed by endothelial cells, causes vascular destabilization and reduces pericyte coverage of the vasculature (von Tell et al., 2006). Ang-2 competes with Ang-1 to bind to the Tie-2 receptor, which leads to phosphorylation of its tyrosine residue and destabilization of the interaction between endothelial cells and pericytes (Maisonpierre et al., 1997). A clinical study reported that compared to in diabetic patients without DR, the serum level of Ang-2 is significantly elevated in patients with DR (Khalaf et al., 2017). Intravitreally injected Ang-2 induces retinal pericyte loss and increases the formation of acellular capillaries in the eyes of healthy rats. Diabetes-induced pericyte loss and acellular capillary formation are rescued in heterozygous Ang-2 deficient mice (Hammes et al., 2004).

(2) TGF- β signaling

TGF- β is a multifunctional cytokine that is widely expressed by endothelial cells and pericytes, and is involved in cellular proliferation and differentiation. TGF- β is required to sustain endothelial-pericyte interactions. Disruption of the TGF- β signaling pathway via ablation of its downstream molecule *Smad4* leads to reduced pericyte coverage of capillaries and enhanced vascular permeability (Li et al., 2011; Winkler et al., 2011). TGF- β prevents vascular pericyte proliferation via the induction of VEGFR-1 in endothelial cells (Shih et al., 2003). Neuronal cadherin (N-cadherin), a vital adhesion junction, is enriched between pericytes and endothelial cells, and reduced N-cadherin expression is observed in DR (Hu et al., 2017). TGF- β signal transduction is essential for endothelial cell communication with pericytes. Activation of the TGF- β signaling pathway upregulates N cadherin (Ma et al., 2018).

(3) PDGF-B/PDGFR- β signaling

PDGF-B is predominantly expressed by retinal endothelial cells and binds to PDGFR- β , which is expressed by pericytes. PDGF-B/PDGFR- β signaling is vital for the recruitment of retinal pericytes. Pericyte-specific PDGF-B- and PDGFRB deficient mice display multitudinous broken microaneurysms. Perinatal death due to extensive microvascular leakage and bleeding are observed in PDGF-B and PDGFRB knockout mice (Leveen et al., 1994; Lindahl et al., 1997). PDGF-B depletion in endothelial cells results in pericyte deficiency

(Enge et al., 2002).

1.4.4 Endothelial cell-cell junctions

Endothelial cell junctions are generally classified into two main types: TJs and AJs (Fig. 5). They both provide essential adhesive contacts between neighboring endothelial cells, although these junctions are composed of different proteins. Structurally, within cells, TJs are localized most apically along cell plasma membranes and act as a fence to separate membrane proteins between apical and basolateral membranes. Each TJ is paired to and associated with another TJ on the cell membrane. AJs are composed of cadherin family members of adhesion proteins found at the cell-cell junction of epithelial and endothelial cells, which are connected to the actin cytoskeletal proteins of adjacent cells. Cadherins regulate intracellular adhesion via Ca^{2+} -dependent and homophilic trans-interactions. Within endothelial cells, they dominantly express two types of cadherin: VE-cadherin and N-cadherin. N-cadherin is also expressed in neural cells and smooth muscle cells. Other cadherins, for example, T-cadherin and P-cadherin, are variously expressed in distinct types of endothelial cells (Zhou et al., 2003).

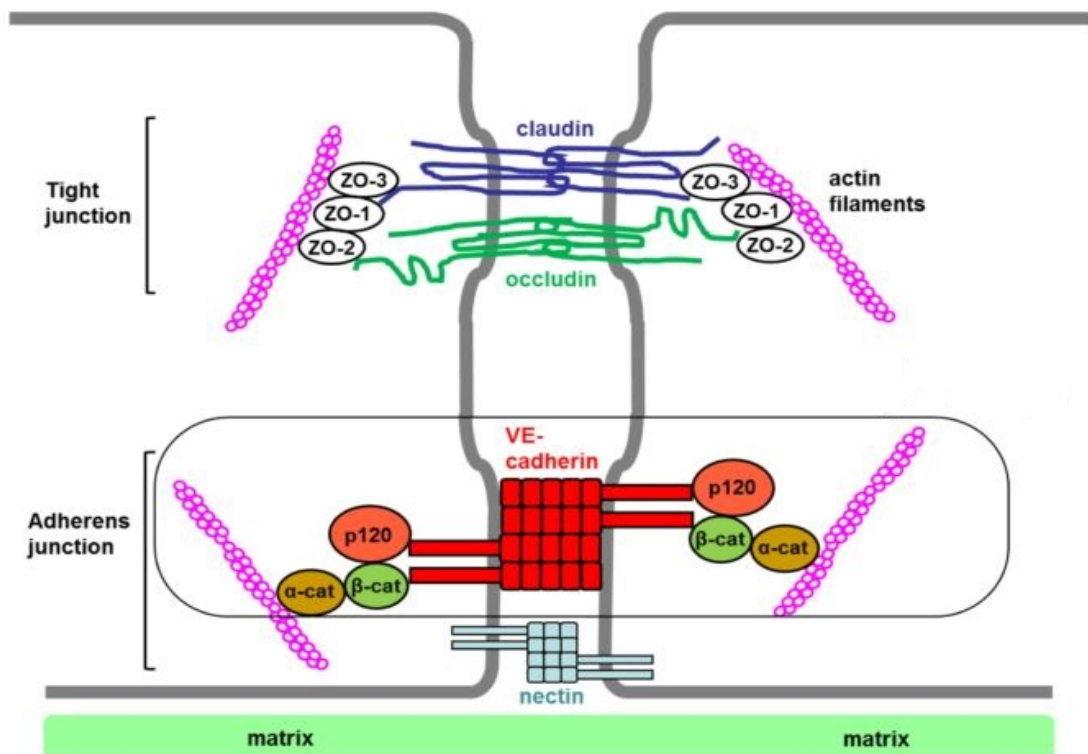


Figure 5: Schematic overview of adhesion junctions and tight junctions. α -cat: α -catenin; β -cat: β -catenin; p120: p120 catenin; ZO: zona occludens. Reprinted from an

1.4.4.1 VE-cadherin structure

VE-cadherin, an endothelial-specific AJ, is the most studied molecule in the cadherin family, which plays a crucial role in endothelial barrier function and maintenance of vascular integrity. It is a transmembrane protein, including an extracellular domain that consists of five homologous repeats from EC1 to EC2 (**Fig. 6**) and a cytoplasmic tail that associates with p120-catenin, β -catenin, and plakoglobin. Structurally, β -catenin binds to the carboxyl-terminal tail of cadherin, whereas p120-catenin binds to the juxtamembrane domain (JMD) of cadherin and modulates cadherin turnover (Cadwell et al., 2016). β -Catenin and plakoglobin directly bind to α -catenin, thereby regulating several cytoskeletal proteins such as actin and zonula occludens-1 (ZO-1). In addition, VE-cadherin also interacts with Src kinase and junctional phosphates (DEP-1 and VE-PTP) (Wallez et al., 2006). Therefore, VE-cadherin directly or indirectly contributes to the intracellular signaling pathways that regulate endothelial cell motility, vascular genesis, angiogenesis, maintenance of cell-cell adhesion, actin protein remodeling, and gene transcription (Corada et al., 1999). Retinal VE-cadherin expression is significantly reduced in patients with diabetes. HG can activate matrix metalloproteinases (MMP) 2 and 9, which results in VE-cadherin degradation (Navaratna et al., 2007). Endothelial cells exposed to HG show increased intracellular fiber contraction, which leads to loss of cell connection, disruption of VE-cadherin signals and reduction in VE-cadherin expression (Nobe et al., 2006; Wu et al., 2017).

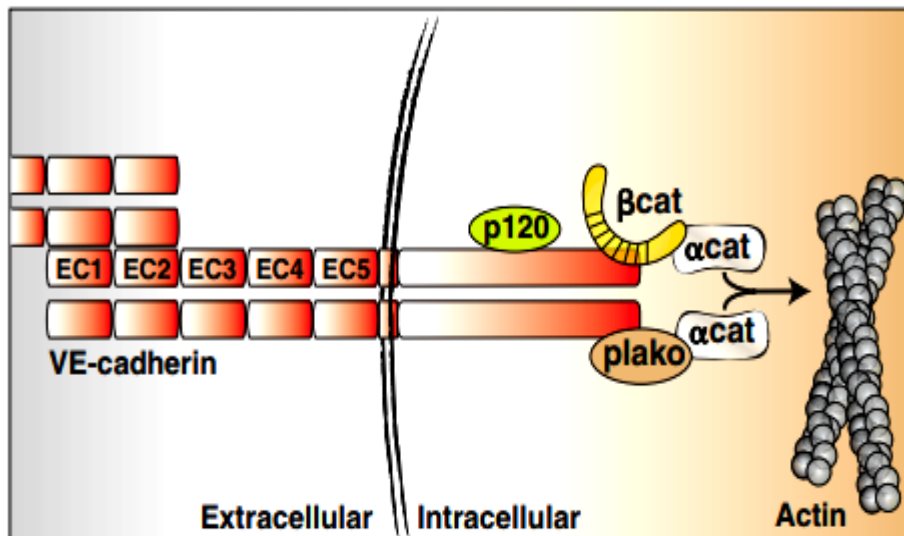


Figure 6: The structure of VE-cadherin. Permission obtained from copyright © 2008 The Company of Biologists Ltd (Dejana et al., 2008).

1.4.4.2 VE-cadherin endocytosis and degradation

Cellular interactions mediated by VE-cadherin are crucial for normal vascular morphogenesis. In the diseased state, such as cancer, inflammation, microvascular disorders, diabetes, and autoimmune diseases, VE-cadherin expression is often dysregulated (Reynolds and Carnahan, 2004). VE-cadherin is a highly dynamic adhesion junction protein that is transported into the cytosol via vesicle molecules. VE-cadherin endocytosis is mainly mediated via clathrin-dependent and clathrin-independent pathways (**Fig. 7**) (Delva and Kowalczyk, 2009). In the quiescent state, VE-cadherin interacts with p120-catenin and β -catenin to protect the plasma membrane from VE-cadherin internalization into the cytosol via the formation of p120-catenin and small GTPase (Rho A, Rac and CDC42) complex (Xiao et al., 2007). Dissociation of the p120-catenin-VE-cadherin complex after knocking down of p120-catenin promotes VE-cadherin internalization (Garrett et al., 2017). Without p120-catenin, VE-cadherin is degraded via the endo-lysosomal degradation pathway (Elia et al., 2006). A study has shown that presenilin-1 competes with p120-catenin for binding to VE-cadherin, which facilitates VE-cadherin endocytosis and degradation (Baki et al., 2001). Furthermore, ubiquitination also assists in the degradation of VE-cadherin. For example, E3 ligase, also known as Hakai, is a c-Cbl-like protein, which ubiquitinates VE-cadherin (Fujita et al., 2002). The K5 ubiquitin ligase directly acts on VE-cadherin, which can drive VE-cadherin endocytosis and

degradation without a constitutive endocytic motif (Nanes et al., 2017). Endocytic adaptors, including adaptor 2 (AP-2), can bind to clathrin and phospholipids at the plasma membrane. Studies have shown that AP-2 interacts with VE-cadherin and is involved in VE-cadherin endocytosis and degradation (Miyashita and Ozawa, 2007).

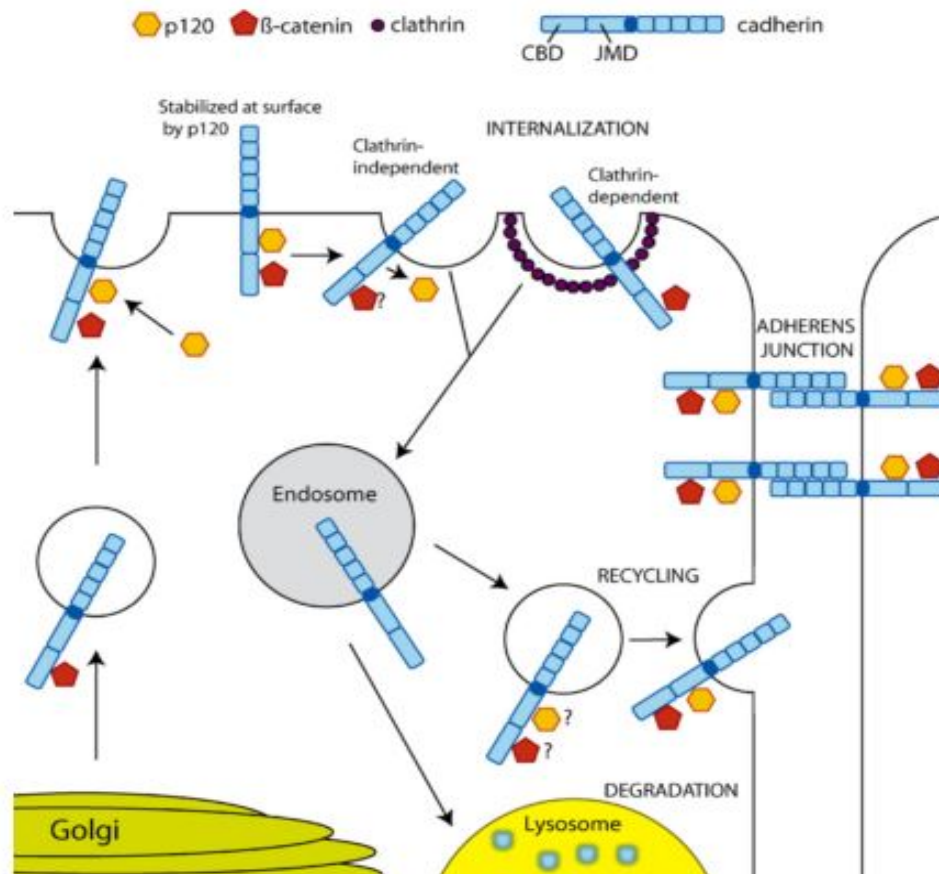


Figure 7: Overview of VE-cadherin trafficking. VE-cadherin is expressed at the cell plasma membrane and interacts with p120-catenin and β -catenin via binding to the cadherin juxtamembrane domain (JMD) and catenin binding domain (CBD). VE-cadherin internalization is regulated via clathrin-dependent and clathrin-independent pathways. Internalized VE-cadherin is degraded in the lysosome or returns to the plasma membrane. Permission obtained from copyright © 2007 Elsevier B. V. (Xiao et al., 2007).

1.4.4.3 VE-cadherin phosphorylation

It is well-known that the phosphorylation of VE-cadherin is associated with weak junctions and vascular permeability. The sites of tyrosine or serine

phosphorylation in the cytoplasmic tail of VE-cadherin are shown in **Fig. 8**. VEGF can phosphorylate VE-cadherin Tyr 658 and Tyr 685 via Src activation (Adam, 2015; Wallez et al., 2007). Leukocytes or lymphocytes also affect VE-cadherin phosphorylation via multiple signaling pathways. VEGF can also regulate the process of VE-cadherin endocytosis. As shown in **Fig. 9**, VEGF triggers the phosphorylation of VEGFR2, Src kinase, and VE-cadherin (Tyr 685) at endothelial junctions, accompanying the generation of reactive oxygen species (ROS). Once VE-cadherin is phosphorylated, p120- and β -catenin dissociate from the VE-cadherin complex, promoting plasma membrane VE-cadherin translocation toward the nucleus. In contrast, the disconnection of p120-catenin from VE-cadherin promotes VE-cadherin endocytosis via the clathrin-dependent pathway and accelerates VE-cadherin capture by lysosomes for degradation (Mukherjee et al., 2006). Once VE-cadherin is internalized into the cytosol, some regulatory proteins such as Hrs, Rab 5, and Rab 7 GTPase mediate the transport of the internalized VE-cadherin to the lysosome (Ogata et al., 2007; Palacios et al., 2005). Reports have shown that VE-cadherin tyrosine phosphorylation (Tyr 658 and Tyr 731) is involved in the induction of vascular permeability and leukocyte transmigration. As a result, increased VE-cadherin phosphorylation leads to gap enlargement between endothelial cells, thereby enhancing vascular permeability (Wessel et al., 2014). Other studies have reported that HG promotes VE-cadherin tyrosine phosphorylation (Tyr731) and Src kinase tyrosine phosphorylation (Tyr 416) via activation of PKC in endothelial cells. HG induces the separation of the VE-cadherin/ β -catenin complex and increases β -catenin translocation to the nucleus (Haidari et al., 2014). The mechanism underlying HG-induced VE-cadherin degradation probably involves increased expression of presenilin-1 (Nagai et al., 2016). The disruption of VE-cadherin internalization might weaken endothelial cell integrity (Gavard, 2014).

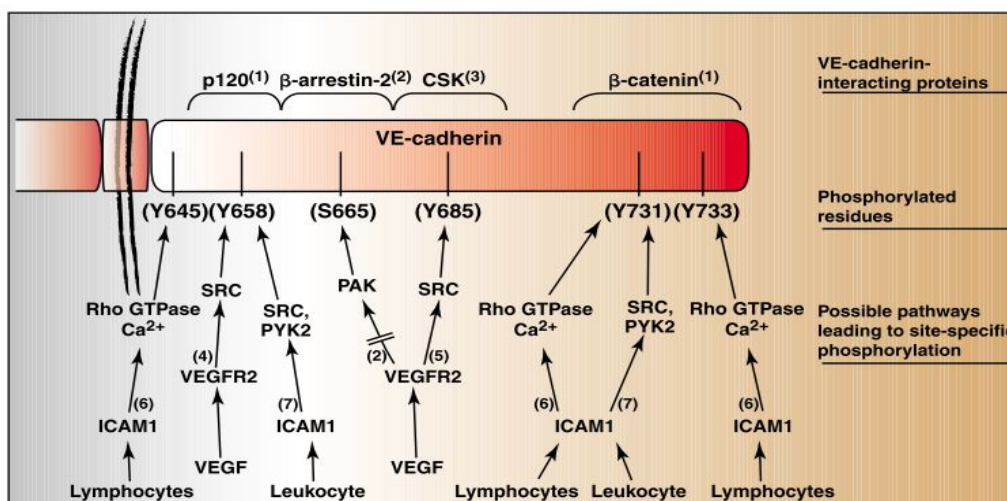


Figure 8: Phosphorylation site of VE-cadherin. Permission obtained from copyright © 2008 The Company of Biologists Ltd (Dejana et al., 2008).

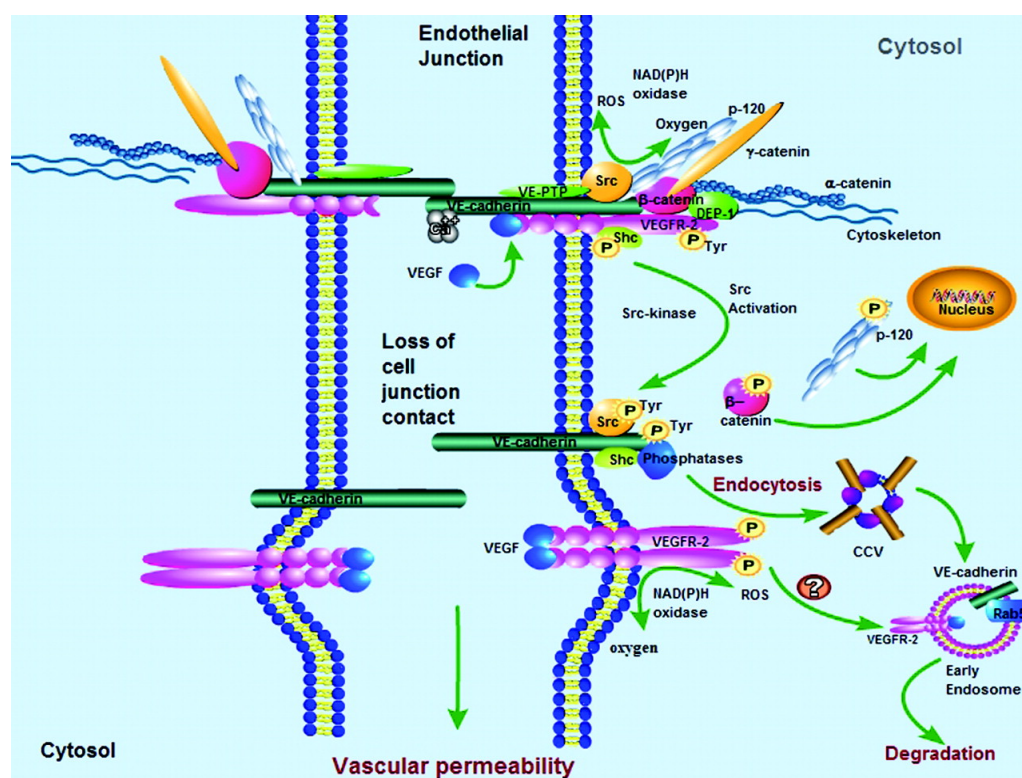


Figure 9: VEGF-mediated VE-cadherin endocytosis and degradation. Permission obtained from copyright © 2006 Wolters Kluwer Health, Inc (Mukherjee et al., 2006).

1.5 The potential mechanism of pericyte loss in retinopathy

Several factors are involved in pericyte loss during the early phase of DR, including HG insult, inflammation, and disruption of endothelial cell-pericyte interaction. Pericytes exposed to HG condition exhibit rapid accumulation of glucose in the cytosol with increased activity of AR (Akagi et al., 1983). HG causes mitochondrial dysfunction, such as decreased membrane potential, reduced oxygen consumption, and extracellular acidification, as well as enhanced mitochondrial fragmentation in retinal pericytes (Trudeau et al., 2011). The NF- κ B signaling pathway in retinal pericytes is activated upon treatment with HG, which leads to cell apoptosis with increased expression of Bax and TNF- α (Romeo et al., 2002). HG reduces the connexin 43 (Cx43) gap junction expression in pericytes and loosens contact between pericytes (Li et al., 2003). Excessive glucose can produce more advanced glycation end products (AGEs) that are toxic to retinal pericytes. High level of AGEs increases Ang-2

expression, which causes pericyte loss via $\alpha_3\beta_4$ integrin and p53 signaling pathways (Park et al., 2014). The increase in HG-induced oxidative stress also involves pericyte loss via the upregulation of pro-apoptotic thioredoxin interacting protein (Devi et al., 2013). Pericytes cultured under HG condition express high levels of IL-1 β , TNF- α , and ICAM-1 (Nehmé and Edelman, 2008).

1.6 Rodent retinopathy models

Studying the pathogenesis of pericyte loss in retinal disease using human patient samples is challenging. Therefore, established animal models are proper tools for mimicking the complications of diseases and for uncovering the underlying mechanism. Among animal models, rodents are used most commonly for early retinopathy research.

1.6.1 *Ins2^{Akita}* mouse

Ins2^{Akita} mouse is one of the common models for the early phase of DR, which harbors a mutation in the insulin gene, resulting in destruction of pancreatic β cells and inability to produce adequate insulin. *Ins2^{Akita}* mice are models for type 1-diabetes, as they develop hyperglycemia in as early as four weeks. Furthermore, *Ins2^{Akita}* mice produce high levels of active caspase-3, which leads to retinal cell apoptosis. After 12 weeks of hyperglycemia, *Ins2^{Akita}* mice display retinal vascular permeability. Pericyte loss and acellular capillary formation occur after 36 weeks of hyperglycemia (Barber et al., 2005; Freeman et al., 2009). Three-month old *Ins2^{Akita}* mice show retinal ganglion cell loss from the peripheral retina and abnormal morphological changes in retinal ganglion cells (Gastinger et al., 2008). Another study has reported that retinal thickness and vasculature do not change within six months in *Ins2^{Akita}* mice. However, increased GFAP expression in Muller cells and reduced GFAP expression in astrocytes are observed in *Ins2^{Akita}* mice (McLenachan et al., 2013). Five- and 7.5-month old *Ins2^{Akita}* mice exhibit deficiency in contrast sensitivity of optomotor behavior and spatial frequency threshold (Akimov and Rentería, 2012). Furthermore, compared to that in age-matched control mice, the retinal microvasculature of 6-month old *Ins2^{Akita}* mice displays reduced erythrocyte velocity, shear rate, and flow rate, as well as transient capillary inflow stoppage (Wright et al., 2012). Older *Ins2^{Akita}* mice, such as 9-month old mice, showed defect in synaptic connectivity in the outer plexiform layer and reduction in the

number of retinal ganglion cells and amacrine cells (Hombrebueno et al., 2014). In *Ins2^{Akita}* mice, formation of new abnormal vessels is accompanied by reduced retinal function until 9 months of age (Han et al., 2013).

1.6.2 Rats with polycystic kidney disease

Rats with polycystic kidney disease (PKD) express a truncated human polycystic-2 protein, which is predominantly located at the cilium, such as in kidney tubular epithelial cells and retinal photoreceptors. This mutation leads to the loss of almost the entire C-terminus of the protein. PKD rats are used to mimic the phenotype of autosomal dominant PKD, which often occurs in human patients. Polycystic-2 is essential for ion channel functions for maintenance of osmotic homeostasis (Liu et al., 2018). Before polycystic formation in the kidney, these rats develop retinal photoreceptor degeneration as an initial impairment at 1 month of age. Starting from the second month to the seventh month, PKD rats develop pericyte and endothelial cell loss and show retinal vascular regression as the secondary damage. Retinal vascular regression in PKD rats progresses over time. PKD rats also display microglia activation, such as upregulation of GFAP expression after one month, along with the increase in the expression of several neurotrophic factors, including FGF2, CTNF, and NGF (Feng et al., 2011; Feng et al., 2009; Gallagher et al., 2006). Muller cells in PKD rats show upregulation of AQP1 and AQP4, reduced Kir channel-mediated potassium conductance, and abnormal distribution of Kir4.1 protein, which contributes to retinal photoreceptor death (Vogler et al., 2013). Muller cells in PKD rats exposed to hypoosmotic conditions swell immediately. This effect is attributed to the induction of oxidative and nitrosative stress, mitochondrial dysfunction, and increased expression of inflammatory lipid mediators (Vogler et al., 2016). PKD rats can be considered as an animal model for retinal vascular regression induced by neurodegeneration without hyperglycemia.

1.6.3 Nucleoside diphosphate kinase B knockout mouse

1.6.3.1 The NDPK family

NDPKs, encoded by the *NME* genes, are ubiquitous enzymes that catalyze the exchange of phosphate between nucleoside diphosphates (NDP) and

triphosphate (NTP) reversibly, which involve the generation of a high energy phosphate intermediate (Abu-Taha et al., 2018; Wieland, 2007) (**Fig. 10**). They were identified in the 1950s in the yeast and pigeon breast muscle and exist as ten isoforms (Berg and Joklik, 1953; Krebs and Hems, 1953). Based on their catalytic activity and sequence homologies, the isoforms are classified into two classes. NDPK A, B, C, and D belong to class I, whereas the rest of the NDPK isoforms belong to class II (Wieland, 2007). In class I, the isoforms are catalytically active and share 58--88% sequence homology. The isoforms in class II share only 25--45% homology (Gilles et al., 1991). Most of the genes in class II are primarily expressed in primary cilia and sperm flagella (Boissan et al., 2009). In mammalian cells, the isoforms form heterohexamers of 17--21 kDa. (Gilles et al., 1991; Janin et al., 2000). NDPKs are multifunctional proteins that are involved in tumor metastasis, cell development, gene regulation, apoptosis, and endocytosis (Fan et al., 2003; Krishnan et al., 2001; Postel, 2003; Rosengard et al., 1989; Steeg et al., 1988). Till now, NDPK A and B are the most studied isoforms.



Figure 10: *The reaction mechanism catalyzed by NDPK. Permission obtained from copyright © 2018 Springer Nature (Attwood and Muimo, 2018).*

1.6.3.2 NDPKs and G-protein activation

G proteins were first identified by Alfred G. Gilman and Martin Rodbell when they stimulated cells with adrenaline (Gilman, 1989). G protein-coupled receptors (GPCR) primarily dominate the activity of heterotrimeric G proteins ($G_{\alpha\beta\gamma}$), which participate in cellular signal transduction. G protein contains two functional units: G_{α} and $G_{\beta\gamma}$ dimers (Hamm, 1998). G_{α} is tightly associated with $G_{\beta\gamma}$ dimers in the internal surface of the cell membrane. In the inactive state, GDP binds to the G_{α} unit. However, upon ligand-induced GPCR activation, GDP is released from G_{α} , which in turn binds to GTP, causing the dissociation of the G_{α} unit from $G_{\beta\gamma}$ dimers (Wall et al., 1995). Reports show that NDPK B interacts with $G_{\beta\gamma}$, which is essential for G protein function. As shown in **Fig. 11**, NDPK B can utilize NTP, preferably ATP, to form GTP. NDPK B triggers its

autophosphorylation on His118 site and subsequently phosphorylates the His266 site of G_{β} to mediate GPCR-independent G protein activation (Mäurer et al., 2005).

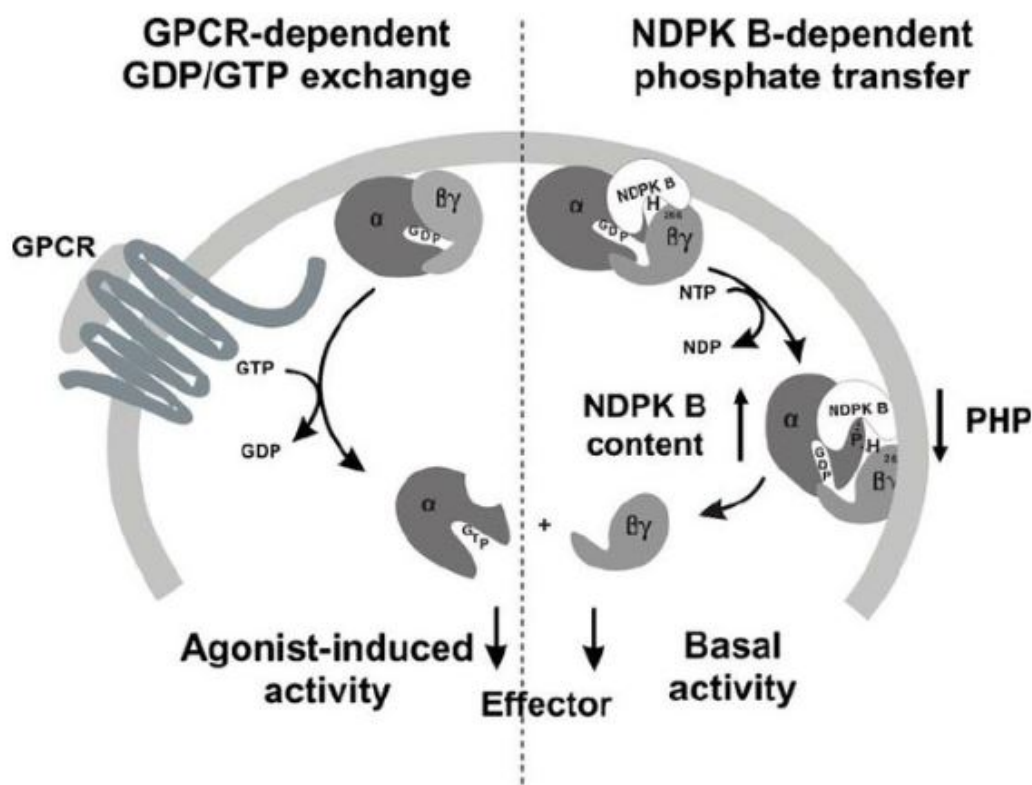


Figure 11: GPCR-dependent and alternative NDPK B dependent G protein activation. Permission obtained from copyright © 2007 Springer Nature (Wieland, 2007).

1.6.3.3 NDPKs and endocytosis

NDPKs interact with dynamin, which is the crucial mediator of the actin cytoskeleton. Three isoforms of dynamin have been identified in mammals, namely dynamin 1, 2, and 3. Among these, dynamin 2 is widely expressed in mammalian cells, whereas dynamin 1 and 3 are mostly presented in the brain. Dynamin 2 is primarily involved in cellular endocytosis (Ferguson and De Camilli, 2012; Menon and Schafer, 2013). Early studies have reported that NDPKs contribute to dynamin-mediated endocytosis of E-cadherin, which leads

to the loss of adhesion junctions (Palacios et al., 2002). The loss of NDPK B results in the inhibition of endocytosis and accumulation of clathrin-coated pits (Snider et al., 2015). Another study has reported that an intimate connection between NDPK B and caveolin proteins is key for caveolae formation, which is a participant in vesicle trafficking and endocytosis (Hippe et al., 2011).

1.6.3.4 NDPKs and diabetes

The Goto-Kakizaki rat model, which is a type 2 diabetic model, exhibits approximately 50% reduction in NDPK activity, histidine kinase activity, and autophosphorylation activity (Kowluru, 2003; Metz et al., 1999). The G protein activation mediated by NDPK B/G $\beta\gamma$ complexes is perturbed in the pancreatic β cells of diabetic animals (Kowluru et al., 2011). The loss of NDPK B induces diabetes-like vascular damage via increased expression of endothelial Ang-2 in the retina (Qiu et al., 2016). O-GlcNAc of FoxO1 mediates NDPK B deficiency-induced Ang-2 elevation and endothelial damage (Shan et al., 2018). Ang2 upregulation is harmful for endothelial-pericyte interaction (Maisonpierre et al., 1997; Yuan et al., 2009). NDPK B also contributes to vascular integrity. NDPK B deficiency displays vascular hyperpermeability and disrupts adhesion junctions between endothelial cells. NDPK B depletion affects VEGF-induced sprouting (Feng et al., 2014). In addition, NDPK B depletion in zebrafish causes a defect in cardiac contractility in conjunction with the downregulation of caveolin-1, caveolin-3, and G $\beta_{1\gamma 2}$ (Hippe et al., 2009). NDPK B is believed to act as histidine kinase that can phosphorylate intermediate conductance potassium channels, including the K $_{Ca}$ 3.1 channel and Ca $^{2+}$ -conducting TRP channel family member 5 (TRPV5).

1.7 Mesenchymal stem cells

Mesenchymal stem cells (MSCs) were first recognized and described in bone marrow by Friedenstein and his colleagues in the 1970s (Owen and Friedenstein, 1988). These cells can be distinguished from hematopoietic stem cells (HSCs) by their fast adherence to vessels, fibroblast-like morphology, and strong proliferative ability (Caplan, 1991). MSCs reside in the perivascular niches where they can sustain self-renewal and preserve the surrounding cells and tissues. MSCs belong to multipotent stem cells derived from developed organs, including bone marrow, adipose, skeletal muscle, dental tissue,

placenta, and umbilical cord, which are capable of differentiating into a variety of cell types including osteoblasts, myocytes, chondrocytes, and adipocytes (**Fig. 12**) (Bianco et al., 2008; Busser et al., 2015; De Bari et al., 2003; Huang et al., 2009; Mackay et al., 1998; Sibov et al., 2012; Vellasamy et al., 2012). In some tissues, MSCs share markers with pericytes such as NG2 and PDGFR β (Feng et al., 2010). Till date, various studies have shown that pericytes can differentiate into chondrocytes, adipocytes, and phagocytes, which strongly suggests that pericytes are similar to MSCs in terms of cell differentiation (Hirschi and D'Amore, 1996; Paquet-Fifield et al., 2009; Richardson et al., 1982). Owing to multiple differentiation properties and similarities with pericytes, MSCs possess enormous potential for the treatment of degenerative diseases such as DR. Indeed, MSCs are the ideal candidates for treating DR as they can replace the damaged pericytes, promote pericyte coverage in retinal capillary vasculature, and stabilize retinal vasculature, and mitigate vascular leakage (Ding et al., 2017; Fiori et al., 2018).

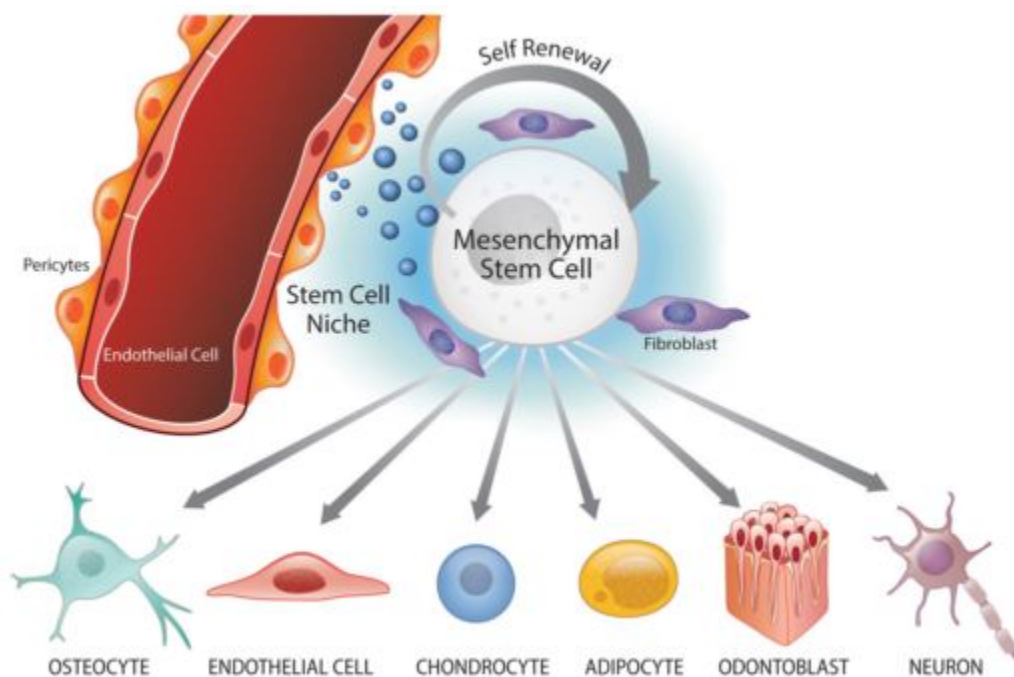


Figure 12: Multipotency of MSCs. MSCs reside in the perivascular niches and have multiple differentiation properties. They maintain cells and tissues. Under special conditions, they can differentiate into osteocytes, endothelial cells, chondrocytes, adipocytes, odontoblasts, and neurons. Reprinted from an open access article distributed under the Creative Commons Attribution License (Oh and Nör, 2015).

1.8 Therapeutic effects of MSCs in retinal degenerative diseases

Till now, most investigations on stem cells have focused on preclinical studies using different animal models with retinal disorders such as DR. Current therapeutic strategies for retinal degenerative diseases using MSC-based therapy involve: 1) MSC replacement in the injured retinas; 2) manipulation of paracrine secretion properties of MSC for preserving retinal damaged cells and restoring retinal cell functions (**Fig. 13**).

1.8.1 MSC plasticity

An early study by Kicic et al. in 2003 has demonstrated that MSCs differentiate into retinal photoreceptor cells when exposed to activin A, epidermal growth factor (EGF), and taurine *in vitro*. More importantly, they also provided evidence that MSCs injected in the subretinal region of a rat model with retinal degeneration can migrate into the photoreceptor layer and express photoreceptor markers *in vivo* without any adverse effects (Kicic et al., 2003). Another report has revealed that the trabecular meshwork- and conjunctiva-derived MSCs can transform into photoreceptor-like cells *in vitro* (Nadri et al., 2013a; Nadri et al., 2013b). Similarly, another study has shown that bone marrow-derived MSCs (BMSCs) can differentiate into retinal neuronal cells in injured rats (Tomita et al., 2002). Adipose-derived MSCs (ASCs) cultured in retinal pigment epithelium (RPE) -conditioned medium with vasoactive intestinal peptide display RPE features and markers (Vossmerbaeumer et al., 2009). Mendel et al. (2013) have reported that ASCs can differentiate into pericytes after treatment with TGF- β (Mendel et al., 2013). Furthermore, BMSCs have been reported to differentiate into neural precursor cells and mature neurons when treated with neural selection and induction medium (Chiou et al., 2005). Chakravarthy et al. have shown that BMSCs can migrate to diabetic mouse retina and express microglial, endothelial, pericyte, and Muller cell markers (Chakravarthy et al., 2016). Catanheira et al. have demonstrated that MSCs injected intravitreally migrate to and are incorporated into the retinal outer nuclear layer in the injured retina of rats. They are even present in the subretinal space. Most of the transplanted cells can express the markers for amacrine cells, bipolar cells, and retinal rod photoreceptor, whereas a few graft cells can express glial cell markers but not retinal pigment epithelial

cell markers (Castanheira et al., 2008). These results strongly indicate the potential of MSC-based cell therapy for retinal degenerative disease.

1.8.2 Paracrine signaling

MSCs can mitigate vascular and neuronal damage via the upregulation of several cytoprotective and neurotrophic factors in DR or retinal degenerative diseases. Otani et al. have reported that intravitreally injected MSCs preserve retinal blood vessels and rescue retinal degeneration in rd1 and rd10 mouse models (retinal degeneration models) via upregulation of antiapoptotic factors (Otani et al., 2004). Thomas et al. have reported that ASCs can differentiate into pericyte-like cells and migrate into retinas in the model of retinopathy of prematurity (ROP), preventing progressive degeneration of the retinal capillary network (Mendel et al., 2013). Yang et al. demonstrated that MSC transplantation reduces blood glucose level and promotes vascular leakage repair in streptozotocin-induced diabetic rats (Yang et al., 2010). A recent study has demonstrated that intravitreal injection of both ASCs or primed condition medium from stem cells exert a protective role in *Ins2^{AKita}* mice, including reduced retinal GFAP expression and retinal vascular hyperpermeability (Elshaer et al., 2018). Intravitreal injection of BMSCs contributes to the survival of retinal ganglion cells in the ischemia/reperfusion injury rat models (Na et al., 2009). In an ocular hypertension model, BMSCs produce neurotrophic factors to reduce retinal ganglion cell death (Johnson et al., 2010a). Subretinal transplantation of BMSCs promotes retinal photoreceptor survival and delay their death in the Royal College of Surgeons (RCS) rats (Inoue et al., 2007).

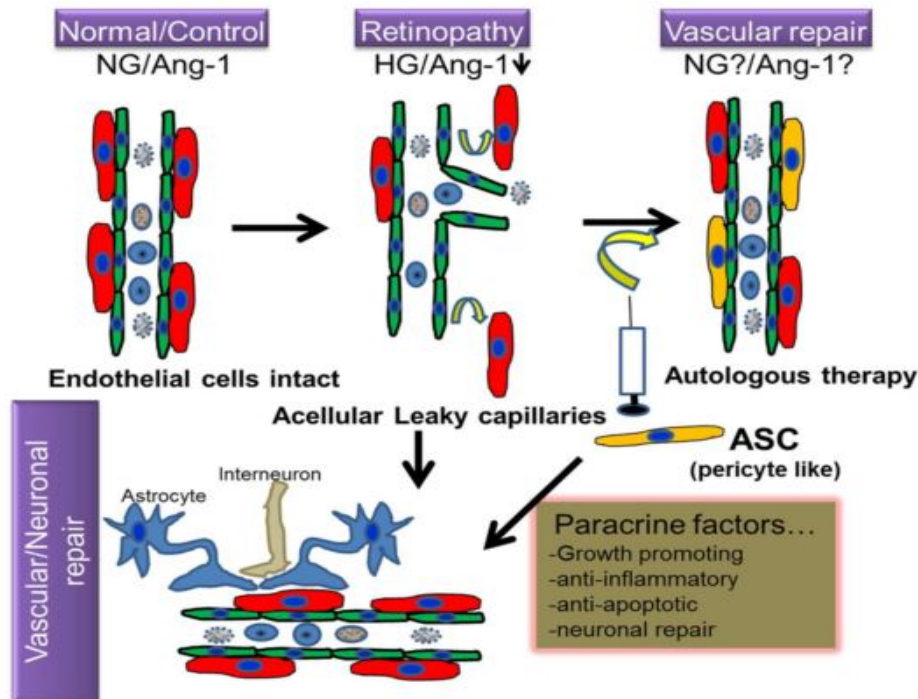


Figure 13: Strategy of MSC-based therapy for DR. MSCs replace the injured pericytes after intravitreal administration. MSCs preserve retinal vascular integrity and promote neurodegenerative repair via paracrine signaling. Reprinted from open access article distributed under the Creative Commons Attribution License (Rajashekhar, 2014).

1.9 Aims of this study

Retinal vasoregression involves pericyte loss and formation of acellular capillary. It is a hallmark of early retinopathy. Retinal pericytes support endothelial cells, control endothelial cell proliferation, and play a vital role in the retinal neurovascular unit. Retinal vascular destabilization, such as dysfunction of endothelial cells, leads to breakdown of the blood-retina barrier, which causes retinal edema and bleeding as well as vision loss. Among the adhesion junction molecules, VE-cadherin is essential for endothelial barrier function and vascular stability. Dysregulation of VE-cadherin, such as downregulation of VE-cadherin or increased phosphorylation of VE-cadherin, impairs barrier functions. Adequate pericyte coverage and VE-cadherin expression facilitate vascular integrity.

We have previously reported that PKD rats, NDPK B^{-/-} mice, and Ins2^{Akita} mice are three different animal models of retinal vasoregression. PKD rats progress

to pericyte loss at 2 months, which is associated with retinal photoreceptor degeneration. NDPK B^{-/-} mice exhibit diabetes-like vascular pathology such as retinal pericyte loss at 5 months. Ins2^{Akita} mice display retinal vasoregression at 3 months. Nevertheless, whether these retinopathy models show abnormal expression of VE-cadherin in retinas and whether the disrupted VE-cadherin expression affects pericyte stability are still unknown.

On the other hand, from a clinical perspective, MSC-based therapy may be used for treating retinal degenerative disorders. MSCs have multipotent functions. For example, they differentiate into pericytes that can rapidly attach to the vessels and migrate to the retinal pericyte position. In addition, they can produce several trophic factors to nourish and repair impaired retinal vessels and protect pericytes and endothelial cells from damage. However, the specific mechanism via which MSCs migrate into the retina, differentiate into pericytes, and repair injured retinal cells *in vivo* is still uncertain. Based on the data on retinal vasoregression and the role of VE-cadherin in the neurovascular unit from our group and those of others, as well as the features shared between MSCs and pericytes, we aimed to investigate the following:

1. a) the characteristic phenotype of retinal VE-cadherin expression in these animal models of retinal vasoregression with and without hyperglycemia; b) the link between VE-cadherin dysregulation and pericyte loss; c) the signal transduction in VE-cadherin-mediated vasoregression.

2. a) whether intravitreal injection of MSCs or MSC secretion can restore pericyte coverage, reduce the formation of acellular capillary and improve the retinal neuronal functions in vasoregressive retinas; b) whether intravitreally injected MSCs can migrate into retinas, integrate with retinal vessels and differentiate into pericyte-like cells *in vivo*; c) the underlying mechanism of action of intravitreally injected MSCs in retinal vasoregression.

2 Materials and Methods

2.1 Materials

2.1.1 Animals

NDPK B^{-/-} mice, Ins2^{Akita} mice, Sprague Dawley (SD) rats, and PKD rats were used in the experiments. Animal care and experimental procedures were performed per the guidelines of the Association for Research in Vision and Ophthalmology (ARVO) and were approved by the local government.

2.1.2 Cells

Human ASCs and rat BMSCs isolated from adult SD rats were obtained from the laboratory of Prof. Karen Bieback (Institute for Transfusion medicine and Immunology, Medical Faculty of Mannheim, Heidelberg University). Human umbilical cord vein endothelial cells (HUVECs) were isolated from the umbilical cords of healthy pregnant women with informed consent. Rat fat pad endothelial cells (RFPECs) were used for intravitreal injection, and human brain pericytes were used for endothelial-pericyte co-culture experiments. The right eyes of rats were intravitreally injected with cells [20,000 in 2 μ L phosphate buffered saline (PBS)], including human ASCs or starved BMSCs, using serum-free medium, or non-starved BMSCs, or HUVECs, or RFPECs, while PBS was administered in the left eyes as control.

2.1.3 Chemical materials

Table 1: chemicals and reagent

Chemicals and reagents	Company
4',6-diamidino-2-phenylindole (DAPI)	Sigma-Aldrich
4% PFA	Merck
10 \times PBS	Thermo Fisher Scientific
Bovine serum albumin (BSA)	Sigma-Aldrich
D-glucose	Sigma-Aldrich
Difco Trypsin 250	BD Bioscience
DMSO	Sigma-Aldrich

DRAQ5	Cell Signaling Technology
Ethanol absolute	Fischer
Isoflurane "Forene 100%."	Abbott
L-glucose	Sigma-Aldrich
Mayer's Hemalum solution	Merck
Methonal	Sigma-Aldrich
Roti®-Mount FluorCare	Carl Roth
Novesine® 0.4% eye drop	OmniVision
Nuclease free water	Promega
Periodic acid	Sigma-Aldrich
PP2	Santa Cruz Biotechnology
Schiff's reagent	Merck
Sucrose	Sigma-Aldrich
TaqMan Fast Advanced Master Mix	Thermo Fisher Scientific
Tris	Carl Roth
Tris-HCl	Carl Roth
Triton X-100	Carl Roth
Trypsin	Merck
Tween 20	Sigma-Aldrich
O.C.T compound	Sakura Finetek

2.1.4 Cell culture medium and substances

Table 2: cell culture media and substances

Media and substances	Company
Endothelial cell medium	Promocell
Dulbecco's modified eagle medium (DMEM) with 1000mg/L glucose	Sigma-Aldrich & Lonza
MCDB 131 medium	Thermo Fisher Scientific
EDTA-Trypsin 0.05%	Sigma-Aldrich
Fetal calf serum (FCS)	GE Healthcare
L-Glutamine 200 mM	Sigma-Aldrich
SD rat serum	Innovative Research
Phosphate-buffered saline (PBS)	Sigma-Aldrich
Penicillin 100 U- Streptomycin 10 mg/mL	Sigma-Aldrich

2.1.5 siRNA

Table 3: siRNA

siRNA	Sequence
Control-siRNA	5'-AACUGGUUGACUACAAGUCUU-3'
NDPK B-siRNA	5'-AGGUAGUGUAAUCGCCUUG-3'
VE-cadherin siRNA	5'-ACCACGAAACGTGAAGTTCAA-3'

2.1.6 Buffers

Table 4: Buffers for immunohistochemistry

Buffer	Contents
Antigen retrieval buffer	Solution A: 2.1 g citric acid monohydrate to 100 mL ddH ₂ O → pH 6.0-6.3 Solution B: 3.6 g trisodium citrate dihydrate to 100 mL ddH ₂ O → pH 6.0-6.3 Working solution: 1.48 mL A + 2.504 mL B to 400 mL ddH ₂ O
Fixation buffer	4% PFA in PBS
Blocking/permeabilization buffer	2.5% BSA, 0.3% Triton in PBS
Antibody diluting buffer	1% BSA, 0.3% Triton in PBS
Wash buffer	1× PBS

Table 5: Buffers for immunocytochemistry

Buffer	Contents
Fixation buffer	4% PFA in PBS
Blocking/permeabilization buffer	1% BSA, 0.3% Triton in PBS
Antibody diluting buffer	1% BSA, 0.3% Triton in PBS
Wash buffer	1× PBS

Table 6: Buffers for retinal digestion

Buffer	Contents
Fixation buffer	4% Formalin
Wash buffer	1× PBS

Retinal digestion buffer

3% Trypsin-Tris

Table 7: Buffers for retinal whole-mount staining

Buffer	Contents
Fixation buffer	4% Formalin
Wash buffer	1× PBS/0.1% Triton in PBS
Blocking/permeabilization buffer	1% BSA and 0.2% Triton in PBS

Table 8: Buffers for immunoblotting

Buffer	Contents
RIPA buffer	50 mM Tris-HCl, pH 7.4, 150 mM NaCl, 1 mM dithiothreitol, 1% Triton X-100, 1% sodium deoxycholate
Protein loading buffer	25 mL 50% glycerol 5 mL 10% 2-mercaptoethanol 7.5% SDS; 15 mL 300 mM Tris, pH 6.8 0.25% Bromophenol Blue; 5 mL H ₂ O
Cell lysis buffer	10 mL RIPA buffer with one tablet proteinase cocktail inhibitor
TBS (10x)	100 mM Tris pH: 7.4; 1.5 M NaCl
TBST (1 L)	100 mL TBS (10x), 890 mL H ₂ O; 10 mL 10% Tween 20
SDS-PAGE electrophoresis buffer	0.125 M Tris; 1.25 M glycine; 0.5% SDS
Tris buffer (stacking gel)	1 M Tris pH: 6.8
Tris buffer (separating gel)	1.5 M Tris pH: 8.8
Western blot buffer (10x) (1L)	32.5 g Tris; 144 g glycine; 1 L H ₂ O
Transferring buffer (1 L)	100 mL western blot buffer (10x); 200 mL Methanol; 700 mL H ₂ O
Ponceau S (100 mL)	5 mL acetic acid; 95 mL H ₂ O; 0.2 g Ponceau S

2.1.7 Antibody

Table 9: Antibodies for FACs

Antibody	Cat. Nr.	Company
CD44-APC	Clone 12K35	LifeSpan BioSciences
CD45-FITC	Clone OX-1	BioRad

Table 10: Primary Antibodies

Antibody	Cat. Nr.	Company
GFAP	Z0334	Dako
	sc-6170	Santa Cruz Biotechnology
HSP27	sc-1048	Santa Cruz Biotechnology
HSP90	4874	Cell Signaling Technology
GS	MAB302	Merck
IL-1 β	AF-501-NA	R&D Systems
Iba1	019-19741	Wako Chemicals
Lectin	L5264	Sigma-Aldrich
VE-cadherin	AF1002	R&D Systems
	ALX-803-305- C100	Enzo Life Science
β catenin	sc-7199	Santa Cruz Biotechnology
p120 catenin	sc-1101	Santa Cruz Biotechnology
NDPK B	MC-412	Kamiya Biomedical Company
G β	Sc-378	Santa Cruz Biotechnology
Phospho-VE-cadherin (Y685)	Ab119785	Abcam
Phospho-src (Y416)	2101	Cell Signaling Technology
src	2108	Cell Signaling Technology
γ -Tubulin	T5168	Sigma-Aldrich

Table 11: Secondary Antibodies

Antibody	Cat. Nr.	Company
Rabbit anti-mouse peroxidase	A-9044	Sigma-Aldrich
Rabbit anti-goat peroxidase	A-8919	Sigma-Aldrich
Goat anti-rabbit peroxidase	A-9169	Sigma-Aldrich
Alexa Fluor 633 conjugate	A-21052	Life Technologies
Alexa Fluor 555 conjugate	A-32727	Life Technologies
Alexa Fluor 594 conjugate	115-585-044	Jackson
		ImmunoResearch
Alexa Fluor 488 conjugate	A-11001	Life Technologies
Swine anti-rabbit FITC	F0205	Dako
Swine anti-rabbit TRITC	R0156	Dako

2.1.8 Primers

Table 12: Primers for QPCR

Gene	Company
IL-1 β	Rn00580432_m1; Thermo Fisher Scientific
IL-6	Rn01410330_m1; Thermo Fisher Scientific
IL-10	Rn01483988_g1; Thermo Fisher Scientific
C3	Rn00566466_m1; Thermo Fisher Scientific
Cfb	Rn01526084_g1; Thermo Fisher Scientific
Arg1	Rn00691090_m1; Thermo Fisher Scientific
NGF	Rn01533872_m1; Thermo Fisher Scientific
BDNF	Rn02531967_s1; Thermo Fisher Scientific
GDNF	Rn01402432_m1; Thermo Fisher Scientific
CNTF	Rn00755092_m1; Thermo Fisher Scientific
FGF2	Rn00570809_m1; Thermo Fisher Scientific
β actin	Rn00667869_m1; Thermo Fisher Scientific
NME2	Hs00897133_g1; Thermo Fisher Scientific
CDH5	Hs00901465_m1; Thermo Fisher Scientific
Notch 1	Hs01062014_m1; Thermo Fisher Scientific
CTNNB1	Hs00355045_m1; Thermo Fisher Scientific
GJA1	Hs00748445_s1; Thermo Fisher Scientific
CAV1	Hs00971716_m1; Thermo Fisher Scientific
ACTB	Hs01060665_g1; Thermo Fisher Scientific

2.1.9 Kits

Table 13: Kits

Kits	Company
Cell Tracker Green CMFDA Dye	Thermo Fisher Scientific
Subcellular Protein Fractionation Kit for cultured Cells	Thermo Fisher Scientific
Lumi-Light Western Blotting	Roche
Super Signal West Femto	Thermo Fisher Scientific
Centrifugal Filter Unit	Microcon® Centrifugal Filters Devices
cOmplete™, EDTA-free Protease	Roche

2.1.10 Consumable materials

Table 14: consumable materials

Material	Type	Company
Cell culture dishes	6 cm, 10 cm	Sarstedt
Cell culture flasks	175 cm ² , 125 cm ²	Sarstedt
Cell culture multi-well plates	6-well, 12-well, 24-well	Sarstedt
Collecting tubes	50 mL, 15 mL	Sarstedt
Filter tips	1000 µL, 100 µL, 10 µL	Greiner Bio One
MicroAmp® Fast Optical Reaction Plate	96-well, 0.1 mL	Applied Biosystems
MicroAmp® Optical Adhesive Film		Applied Biosystems
Microscope object slides	76×26 mm	R. Langenbrinck
Microscope round coverslips	Ø 12 mm	Menzel
Microscope square coverslips	24×24 mm, 24×60 mm	Carl Roth
PCR tubes	Multiply® µStrip Pro 8-strip	Sarstedt
Pipette tips	1000 µL, 100 µL, 10 µL	Sarstedt
Protran nitrocellulose transfer membrane	2.5 µm	Whatman
Serological pipettes	5 mL, 10 mL, 25 mL	Sarstedt
Sterile syringes	Omnifix® solo 1 mL	B. Braun
Whatman® filter paper		Whatman

2.1.11 Apparatuses

Table 15: Apparatuses

Apparatuses	Company
--------------------	----------------

Laminar flow bench	Heraeus/Thermo Fisher Scientific
Incubator (37°C, 5% CO ₂)	Memmert
Water bath	Thermo Fisher Scientific
Centrifuge	Eppendorf/Thermo Fisher Scientific
Gel imager	Alpha imager 2000
Shaker	Neolab
Electrophoresis chamber and apparatus	Bio-Rad
Mini-protein casting module	Bio-Rad
Heating block	Eppendorf
Voltmeter	Biometra
Vortex	Janke & Kunkel
Pipette	Sartorius
Weighing machine	Sartorius
Pump	
Microprocessor PH meter	WTW
Spectrophotometer	Thermolabsystems Multiscan EX
NanoDrop Spectrophotometer	PeQLab
Stereomicroscope	Zeiss/Olympus
Fluorescence microscope	Leica
Confocal microscope	Leica
Scanning machine	Zeiss Axio Scan Z1
QPCR machine	Applied Biosystems
Millipore water machine	Milli-QR
Needle for intravitreal injection	World Precision Instruments
4°C fridge	Bosch
-20°C fridge	Bosch
-80°C fridge	Thermo Fisher Scientific

2.1.12 Software

Table 16: Software

Software	Company
Alpha imaging software	Alphamager® Innotech
Confocal microscope software	Leica Application Suite X
Zen blue	Zeiss
AnalysisPro	Olympus

Image J	National Institutes of Health
Bradford	Thermolabsystems Multiscan EX
Blot image	IrfanView
Statistical software	GraphPad Software Inc
Reference software	Endnote

2.2 Methods

2.2.1 Isolation of HUVECs

Fresh human umbilical cords were put on clean pad and excess blood was removed. Fresh cuts were made on both ends of the cords. One end of the cord was sealed using a clamp and the other end was attached to a 3-way stopcock, allowing bidirectional flow of fluid through the vein, which was further washed using pre-warmed low glucose DMEM to remove the internal blood of the vein completely. 1×DMEM-Dispase II was used to digest the vein endothelial cells. The cord was incubated (37°C, 5% CO₂) for 30 min. The digested cells were collected by a 50-mL Falcon tube with 5-mL FCS to stop the enzymatic digestion. After centrifugation, the cells were collected and cultured in complete endothelial cell growth medium.

2.2.2 HUVEC and pericyte culturing

HUVECs were cultured on gelatin-coated flasks using endothelial cell growth medium supplemented with 10% FCS. Human pericytes were purchased from the company (ScienCell Research Laboratories) and were grown on gelatin-coated flasks in the DMEM/F12 medium supplemented with 5% FCS, 1% penicillin-streptomycin, insulin (5 µg/mL), and bFGF (2 ng/mL).

2.2.3 HUVEC-pericyte co-culture

HUVECs were cultured in a 6-well plate coated with 1% gelatin. Cells were transfected with control siRNA or VE-cadherin siRNA, followed by changing of fresh complete endothelial cell medium 4 h after transfection. The next day, pericytes were added on the top of the HUVEC monolayer (pericytes: HUVECs = 1:3) and further co-cultured for 24 h in mixed medium containing 50% HUVEC

culturing medium and 50% pericyte culturing medium.

For the quantification of attached pericytes, pericytes were incubated with anti-NG2 antibody, and HUVECs were incubated with the anti-VE-cadherin antibody overnight at 4 °C. Then, after washing with PBS, the cells were incubated with the commensurate secondary antibodies at RT for 1 h. The slices were mounted with Roti-mount. Pericyte coverage was quantified from the average fluorescent intensity of five microscopic fields at 40× magnification using the ImageJ software.

For the quantification of detached pericytes, before co-culture, pericytes were stained with Cell-Tracker™ Green dye (5µM) in a serum-free medium at 37 °C for 30 min; they were further incubated in a complete medium at 37 °C for 30 min. The labeled pericytes were added on the HUVEC monolayer according to their seeding ratio. The detached pericytes were collected from the medium and were quantified using the cell counting chamber. The quantification was performed under a fluorescent microscope and the cell number was randomly measured in five microscopic fields at 10× magnification.

2.2.4 RNA interference

HUVECs were cultured in gelatin-coated 6-well plates using ECBM supplemented with 10% FCS. HUVECs at 70% confluence cultured in serum-free OptiPRO medium (Life Technologies, Darmstadt, Germany) were transfected with NDPK B siRNA, VE-cadherin siRNA, and control siRNA using lipofectamine (Life Technologies, Darmstadt, Germany) according to the manufacturer's protocol and incubated for 4 h. After transfection, the cells were re-cultured in ECBM supplemented with 10% FCS. Then, cells were starved in ECBM with 0.5% FCS overnight at 37°C, followed by stimulation with normal glycemic condition (5.5mM D-glucose) or hyperglycemic condition (30mM D-glucose) for 24 h. The NDPK B and VE-cadherin knockdown were validated using western blot analysis.

2.2.5 VE-cadherin internalization assay

HUVECs were cultured in a cell chamber (Merck, Germany) coated with cross-linked gelatin and glutaraldehyde. The cells were transfected with the NDPK B siRNA or control siRNA for 4 h at 70% confluence. The next day, cells were cultured in 2% FCS medium overnight. Then, the cells were incubated with VE-

cadherin primary antibody (clone BV6, ALX-803-305, Enzo Life Sciences) at 4°C for 1 h in MCDB 131 medium containing 1% BSA. After washing thrice with ice-cold MCDB 131 medium, the cells received 5 mM NG/30 mM HG for 30 min or VEGF (50 ng/mL) for 15 min at 37°C in the incubator. For assessment of VE-cadherin internalization, cells were washed with ice-cold acid washing buffer (Hanks buffer, pH 2.7, containing 25 mM glycine and 1% BSA), and were fixed with 4% paraformaldehyde (PFA) for 15 min on ice. Then, the cells were incubated with 1% BSA containing 0.2% Triton X-100 in PBS overnight at 4°C. Subsequently, cells were incubated with rabbit anti-EEA1 (1:200, Thermo Fisher Scientific, USA) or rabbit anti-LAMP1 (1:200, Cell Signaling Technology, USA) overnight at 4°C. After washing thrice with PBS, the cells were incubated with the corresponding secondary antibodies, goat-anti-mouse Alexa Fluor 488 (1:200, Life Technology, USA), and swine-anti-rabbit TRITC (1:30, Dako, Denmark) at RT for 1 h. The nuclei were stained with DRAQ5 (1:1000, Cell Signaling Technology, USA) for 5 min. The images were acquired using a fluorescent microscope or confocal microscope (Leica, Germany).

2.2.6 Membrane protein extraction

HUVECs were cultured in 6-well plates till they reached 70% confluence. After transfection and starvation, the cells were stimulated with or without HG (30 mM) for 24 h. Subsequently, the cells were harvested using trypsin-EDTA and collected via centrifugation at 500 × *g* for 5 min. The subcellular protein fractionation kit was used for preparing the membrane extract.

2.2.7 Isolation of human ASCs

Human ASCs were isolated from lipoaspirate samples. ASCs were cultured in complete medium (DMEM, 10% fetal calf serum, penicillin, and streptomycin) and were characterized based on fibroblastoid morphology, adipose- and osteogenic differentiation potential, and immune phenotype.

2.2.8 Isolation of rat BMSCs

The femur and tibia isolated from healthy SD rats were dissected and used for isolating BMSCs. Tissues were immersed in PBS containing 2 mM EDTA, 100 U/mL penicillin, and 100 µg/mL streptomycin (PS). A syringe was used for flushing the bone marrow cavity using PBS/2mM EDTA/PS. The liquid collected was centrifuged at 420 × *g* for 5 min. The cell pellet was then re-suspended in complete medium (DMEM, 10% rat serum, PS) and transferred to a 25 cm²

plastic flask and incubated overnight at 37 °C in a 5% CO₂ incubator. The next day, the flasks were washed using PBS/EDTA, and the cells were cultured until they were subconfluent.

2.2.9 Human ASC, rat BMSC, and RFPEC culturing

Human ASCs were typically cultured in T75 or T125 flasks, and the medium (DMEM (low glucose) with 1% L-glutamine, 1% PS, and 10% FSC) was changed after every two days. Cells were split once till they reached 70–80% confluence. For passaging, the cells were first washed twice with PBS and then digested with trypsin at 37°C for 5 min. After all the cells had detached, complete medium was used to stop the digestion. Cells were plated in the new culturing flask at the density of 1×10^6 cells/cm².

Rat BMSCs were cultured in complete medium (DMEM (low glucose) with 1% L-glutamine, 1% PS, and 10% FSC). Upon reaching 70–80% confluence, the cells were digested using trypsin/EDTA. Afterward, the cells were seeded at the density of 3×10^5 cells in a T75 flask and cultured for 3 days.

RFPECs were cultured in DMEM (1000mg/L glucose) supplemented with L-glutamine, PS, and 10% FCS in a 5% CO₂ incubator at 37°C.

2.2.10 Concentration of human ASC supernatant

Ten milliliters of human ASC culture supernatant were collected from the cell culturing flasks and concentrated using Microcon® centrifugal filters devices. First, the tube was inserted in the Microcon® centrifugal filters devices. Second, culture supernatant was pipetted into the device and was centrifuged at 14,000 × *g* for 20 min. The liquid at the bottom of the tube was discarded, and the concentrated supernatant in the inserted tube was collected for the following concentration step. Finally, the injected culture supernatant was concentrated 100 times from 100 mL.

2.2.11 Cell labeling

MSCs were labeled with Cell-Tracker™ Green CMFDA for monitoring their location in the eye post-injection. Initially, cells were washed with PBS and then collected after trypsin digestion. Subsequently, the cells were incubated in 1.5

mL Eppendorf tubes with a serum-free culture medium containing 5 μ M Cell-Tracker™ Green CMFDA dye at 37 °C for 30 min. Afterward, the cells were re-incubated in a complete fresh medium at 37°C for 30 min. Finally, the cells were diluted in sterile PBS at the concentration of 10,000 cells/ μ L.

2.2.12 Intravitreal injection

Rats were anesthetized with isoflurane for the whole injection procedure. An anesthetic solution, Novesine® 0.4% eye drop, was applied to both eyes. A 35-gauge fine needle connected with a 10 μ L syringe was used for injection into the vitreous cavity, under monitoring using an ophthalmic microscope. The left eyes were intravitreally injected with 2 μ L of sterile PBS. The right eyes received injection of 20,000 cells in 2 μ L.

2.2.13 Retinal digestion and quantitative retinal morphometry

The frozen eyes were immersed in 4% formalin solution at RT for 48 h. The eyes were washed thrice with PBS to remove the remaining fixation solution. Retina isolation was performed under the microscope. First, the eyeball was positioned forward by placing the forceps around the posterior part. After that, the cornea was removed using sharp scissors. After eliminating the lens and vitreous, the retina was carefully isolated using a micro-spatula.

The retinas were initially sunk in deionized water at 37°C for 1 h and further incubated in Tris-HCl buffer (pH 7.0) containing 3% trypsin at 37°C for about 3 h. The retinas were carefully moved onto a clean glass slide and washed with deionized water using a pump until no debris was left in the water, and the retinal vasculature network observed under the microscope. The retinas dried entirely at RT and subjected to period-acid-schiff (PAS) staining procedure for visualization of the retinal vasculature. The protocol of PAS staining was as follows:

ddH ₂ O	5 min
1% Periodic acid	30 s
ddH ₂ O	Short time
Schiff's reagent	30 s
Running tap water	5 min
ddH ₂ O	Short time

Mayer's Hemalum	30 s
Running tap water	7 min
ddH ₂ O	Short time
70% ethanol	Short time
80% ethanol	Short time
96% ethanol	5 min
100% ethanol	5 min
Roti®-histol ×3	5 min each
Embed with Entellan®	

The number of pericytes and the acellular capillaries in 40× magnification images were used for quantification. Briefly, ten microscopic fields were selected randomly for each image. AnalysisPro (Olympus) was used for calculating cell and acellular capillary number. A special ocular containing a grid of 100 squares was required for the observation of acellular capillaries. The acellular capillaries present in the squares was recorded in ten randomly-selected microscopic fields.

2.2.14 Immunofluorescence staining

The eyes were embedded in paraffin blocks, and retinal paraffin sections of 6-µm thickness were made and deparaffinized after incubation at 60°C for 1 h. After cooling, the sections were further immersed in Roti-Histol, and subsequently in decreasing concentrations of ethanol (100% to 70%). After antigen retrieval using a citric buffer, the sections were immersed in a solution containing 2.5% BSA and 0.3% Triton X-100 for 2 h at RT. Next, the sections were immersed in primary antibody overnight at 4°C and were incubated with the corresponding secondary antibodies for 1.5 h at RT in the dark on the next day. DRAQ5 was used for nuclear staining.

HUVECs were fixed using 4% PFA for 15 min on ice. After PBS washing, the cells were blocked and permeabilized overnight using 1% BSA + 0.2% Triton X-100 at 4°C. The cells were stained overnight with corresponding primary antibodies at 4°C. The next day, the cells were stained with the corresponding secondary antibodies at RT for 1 h in the dark. DRAQ5 was used for nuclear staining.

For retinal whole-mount staining of VE-cadherin and lectin, the eyes were fixed

in 4% PFA on ice for 2 h. After three PBS washes, the retinas were dissected and incubated overnight in the blocking/permeabilization buffer (1% BSA+0.2% Triton X-100) at 4°C. Afterward, the retinas were incubated overnight with anti-VE-cadherin antibody and anti-lectin conjugated with the TRITC antibody at 4°C. The retinas were incubated with a goat anti-mouse antibody at RT for 1 h. Finally, the retinas were mounted on the glass slides with Roti-mount. The images were acquired using a confocal laser scanning microscope. Retinal vascular VE-cadherin expression was quantified from the fluorescent intensity using the ImageJ software.

2.2.15 Microglia quantification

Microglia were quantified using immunofluorescence staining images. The eyes were fixed in 4% formalin for 24 h, and the retinas were isolated. After PBS washing, the retinas were blocked and permeabilized in a buffer containing 0.5% Triton X-100 and 1% BSA in PBS for 30 min. The retinas were then co-incubated with the anti-Iba1 and anti-lectin antibody overnight at 4°C. After PBS washes, the retinas were then co-incubated with the corresponding secondary antibodies for 1 h at RT. Finally, the retinas were flat-mounted with Vectashield hard set mounting medium. Images were captured from five randomly-selected fields in the deep capillary layer using a confocal microscope. Iba1-positive cells were counted using ImageJ (v 1.50i) and calculated as a microglia/mm² retinal area.

2.2.16 Multifocal electroretinography

Multifocal electroretinography (mfERG) was performed in this study. The rats were positioned in front of the RETImap machine, with a DTL electrode touching the cornea. Subcutaneous silver needle electrodes were inserted into the neck skin of the rats as the reference and ground electrodes. A contact lens with ninety dioptics was mounted over viscous 2% methocel gel, which was then placed on the eyes of the mice. An array of seven equally-sized hexagons was selected. The stimulation was conducted using 150 cd/m² and 1 cd/m² for the m-sequence with four dark frames in between the stimuli. An average of eight cycles was used for the final analyses. mfERG was recorded under photopic conditions, where both rod and cone photoreceptors were activated in rats. In terms of analysis, the response from the internal retina was quantified as a positive wave 1 (P1) regarding signal strength represented by P1 amplitude,

and signal velocity indicated by P1 implicit time. In this experiment, the P1 amplitude, acting as an indicator of the inner retinal function and mainly generated by the Müller cells. was represented the b-wave in standard ERGs,

2.2.17 Cryosectioning

The eyes were fixed using 4% PFA for 4 h, followed by three washes with PBS. After the removal of the cornea and lens, the remaining tissue was placed in a 20% sucrose solution for 30 min. Subsequently, the eye tissue was positioned vertically in a small cutting form with O.C.T compound and frozen at -20°C . Sectioning was performed with a cryostat. Cryosections were stained with DAPI for observing the nuclei and were finally mounted with the Roti-mount solution.

2.2.18 Immunoblotting

The proteins from retinas and cells, extracted using radioimmunoprecipitation assay (RIPA) buffer supplemented with protease inhibitor cocktail, were separated using sodium dodecyl sulfate-polyacrylamide gel electrophoresis (SDS-PAGE) and were further electrically transferred onto nitrocellulose membranes that were blocked with Roti-block at RT for 1 h. After washing with Tris-buffered saline with Tween-20 (TBST), the membranes were incubated with targeted primary antibodies in a Falcon tube on a shaker overnight at 4°C . Then, the blots were incubated with corresponding secondary antibodies at RT for 1 h. The blot was visualized using a chemiluminescent substrate and an imaging machine. Protein expression was analyzed using the ImageJ software.

2.2.19 Dot blot

One microliter of the aqueous humor from eyes dropped was onto a nitrocellulose membrane that was allowed to completely dry at RT. After blocking for 1 h, the blot was incubated overnight with goat anti-rat IL-1 β primary antibody at 4°C . After washing thrice with TBST, the membrane was incubated with the corresponding secondary rabbit-anti-goat antibodies at RT for 1 h. Protein expression was analyzed using the ImageJ software.

2.2.20 Ex vivo experiments

The eyes of PKD rats were intravitreally injected with 2×10^4 human ASCs labeled with Cell-Tracker™ Green and cultured in a 12-well plate in complete medium. Eyes were fixed in 4% PFA for 2 h on ice three days after the injection. After washing with PBS, the retinas were carefully dissected for whole-mount staining with an antibody against lectin conjugated with TRITC. The images were captured using an immunofluorescence microscope.

2.2.21 Retinal RNA isolation

The dissection instruments were sequentially disinfected with 70% ethanol, distilled water, and RNaseZAP. Rat retinas were isolated from eyes and were transferred to a 1.5 mL Eppendorf tube filled with 300 μ L Trizol. Retinas were homogenized through a syringe connected sequentially with 22G, 25G, and 27G needles in this order. Subsequently, 700 μ L Trizol was added to the tubes with the retina solution and mixed well manually. The tube was placed at RT for 5 min, followed by the addition of 200 μ L chloroform into 1 mL Trizol solution. Subsequently, the tube was intensely shaken manually for 15–20 s and was placed at RT for 2–3 min. After centrifuging at $12,000 \times g$ for 15 min at 4°C, 500 μ L of the top aqueous phase was aspirated out and transferred into another new tube, to which 500 μ L isopropanol was added to precipitate RNA via centrifugation at $12,000 \times g$ for 30 min at 4°C. The RNA pellet was washed using 75% ethanol. Finally, the RNA was completely air-dried and dissolved in 20 μ L diethyl pyrocarbonate (DEPC)-treated water.

2.2.22 Real-time polymerase chain reaction (PCR)

The RNA concentration was measured with a Nanodrop machine. RNA was reverse-transcribed to cDNA using the GoScript™ reverse transcription kit. The program for cDNA synthesis was as follows: annealing at 25°C (5 min)—extension at 42°C (60 min)—inactivation of reverse transcriptase at 70°C (15 min). The cDNA was diluted 1:5 in RNase-free water for real-time PCR. TaqMan Fast advanced master mix was utilized for real-time PCR. All primers and MGB probes labeled with FAM dye for amplification were purchased from Applied Biosystems-Thermo Fisher Scientific. Gene expression was analyzed using the $-\Delta\Delta CT$ method. The expression of each target gene was standardized to that of the housekeeping gene encoding β actin.

2.2.23 Retinal perfusion

Mice were anesthetized using isoflurane inhalation. Cervical dislocation was performed after short anesthesia. Mice were immobilized firmly in a stereotactic device. Medical scissors were used to carefully open the chest cavity and a perfusion syringe was inserted in the left ventricle. The right atrium was pierced with a needle for inducing blood outflow. For removal of retinal vessel blood, 10 mL of saline was slowly perfused in the left ventricle of mice for 5 min until the mice's eyes turned white. Immediately after the perfusion, the eyes were enucleated and stored in liquid nitrogen.

2.2.24 Statistical analysis

All the data were presented as mean \pm SD. Student t-test or two-way analysis of variance (ANOVA) was performed using GraphPad Prism 5 (GraphPad Software, La Jolla, CA, USA). *P* values < 0.05 were considered significant.

3 Results

3.1 The role of VE-cadherin in retinal vasoregression

3.1.1 VE-cadherin expression is reduced in NDPK B deficient retinas before pericyte loss

To investigate the role of VE-cadherin in the progression of retinal vascular degeneration, we detected the expression of retinal VE-cadherin in NDPK B^{-/-} mice. As shown in **Fig. 14**, western blot analysis confirmed the deficiency of NDPK B in knockout retinas. Retinal VE-cadherin expression was evaluated in NDPK B^{-/-} mice at different ages (from 1 to 5 months). Retinal VE-cadherin expression in 1- and 3-month old NDPK B^{-/-} mice did not vary significantly from that of their age-matched control mice. However, 4-month-old NDPK B^{-/-} mice started to show a substantial decrease in retinal VE-cadherin expression, which was further reduced in 5-month-old NDPK B^{-/-} mice (**Fig. 15A and B**). We had previously detected pericyte loss in 8-month-old NDPK B-deficient retinas (Qiu et al., 2016). To identify the initial time point of pericyte loss in NDPK B^{-/-} retinas, we assessed the pericyte coverage of retinal capillary in WT and NDPK B^{-/-} mice at 4 and 5 months. Retinal pericyte coverage between NDPK B^{-/-} and WT retinas did not vary significantly at 4 months. However, as shown in **Fig. 16A and B**, the number of pericytes in 5-month-old NDPK B-deficient retinas was significantly lower than that in WT retinas ($P < 0.05$). These data suggest that the reduced expression of retinal VE-cadherin occurs before pericyte loss, which is the first sign of hyperglycemia-independent retinal vasoregression in NDPK B^{-/-} mice.

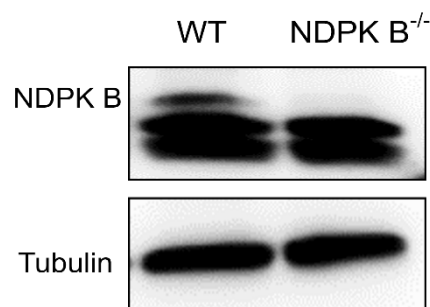


Figure 14: NDPK B depletion in retinas of NDPK B^{-/-} mice. NDPK B was not expressed in the retinas of NDPK B^{-/-} mice as shown using western blot analysis

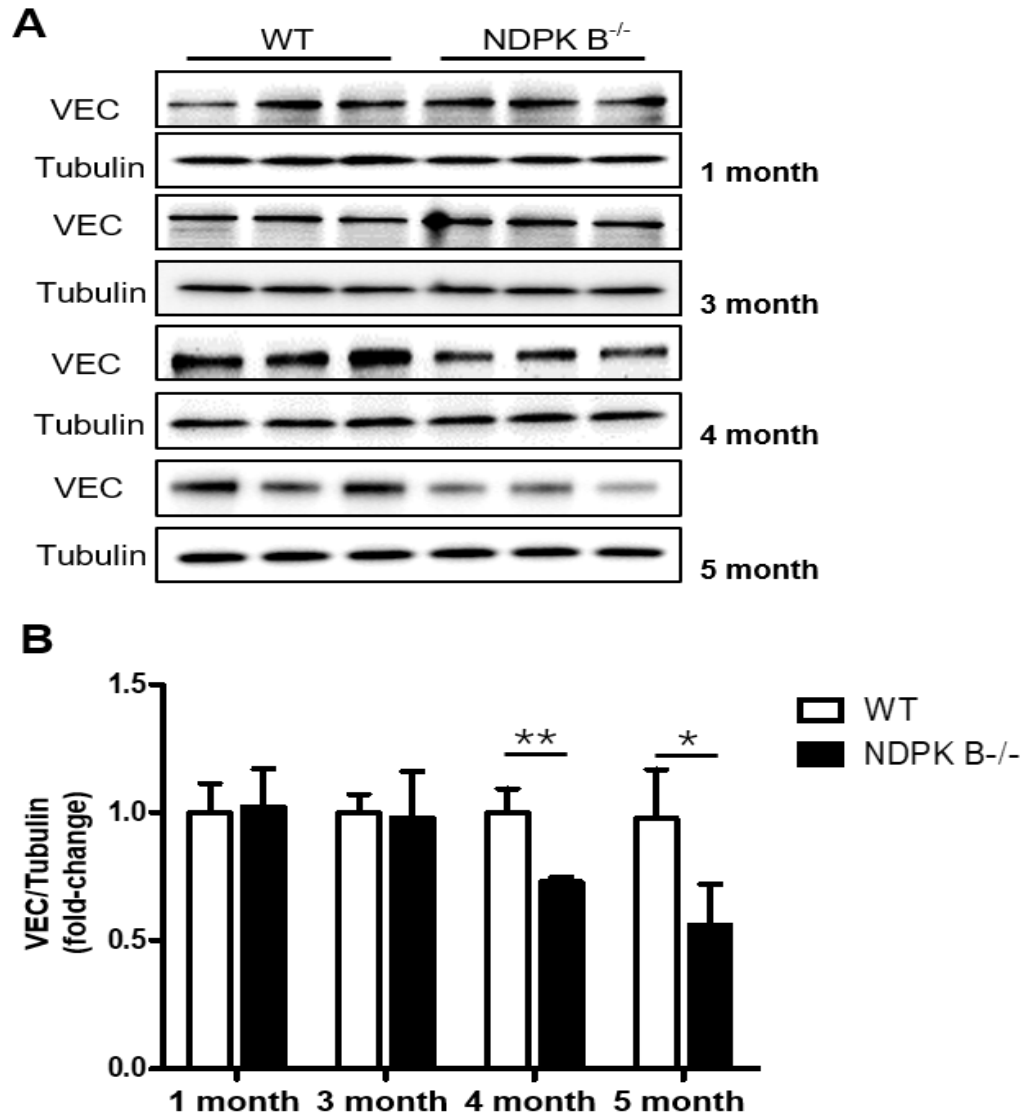


Figure 15: VE-cadherin expression is reduced in NDPK B-deficient retinas. (A) VE-cadherin expression in the retinas of WT and NDPK B^{-/-} mice of different ages (1, 3, 4, and 5 months) determined using western blot analysis. Reduction in the expression of VE-cadherin in the retinas of NDPK B^{-/-} mice was initiated at 4 months and progressed at 5 months. (B) Quantification of western blot data. VEC: VE-cadherin; NDPK B^{-/-}: NDPK B knockout. * $P < 0.05$. ** $P < 0.01$. $n = 3$.

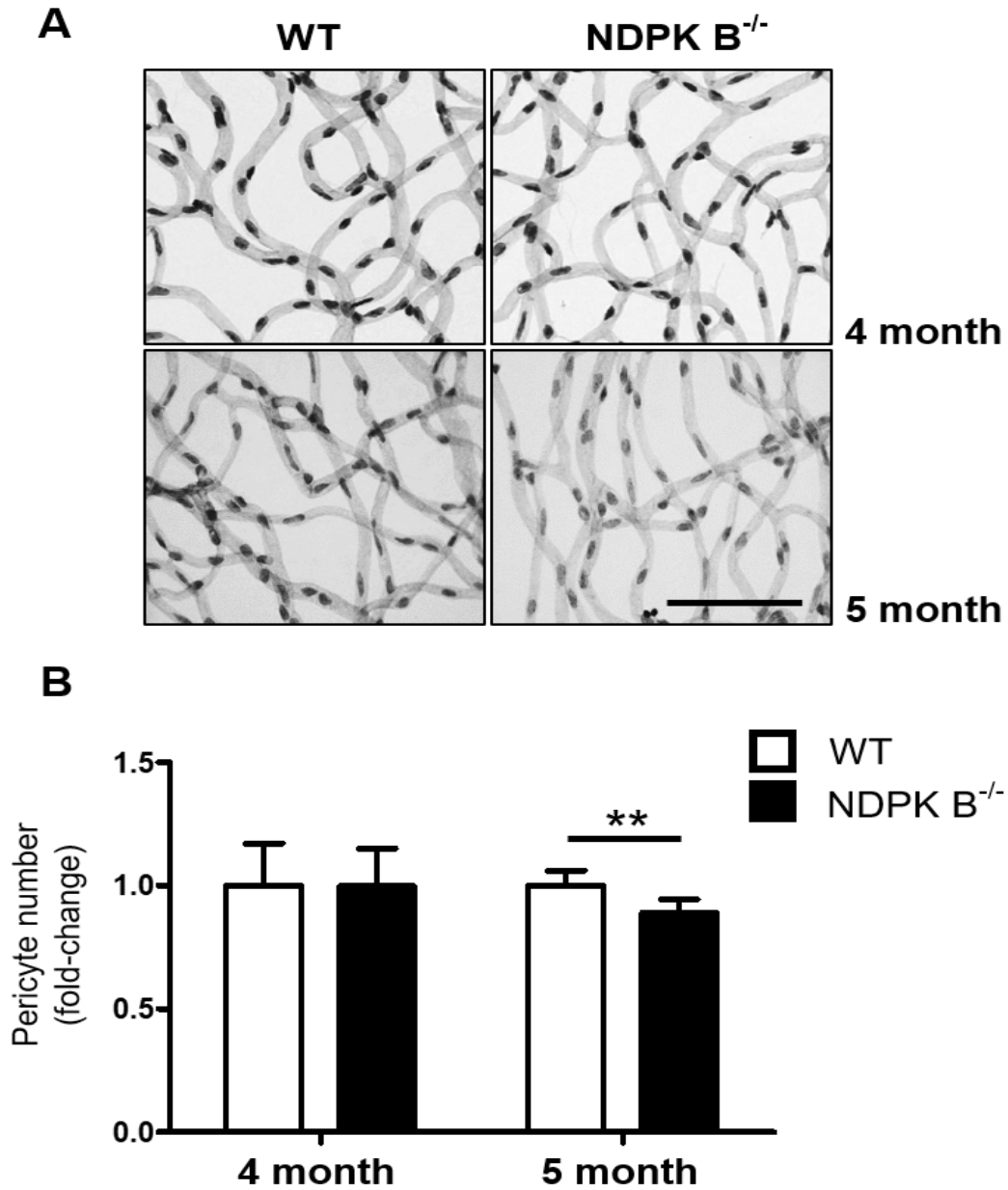


Figure 16: Retinal pericyte loss is observed in 5-month-old NDPK B^{-/-} mice. (A) Retinal digestion was performed in 4- and 5-month-old WT and NDPK B^{-/-} mice. Retinal digestion preparations were stained with PAS stain to show retinal endothelial cells, pericytes, and capillary. (B) Quantification of retinal pericyte coverage in 4- and 5-month-old WT and NDPK B^{-/-} mice. The number of retinal pericytes decreased significantly in 5-month-old NDPK B^{-/-} mice compared to in age-matched control mice. ** $P < 0.01$; $n = 6-8$.

3.1.2 VE-cadherin expression is reduced in the retinas of PKD rats before pericyte loss

We have previously reported that PKD rats develop retinal vasoregression at 2 months, which is driven by retinal photoreceptor degeneration. To determine whether the reduction in the expression of retinal VE-cadherin precedes pericyte loss in PKD rats, we analyzed the expression of retinal VE-cadherin in 1- and 3-month-old rats. Results demonstrated that the expression of retinal VE-cadherin was significantly lower in both 1- and 3-month-old PKD rats than in the age-matched control rats (**Fig. 17A and B**). This indicates that the reduction in the expression of VE-cadherin in retinas occurs earlier than pericytes loss in the retinopathy models associated with neurovascular unit damage and without hyperglycemia.

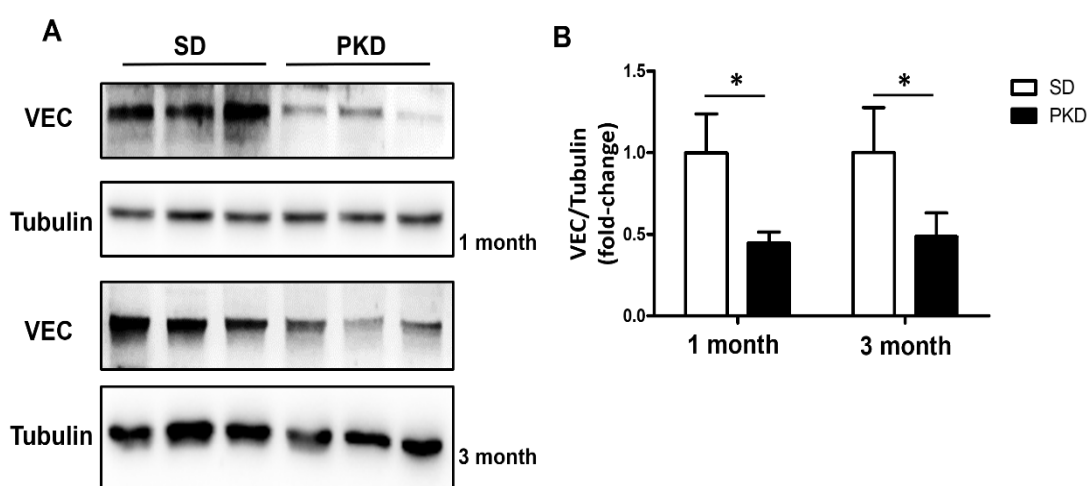


Figure 17: Reduced expression of VE-cadherin in the retinas of PKD rats. (A) The assessment of VE-cadherin expression in retinas of 1- and 3-month-old SD and PKD rats using western blot analysis. (B) Quantification of retinal VE-cadherin expression in SD and PKD rats. Retinal VE-cadherin expression was markedly reduced in both 1- and 3-month-old PKD rats. VEC: VE-cadherin. * $P < 0.05$. $n = 3$.

3.1.3 VE-cadherin expression is reduced in the retinas of *Ins2^{Akita}* mice before pericyte loss

Ins2^{Akita} mice harbor mutation in the insulin gene, which causes hyperglycemia in as early as 4 weeks; hence they are considered proper models of early retinopathy in diabetes and developed pericyte loss in retinas at 8 weeks of age (Barber et al., 2005). To investigate whether reduced expression of retinal VE-

cadherin arises before pericyte loss in $Ins2^{Akita}$ mice, we evaluated retinal VE-cadherin expression in 6-week-old $Ins2^{Akita}$ mice. As expected, in 6-week-old $Ins2^{Akita}$ mouse retinas, we detected a significant reduction in VE-cadherin expression compared to that in the age-matched control mouse retinas (**Fig. 18A and B**). These results indicate that hyperglycemia-induced retinal vasoregression is associated with the reduction of retinal VE-cadherin expression.

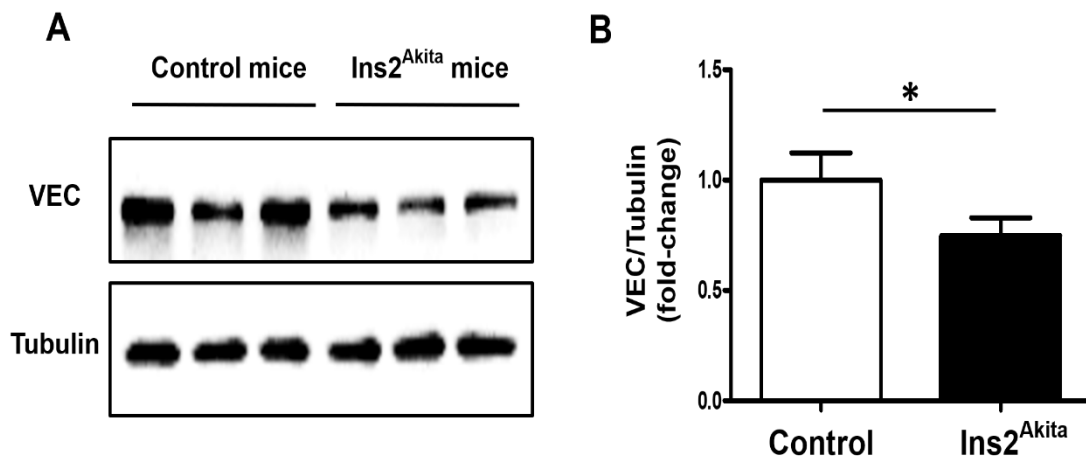


Figure 18: VE-cadherin expression is reduced in the retinas of $Ins2^{Akita}$ mice. (A) VE-cadherin expression was detected in the retinas of 6-week-old $Ins2^{Akita}$ and control mice by Western blot. (B) $Ins2^{Akita}$ mice displayed significantly reduced VE-cadherin expression in retinas. VEC: VE-cadherin. * $p < 0.05$. $n = 3$.

3.1.4 VE-cadherin expression is reduced in deep retinal capillaries of NDPK B^{-/-} mice

Considering the general link between VE-cadherin and pericyte loss and slow development of pericyte loss within three models, we next mainly focused on NDPK B^{-/-} mice. The retinal vascular network includes a superficial layer, an intermediate layer, and a deep capillary layer (Spaide et al., 2015; Stone et al., 1995). To determine which retinal vascular layer is mainly impaired, the morphology of retinal vasculature was assessed using retinal whole-mount staining. Immunofluorescent staining showed no significant change in VE-cadherin expression of retinal arteries and veins; however, a significant decrease in VE-cadherin expression was observed in deep retinal capillaries (**Fig. 19**). These observations indicate that NDPK B deficiency-induced VE-cadherin reduction mainly involves retinal capillaries, which initially develop pericyte loss.

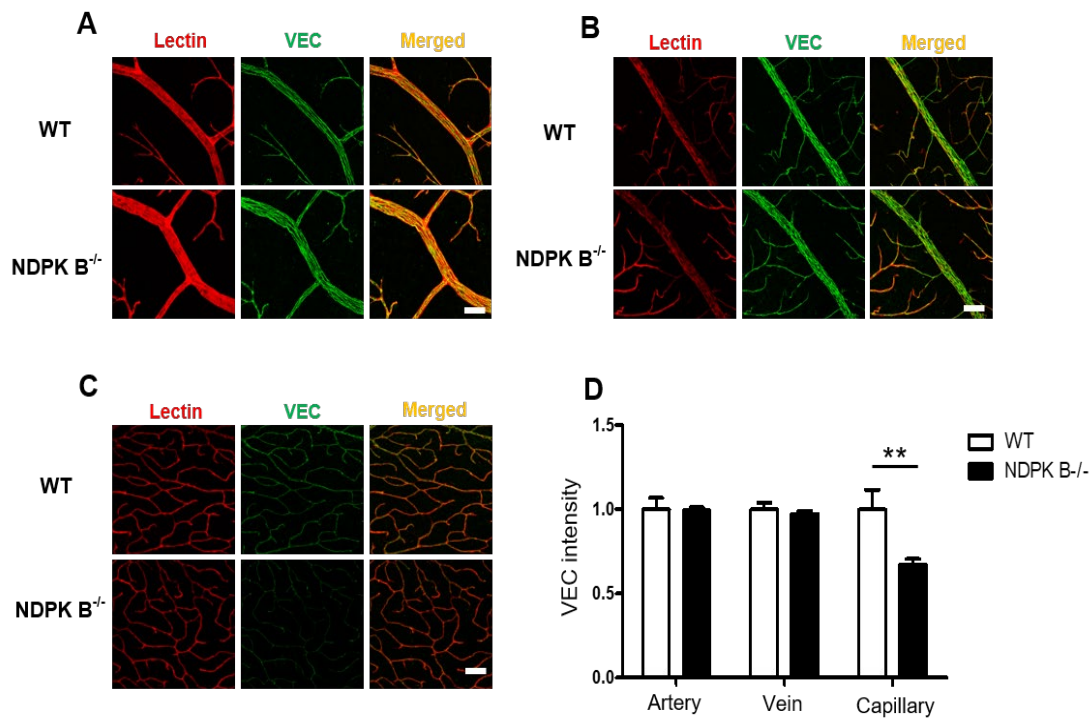


Figure 19: VE-cadherin level is reduced in deep retinal capillaries of NDPK B^{-/-} mice. (A, B, and C) Retinal vasculatures were visualized with lectin (red) and VE-cadherin (green). The images were captured using a confocal microscope. (D) Quantification of VE-cadherin fluorescence intensity in the retinal artery, vein, and capillary was measured using the ImageJ software. ** $P < 0.01$; $n = 3$.

3.1.5 Reduced expression of VE-cadherin in endothelial cells is associated with pericyte loss

As the reduced expression of retinal VE-cadherin preceded pericyte loss in three retinopathy models, we next investigated whether VE-cadherin deficiency in endothelial cells induces pericyte loss *in vitro*. We used siRNA targeting VE-cadherin mRNA to silence VE-cadherin expression in HUVECs. As shown in **Fig. 20A and B**, the knockdown efficiency at the protein level was significant at 24 h and remained so until 96 h, compared to that observed using scrambled siRNA-transfected cells. We further assessed whether VE-cadherin deficiency in endothelial cells destabilizes pericytes in a co-culture system. The quantification of pericytes in medium revealed no significant difference between control and VE-cadherin knock-down groups after co-culture until 10 h. However, we detected a significant elevation in the number of medium pericytes in the VE-cadherin knock-down group post-co-culture for 24 h (**Fig. 21C**). Consistently, the data from immunofluorescent staining demonstrated that the

coverage of pericyte to endothelial cells in the VE-cadherin knock-down group was significantly lower than that in the control group (Fig. 21D and E). These data indicate that VE-cadherin stabilizes the contact between endothelial cells and pericytes.

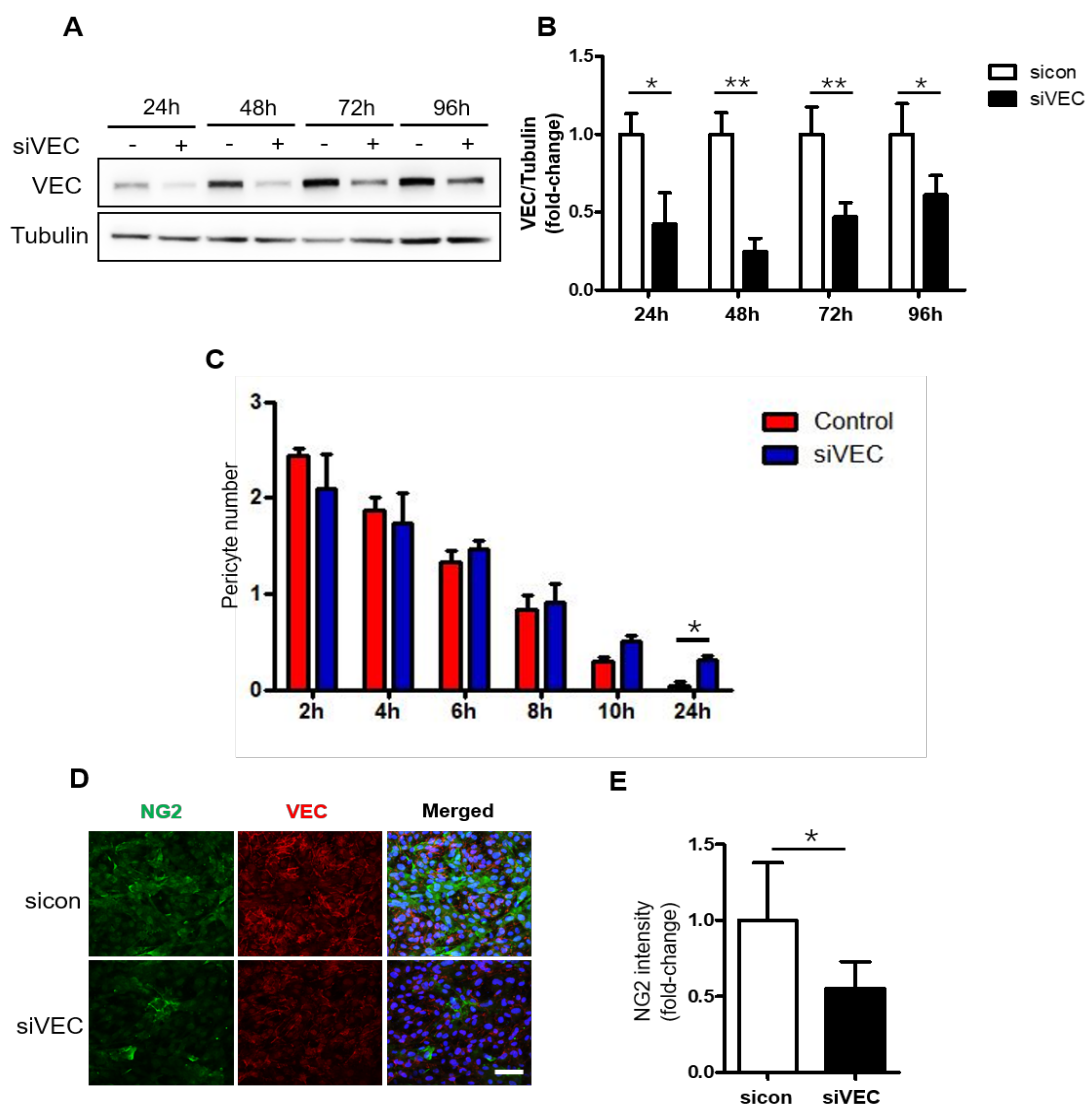


Figure 20: Reduced expression of VE-cadherin in endothelial cells is associated with pericyte loss. (A) HUVECs were transfected with either scrambled siRNA or VE-cadherin siRNA, and the knockdown efficiency of VE-cadherin was detected using western blotting until 96 h. (B) A significant reduction in VE-cadherin expression was detected in HUVECs within 96 h. (C) After knockdown of VE-cadherin in HUVECs for 24 h, human pericytes labeled with Cell-Tracker™ Green were seeded on the top of endothelial cell monolayer in 1:3 ratio (pericytes: HUVECs). The quantification of medium pericytes was measured using a fluorescent microscope by counting cell numbers in five random 10x fields. (D) After co-culture of pericytes and endothelial cells for 24 h, the cells were stained with NG2 (green), VE-cadherin (red), and DRAQ5

(blue). (E) Pericyte coverage was quantified using the ImageJ software. * $P < 0.05$, ** $P < 0.01$, $n = 3$.

3.1.6 NDPK B^{-/-} mice display increased permeability of retinal vasculature

To investigate whether NDPK B deficiency induces hyperpermeability of retinal vessels, we evaluated the endogenous albumin level of the retina after saline perfusion in WT and NDPK B^{-/-} mice (5-month-old). Results of western blotting demonstrated that the endogenous albumin level in the retina of NDPK B^{-/-} mice was significantly higher than that in control mice (**Fig. 21A and B**). This indicates that NDPK B deficiency causes hyperpermeability of retinal vessels.

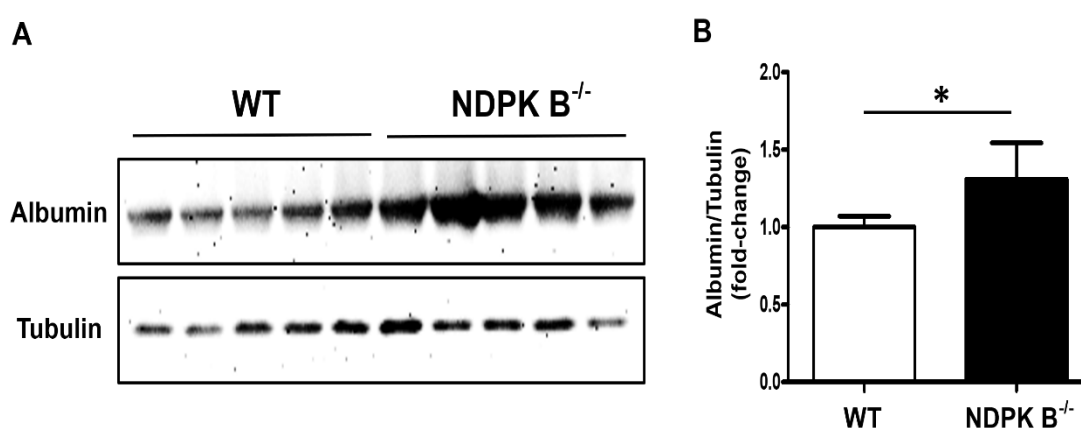


Figure 21: Retinal vascular hyperpermeability in NDPK B^{-/-} mice. (A) Retinal blood was removed via saline perfusion. Retinal albumin levels were used to evaluate retinal vascular leakage via western blotting. (B) NDPK B^{-/-} mice displayed significant increase in retinal vascular permeability. * $P < 0.05$; $n = 5$.

3.1.7 NDPK B loss or HG reduces plasma membrane VE-cadherin levels in endothelial cells

In endothelial cells, NDPK B contributes to barrier integrity. The brains of NDPK B^{-/-} mice showed increased vascular permeability (Gross et al., 2017). Early studies have reported that HG downregulates VE-cadherin (Cao et al., 2014; Rangasamy et al., 2011). To better analyze how NDPK B deficiency or HG induces VE-cadherin degradation, we treated endothelial cells with scrambled siRNA or siNDPK B and then stimulated them with HG for 24 h. The results of western blotting demonstrated that membranous VE-cadherin expression in NDPK B-depleted cells and HG-treated cells was significantly lower than that

in control cells (**Fig. 22A and B**). Immunofluorescent images further showed that in endothelial cells treated with scrambled siRNA, VE-cadherin was distributed in zipper-like pattern, whereas NDPK B-depleted cells and HG-treated cells displayed linear distribution of membranous VE-cadherin (**Fig. 22C**). Quantification demonstrated a significant reduction in membranous VE-cadherin expression in either NDPK B deficient or HG-treated endothelial cells (**Fig. 22D**). However, we did not examine further VE-cadherin reduction in NDPK B-depleted endothelial cells treated with HG.

To exclude HG-induced osmotic effects on endothelial VE-cadherin expression, endothelial cells were exposed to L-glucose as an osmotic control. The results showed lack of any significant difference in VE-cadherin expression between L-glucose-treated cells and non-treated cells. On the contrary, VE-cadherin expression in D-glucose-treated cells was significantly lower than that in the osmotic control (**Fig. 23**).

We further investigated whether NDPK B deficiency or HG treatment alters the expression of junctional molecules in endothelial cells using qPCR. The results demonstrated that the expression of VE-cadherin and other junctional molecules at the mRNA level are unaltered (**Fig. 24**).

p120-catenin stabilizes VE-cadherin and regulates VE-cadherin turnover (Oas et al., 2013). Therefore, we next investigated the expression of β -catenin and p120-catenin in NDPK B-deficient cells and HG-stimulated cells. Results demonstrated that NDPK B deficiency or HG stimulation in HUVECs did not affect the expression of β -catenin and p120-catenin (**Fig. 25**). Thus, these data suggest that NDPK B deficiency induces similar effects as HG on endothelial VE-cadherin, leading to linear arrangement and reduced expression of membranous VE-cadherin.

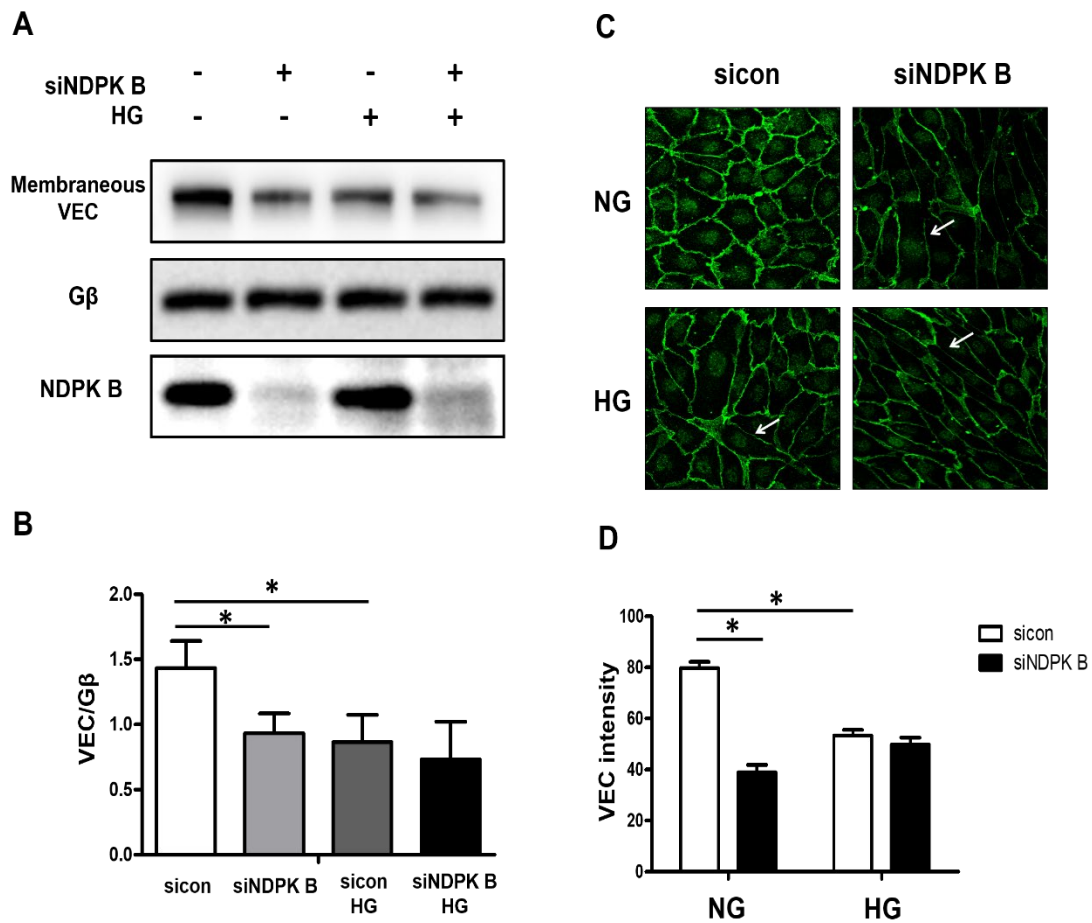
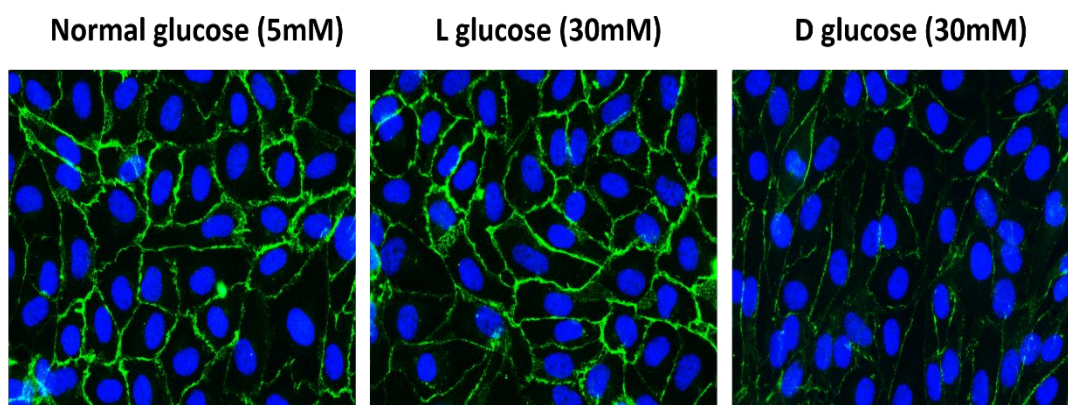
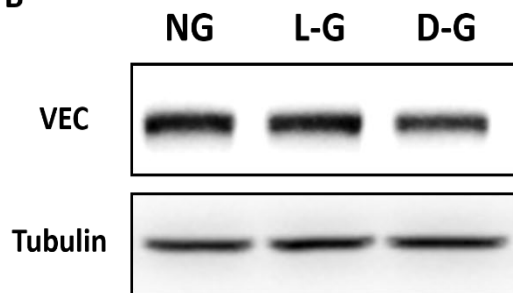


Figure 22: NDPK B loss or HG reduces levels of membranous VE-cadherin. HUVECs were transfected with either NDPK B siRNA or scrambled siRNA and incubated for 4 h. Afterward, the cells were starved in 0.5% FCS culture medium for 24 h. Cells were stimulated with either normal glucose (5.5 mM) or HG (30 mM) for 24 h. (A) Membranous VE-cadherin was extracted. Both NDPK B loss and HG reduced membrane VE-cadherin expression. The NDPK B-depleted HUVECs treated with HG did not exhibit any further decrease in membranous VE-cadherin expression. (B) Membrane VE-cadherin was quantified in these four different groups. (C) HUVECs were stained with VE-cadherin (green) to show cellular VE-cadherin distribution. The linear change in VE-cadherin distribution was observed in treated groups (NDPKB knockdown, HG treatment, and combination). (D) Membrane VE-cadherin expression was quantified from the fluorescent intensity using the ImageJ software. NG: normal glucose; HG: high glucose; sicon: control siRNA; siNDPK B: NDPK B siRNA. * $P < 0.05$; $n = 3$.

A



B



C

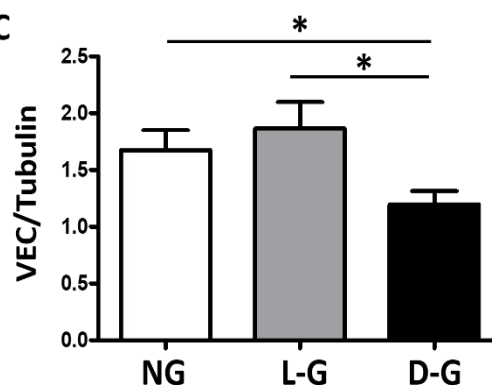


Figure 23: VE-cadherin localization and expression in NG-, L-G- and D-G-treated endothelial cells. (A) VE-cadherin distribution was detected using immunofluorescent staining. Compared to the control, L-glucose-treated cells did not show any differences in VE-cadherin localization and distribution, whereas D-glucose-treated cells displayed decreased expression of VE-cadherin at cell-cell contacts. (B) Evaluation and (C) quantification of VE-cadherin expression was performed using western blotting and statistical analysis, respectively. D-glucose significantly reduced the expression of VE-cadherin, whereas L-glucose did not affect the expression of VE-cadherin in the endothelial cells. NG: normal glucose; L-G: L-glucose; D-G: D-glucose. * $P < 0.05$; $n = 3$.

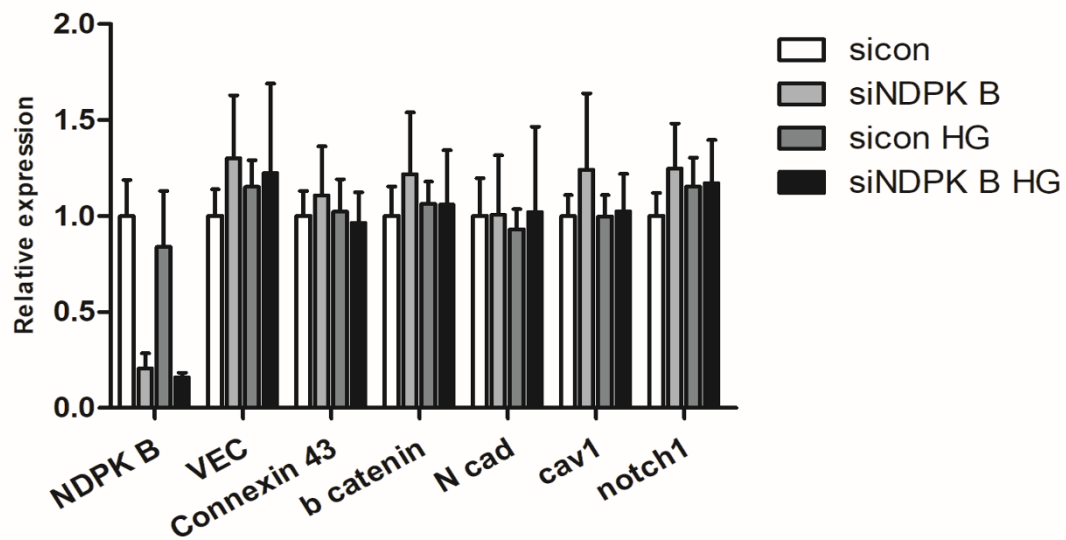


Figure 24: NDPK B depletion or HG does not affect the mRNA expression of junctional molecules in endothelial cells. Quantification of the transcription of adhesion junction molecules using qPCR. NG: normal glucose; HG: high glucose; sicon: control siRNA; siNDPK B: NDPKB siRNA. *n* = 3.

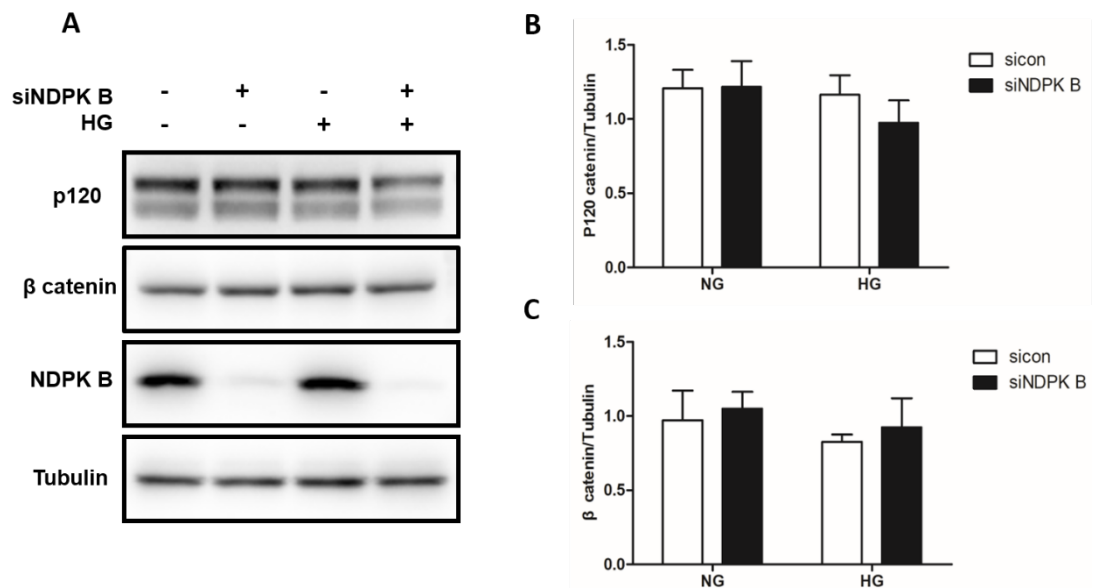


Figure 25: NDPK B deficiency or HG dose not affect the expression of β catenin and p120-catenin in endothelial cells. HUVECs were transfected with scrambled siRNA or NDPK B siRNA for 4 h and were starved in culture medium with 0.5% FCS for another 24 h. Subsequently, cells were treated with or without HG (30 mM) for 24 h. The cell lysate was used for the evaluation of target protein using western blotting.

(A) NDPK B deficiency or HG did not change the expression of β catenin and p120-catenin. (B and C) Quantification of western blotting data from graph A. NG: normal glucose; HG: high glucose. sicon: control siRNA; siNDPK B: NDPK B siRNA. $n = 3$.

3.1.8 NDPK B loss or HG promotes VE-cadherin internalization and VE-cadherin Tyr 685 phosphorylation in endothelial cells

Increased VE-cadherin internalization induced gap formation between endothelial cells (Cao and Schnittler, 2019). Therefore, we further investigated whether either NDPK B deficiency or HG treatment leads to VE-cadherin internalization in endothelial cells. Immunofluorescent images demonstrated that VE-cadherin is predominantly located at cell-cell contact sites without acid washing. After acid washing, membranous VE-cadherin disappeared, and internalized VE-cadherin remained in the cytosol of control cells. VE-cadherin internalization was significantly lower after NDPK B knockdown and HG stimulation for 30 min than in the control cells. VEGF, as a positive control, remarkably induced VE-cadherin internalization after stimulation for 15 min (**Fig. 26**). We did not observe further increased VE-cadherin internalization in NDPK B-depleted endothelial cells treated with HG.

An early study showed that increased Tyr 685 phosphorylation of VE-cadherin is associated with its internalization (Wu et al., 2016). Therefore, we further analyzed whether either NDPK B deficiency or HG treatment in endothelial cells may increase Tyr 685 phosphorylation of VE-cadherin. Immunoblotting showed that VE-cadherin phosphorylation at the Tyr 685 site is significantly enhanced under either NDPK B knockdown or HG condition (**Fig. 27**). The NDPK B-depleted endothelial cells treated with HG did not display further increase in Tyr 685 phosphorylation of VE-cadherin compared to that in the control group. Hence, these results indicate that increased VE-cadherin internalization caused by NDPK B loss or HG stimulation is mediated via increased Tyr 685 phosphorylation of VE-cadherin.

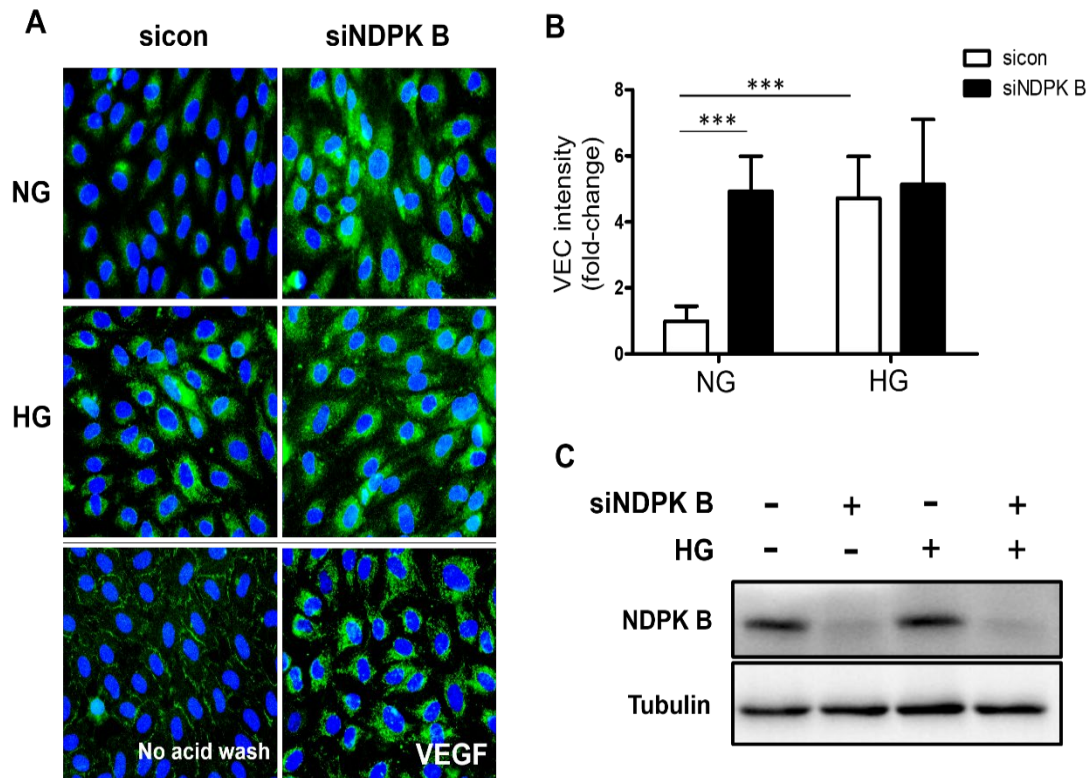


Figure 26: NDPK B deficiency or HG promotes VE-cadherin internalization in endothelial cells. After transfection with either scrambled siRNA or NDPK B siRNA for 4 h in HUVECs, cells were further starved in 0.5% FCS culture medium for another 24 h. Cells were stained with an antibody against VE-cadherin extracellular domain (BV6) on ice for 1 h and were then stimulated with either normal glucose (5 mM) or HG (30 mM) for 30 min. (A) Both NDPK B deficiency and HG treatment promoted VE-cadherin internalization, similar to the effects induced by VEGF treatment as a positive control. Acid washing was used to remove the remaining membrane-bound VE-cadherin. All the membrane-bound VE-cadherin persisted in the absence of acid washing. (B) Quantification of internalized VE-cadherin from the fluorescent intensity of internalized VE-cadherin using ImageJ. (C) NDPK B knockdown efficiency was detected using western blotting. NG: normal glucose; HG: high glucose; siCON: control siRNA; siNDPK B: NDPK B siRNA. *** $P < 0.001$; $n = 3$.

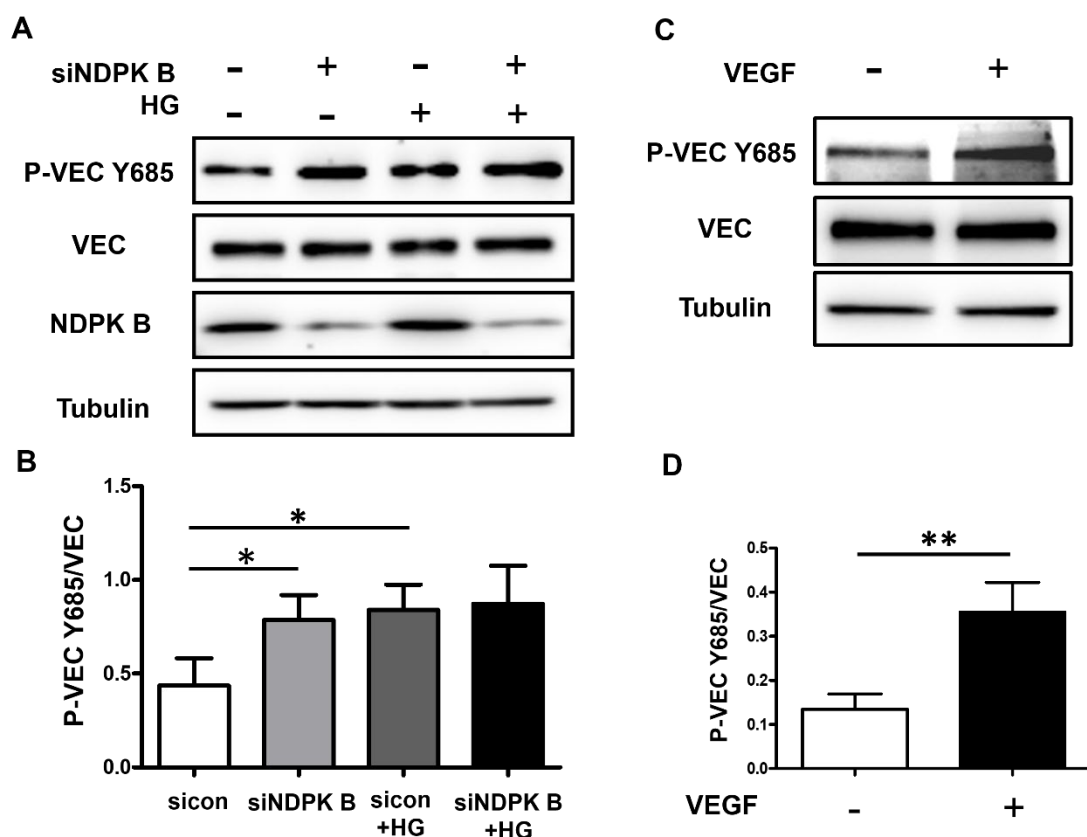


Figure 27: NDPK B deficiency or HG increases VE-cadherin Tyr 685 phosphorylation in endothelial cells. HUVECs were transfected with scrambled siRNA or NDPK B siRNA for 4 h. After starvation in culture medium with 0.5% FCS for 24 h, the cells were treated with or without HG (30 mM) for 30 min. (A) Increased VE-cadherin Tyr 685 phosphorylation was observed under NDPK B deficiency and in HG-treated groups. (B) The graph shows the quantification of western blotting data. (C) VEGF stimulation for 15 min increased VE-cadherin Tyr 685 phosphorylation compared to that in the non-VEGF treatment group. (D) Quantification of western blotting data from graph C. NG: normal glucose; HG: high glucose; sicon: control siRNA; siNDPK B: NDPK B siRNA. * $P < 0.05$, ** $P < 0.01$; $n = 3$.

3.1.9 NDPK B loss or HG induces lysosome-mediated VE-cadherin degradation in endothelial cells

Internalized VE-cadherin was captured by lysosomes for degradation (Chichger et al., 2016). Therefore, we investigated whether NDPK B deficiency or HG treatment promoted lysosome-mediated degradation. Endothelial cells were stained with extracellular VE-cadherin, EEA1 (a marker for early endosome), and LAMP1 (a marker for lysosome). We analyzed the colocalization of

internalized VE-cadherin with EEA1 and LAMP1 under the NDPK B deficiency and HG conditions. Immunofluorescent images demonstrated that internalized VE-cadherin triggered by the loss of NDPK B or HG was first captured by early endosomes in the cytosol, and they further were transported to lysosome with continuous loss of NDPK B or HG treatment (**Fig. 28**). These results suggest that the loss of NDPK B or HG treatment in endothelial cells induces lysosome-mediated degradation.

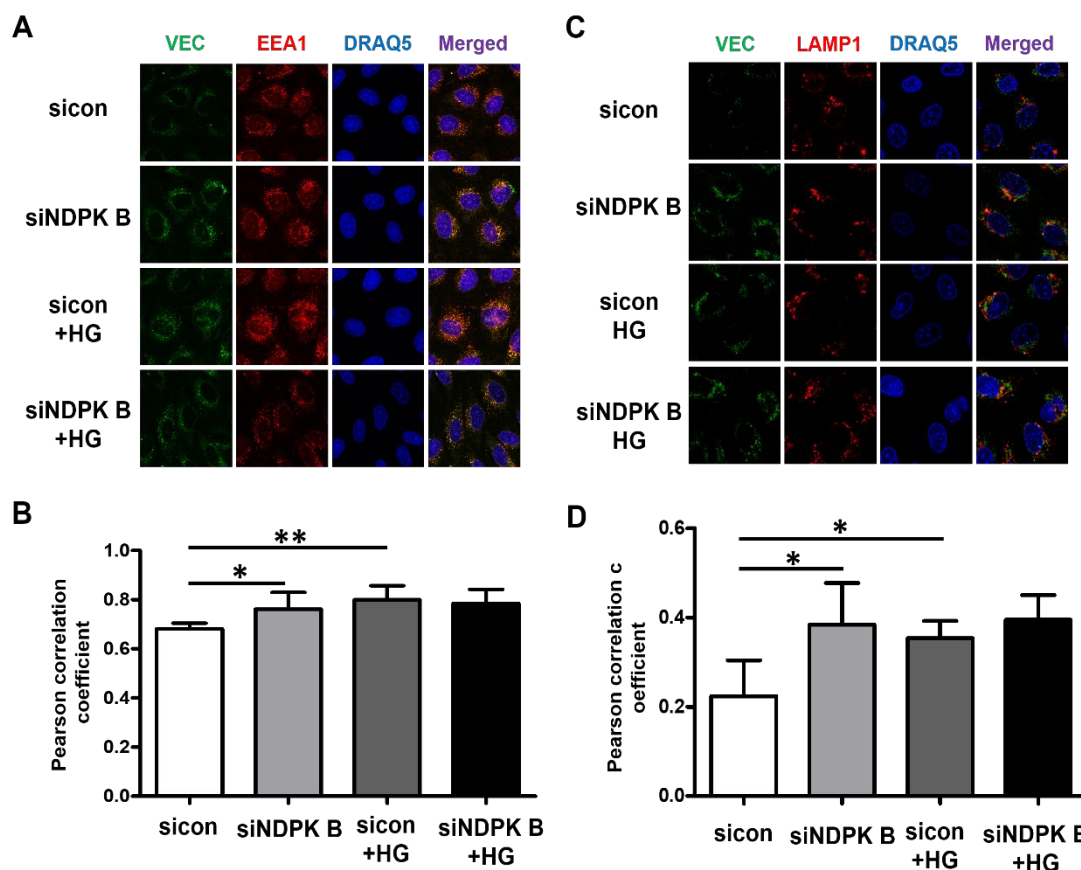


Figure 28: NDPK B deficiency or HG promotes lysosomal-mediated VE-cadherin degradation in endothelial cells. HUVECs were transfected with either scrambled siRNA or NDPK B siRNA for 4 h and were starved in 0.5% FCS culture medium for 24 h. Then, the cells were incubated with an antibody against the extracellular domain of VE-cadherin on ice for 1 h. For evaluation of colocalization of internalized VE-cadherin and EEA1, cells received either NG or HG treatment for 30 min. For evaluation of colocalization of internalized VE-cadherin and LAMP1, cells received either NG or HG treatment for 24 h. (A) Either NDPK B deficiency for 48 h or HG treatment for 30 min promoted colocalization of internalized VE-cadherin (green) combined with endosome marker (EEA1, red). (B) Either NDPK B deficiency for 72 h or HG treatment for 24 h promoted colocalization of internalized VE-cadherin (green) combined with lysosome marker (LAMP1, red). (C and D) Quantification of the colocalization of internalized VE-cadherin, EEA1, and LAMP1 using Pearson correlation coefficient analysis. NG: normal glucose; HG: high glucose; sicon: control siRNA; siNDPK B: NDPK B siRNA. * $P < 0.05$, ** $P < 0.01$; $n = 3$.

3.1.10 NDPK B deficiency or HG induces phosphorylation of VE-cadherin at Tyr 685 via Src kinase activation

Src tyrosine kinase plays a key role in many cellular events, including cell proliferation, adhesion, migration, and differentiation (Krymskaya et al., 2005). Early reports revealed that VE-cadherin phosphorylation relies on Src kinase activation (Alcaide et al., 2012). To address these issues, we investigated whether NDPK B loss or HG induces increase in VE-cadherin phosphorylation via Src kinase. Compared to that in the control, we detected a significant increase in endothelial VE-cadherin tyrosine 685 phosphorylation and Src tyrosine 416 phosphorylation under either NDPK B knockdown or HG treatment condition. Furthermore, these increased effects on VE-cadherin and Src phosphorylation induced by NDPK B loss or HG stress in endothelial cells were partially inhibited by stimulation with pp2 (Fig. 29). These results suggest that increased VE-cadherin phosphorylation caused by NDPK B deficiency or HG treatment is mediated by the Src kinase.

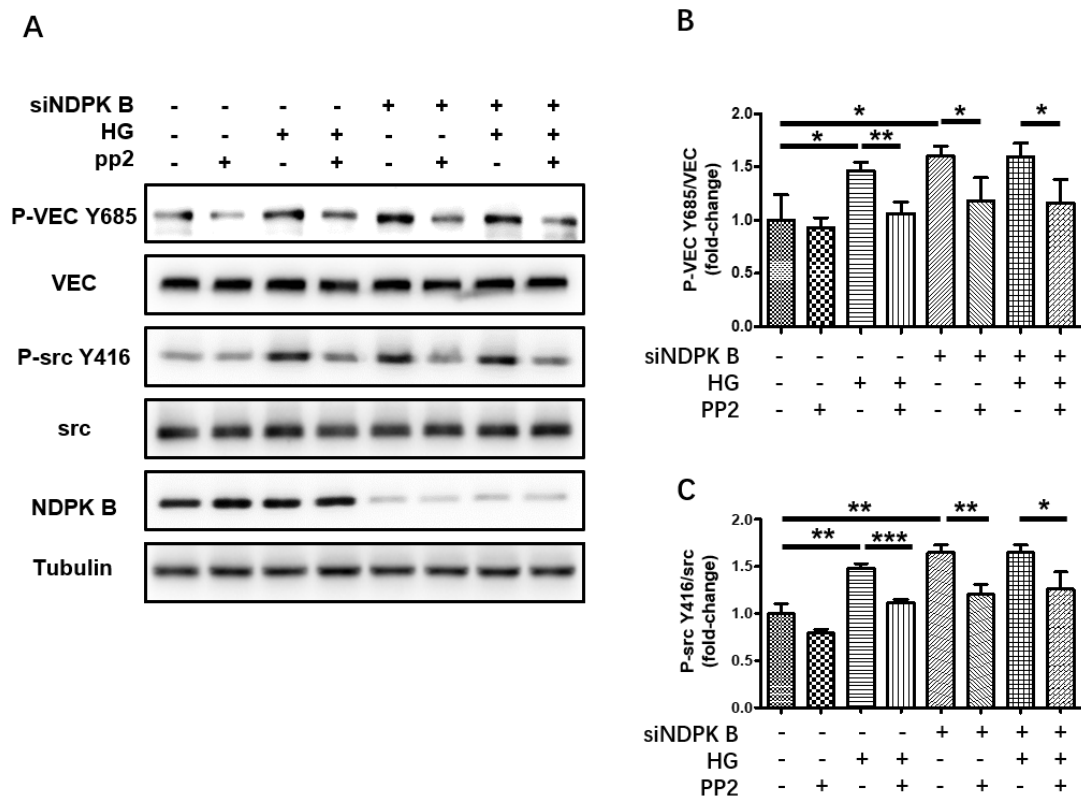


Figure 29: NDPK B deficiency or HG induces phosphorylation of VE-cadherin at Tyr 685 via Src kinase activation. HUVECs were transfected with either non-targeting siRNA or NDPK B siRNA for 4 h and were then cultured in a 0.5% FCS culture

for 24 h. Afterward, cells were pre-treated with either DMSO or pp2 inhibitor (10 μ M) for 1 h. Then, the cells were treated with either NG or HG for a further 30 min. (A) Representative immunoblots of VE-cadherin Tyr 685 phosphorylation, VE-cadherin, Src Tyr 416 phosphorylation, Src, NDPK B, and tubulin. (B and C) Quantification of p-VEC Y685 to total VEC and p-Src Y416 to total Src. NDPK B deficiency or HG treatment increased the VE-cadherin Tyr 685 phosphorylation and Src Tyr 416 phosphorylation. These effects were reversed by treatment with Src inhibitor (PP2). NG: normal glucose; HG: high glucose; sicon: control siRNA; siNDPK B: NDPK B siRNA. * $P < 0.05$, ** $P < 0.01$, *** $P < 0.001$; $n = 4$.

3.2 Intravitreal injection of MSCs as a therapeutic intervention in vasoregressive retina

3.2.1 Characterization of MSCs

Prior to intravitreal injection of MSCs derived from rat bone marrow, we analyzed the cell surface markers of MSCs using FACs. Results indicated that MSCs were positive for CD44 (99.8%) and CD90 (99.7%), but were negative for CD45 (2%), which is considered as the marker for leukocytes and hematopoietic stem cells (**Fig. 30**).

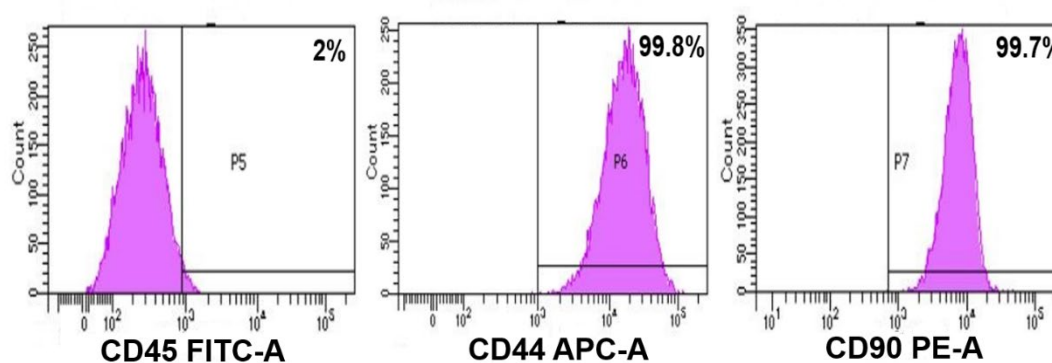


Figure 30: Characterization of rat BMSCs. BMSCs highly express CD90 (p7) and CD44 (p6) as typical MSC markers, but not CD45 (p5), a hematopoietic stem cell marker. Permission obtained from copyright © 2019 John Wiley and Sons (Huang et al., 2019b).

3.2.2 Intravitreally injected MSCs are unable to migrate into the retina of the rat eye

To determine whether MSCs may migrate into the retina, we initially injected human ASCs labeled with fluorescent dye using Cell-Tracker™ Green into the

vitreous cavity of PKD rat *ex vivo*. Three days after injection, we observed that most labeled cells remained in the vitreous cavity (**Fig. 31A**). We further injected labeled rat BMSCs into the rat vitreous cavity *in vivo*. Seven days after the injection, retinal whole-mount staining showed that only a few labeled cells were dispersed on the superficial layer of retinal capillary and that these labeled cells were unable to reach the deep layer of the retinal capillary (**Fig. 31B**). To further verify inability of MSCs to migrate into the retina, we analyzed the location of labeled cells in the retina after intravitreal injection using retinal cryosections. The images showed that labeled cells were limited to the retinal ganglion cell layer (GCL) and were blocked by the retinal inner limiting membrane (ILM). No labeled cells were seen in the inner retina (**Fig. 31C**). These data suggest that intravitreally injected MSCs are incapable of migrating into the retina.

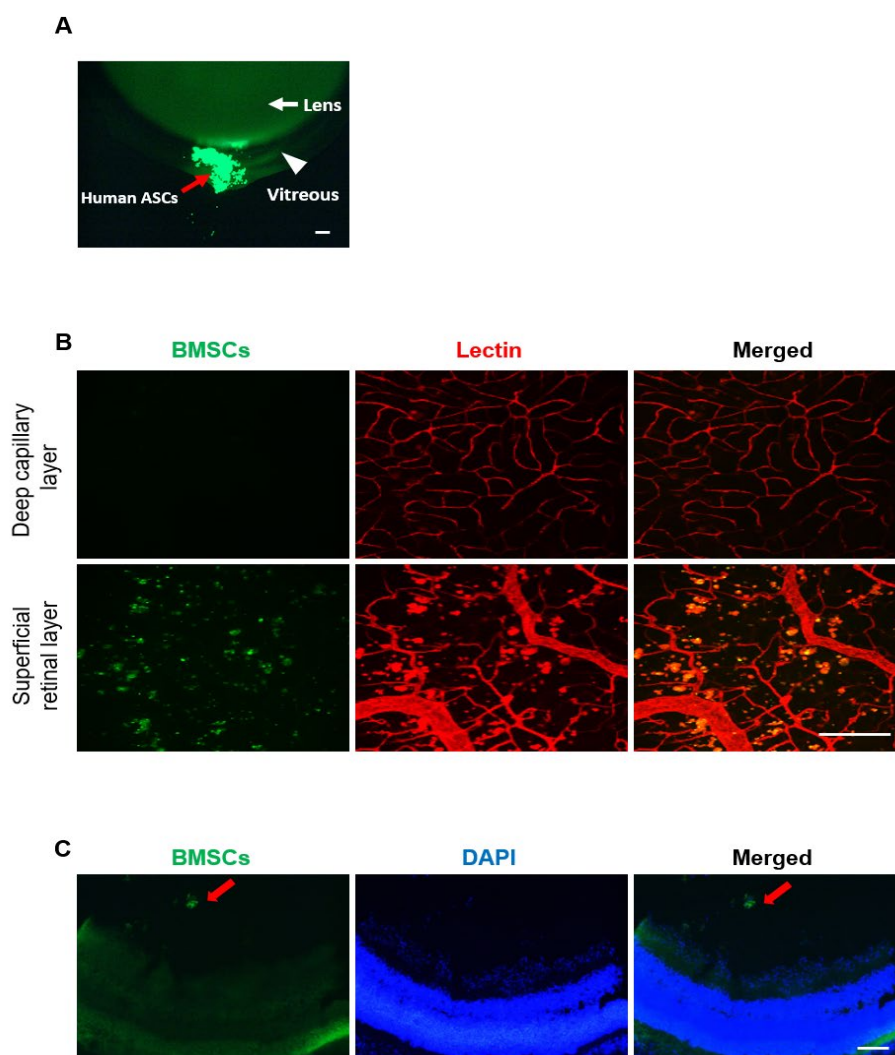


Figure 31: Intravitreally administrated MSCs can not migrate into the retina *ex vivo*

vivo and in vivo. The eyes of PKD rats were intravitreally injected with either human ASCs or rat BMSCs labeled with Cell-tracker Green (2×10^4 in $2 \mu\text{L}$ PBS) *ex vivo* and *in vivo*. A) Three days after injection, most of the labeled human ASCs remained in the vitreous cavity *ex vivo*. The white arrow indicates the lens. The red arrow indicates human ASCs. White arrowhead indicates the vitreous cavity. The labeled cells (green) indicate human ASCs. B) Seven days after injection *in vivo*, visualization of retinal whole-mount staining using confocal microscopy demonstrated that a few labeled BMSCs (green) were confined on the superficial retinal layer in the whole mount staining and did not migrate into the deep retinal capillary layer. C) Cryosection staining demonstrated that labeled BMSCs (red arrow) cannot migrate into inner retinas 7 days after intravitreal injection *in vivo*. Lectin: retinal vessel staining; DAPI: nuclear staining. Scale = $50 \mu\text{m}$. Permission obtained from copyright © 2019 John Wiley and Sons (Huang et al., 2019b).

3.2.3 Intravitreally injected BMSCs induce cataract and retinal vasoregression in SD rats

To evaluate the effect of intravitreally injected MSCs on rat retina, we administrated BMSCs isolated from healthy SD rats (8-week-old) into the vitreous space of 1-month-old SD rats. The eyes were evaluated after a four-week injection. As shown in **Fig. 32A**, the lenses of SD rats injected with BMSCs, either isolated immediately after enucleation of the eyes or during retinal digestion, demonstrated opacity (100%) comparable to that of the control. We further evaluated the retinal vascular outcomes upon intravitreally administering BMSCs using retinal digest preparations. Surprisingly, intravitreal injection of BMSCs led to a 21% reduction in pericyte coverage in the retinal capillaries (1661 ± 52 in the BMSC-injected right eye vs. 2096 ± 29 cells per mm^2 of the capillary area in control left eye, $P < 0.01$, **Fig. 32B and C**). Furthermore, the formation of acellular capillary was significantly increased after BMSC injection in retinas of SD rats by 205% (63.6 ± 2.9 in the BMSC-injected eye vs. 18.8 ± 1.59 per retinal area in the control eyes, $P < 0.001$, **Fig. 32B and D**). These results suggest that intravitreal injection of BMSCs induces lens opacity and retinal vasoregression in healthy rat eyes.

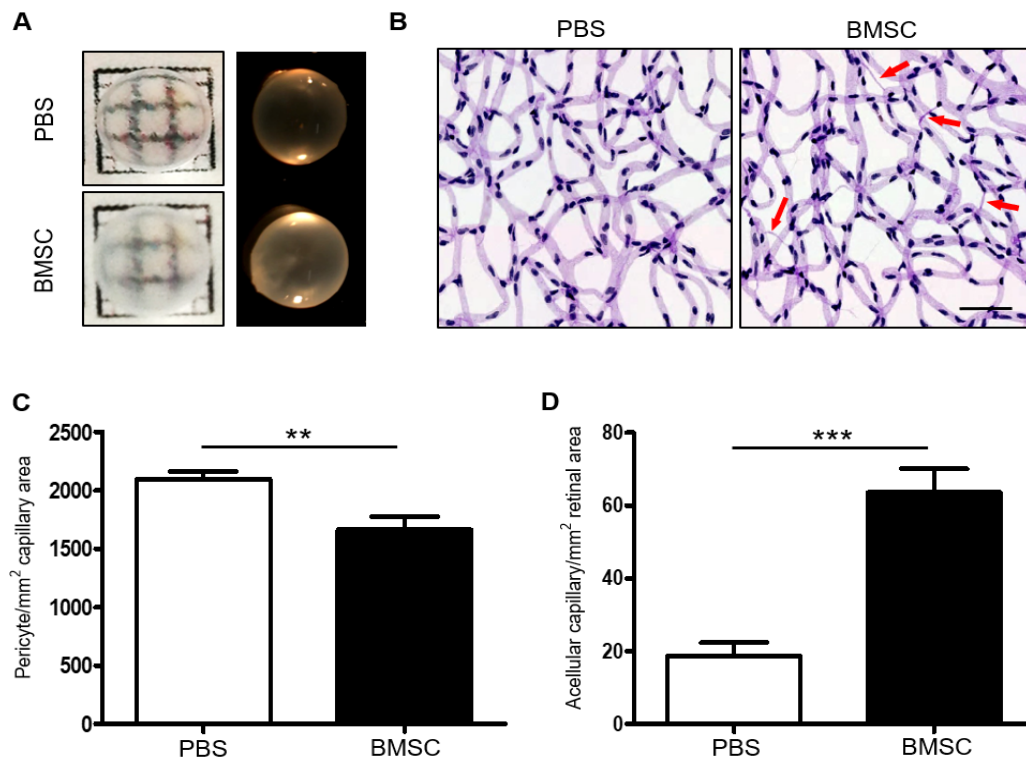


Figure 32: Intravitreally injected BMSCs lead to cataract formation and retinal vasoregression in SD rats. The eyes of SD rats were injected with PBS (left eye; 2 μ L) or BMSCs (right eye; 2×10^4 in 2 μ L PBS) at P30. A) Four weeks post-injection, the lenses were isolated from the eyes and were immediately placed on the grid for evaluation of lens transparency, as shown in the left image. The right image displays the lens isolated from eyes after 4% formalin fixation for 48 h during retinal digestion. BMSC injection-induced cataract/lens opacity compared to PBS injection. B, C, D) Retinal digestion stained with PAS showed that BMSC injection significantly decreased the number of pericytes (C) and increased acellular capillary formation (D) compared to that in the controls. Red arrows indicate acellular capillaries. ** $P < 0.01$, *** $P < 0.001$. Scale bar = 100 μ m. $n = 5$. Permission obtained from copyright © 2019 John Wiley and Sons (Huang et al., 2019b).

3.2.4 Intravitreally injected BMSCs aggravate retinal vasoregression in PKD rats

We further assessed the effects of intravitreally injected BMSCs on PKD rat retinas with obvious vasoregression. Our early data already demonstrated that retinal vasoregression progressed in PKD rats at 2 months, mimicking the retinal vascular pathology that constantly occurs in DR. As mentioned before, we intravitreally administrated BMSCs into the vitreous space of 1-month-old PKD rats and evaluated the effects of retinal vasculature after a 4-week

injection. Interestingly, we observed that BMSC-injected PKD eyes have opaque lens (3 out of 5) (**Fig. 33A**). The data from retinal digestion showed 23% decrease in pericyte coverage (BMSC-injected vs. control: 1321 ± 93 and 1742 ± 47 per mm^2 of capillary area; $P < 0.05$, **Fig. 33B and C**), and 72% increase in acellular capillaries (BMSCs-injected vs. control: 122 ± 11 vs. 71 ± 3.7 per retinal area; $P < 0.01$, **Fig. 33B and D**). We further intravitreally injected non-starved BMSCs into PKD rats, showing that BMSCs induced 21% reduction in pericyte coverage (BMSCs-injected vs. control: 1608 ± 87 and 2040 ± 92 per mm^2 of capillary area; $P < 0.001$, **Fig. 34A and B**) and 56% increase in acellular capillaries (BMSC-injected vs. control: 103 ± 10 vs. 65 ± 7 per retinal area; $P < 0.001$, **Fig. 34A and C**). Therefore, these results suggest that intravitreal administration of BMSCs aggravates retinal vasoregression in PKD rats.

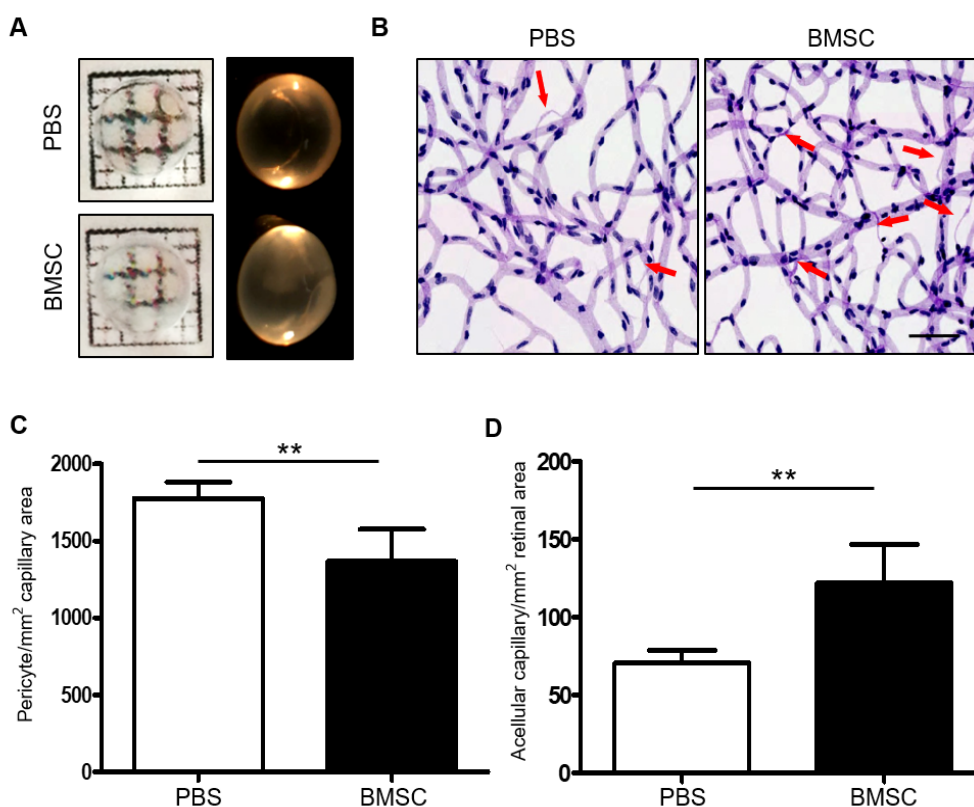


Figure 33: Intravitreally injected BMSCs induce cataract formation and aggravate retinal vasoregression in PKD rats. PBS (left eye; 2 μL) or BMSCs (right eye; 2×10^4 in 2 μL PBS) were injected into the vitreous cavity of PKD rats at P30. A) The lens transparency was analyzed 4 weeks post-injection using the grid, as shown in the left image. The right image displays the lens isolated from the eyes after 4% formalin fixation for 48 h during retinal digestion. Lens opacity was observed peripherally in the BMSC-injected eyes. B-D) PAS staining (B) shows that pericyte loss (C) and formation

of acellular capillaries (D) was further increased after BMSC injection compared to that observed after PBS injection. A red arrow indicates acellular capillaries. ** $P < 0.01$. Scale bar = 100 μm . $n = 5$. Permission obtained from copyright © 2019 John Wiley and Sons (Huang et al., 2019b)

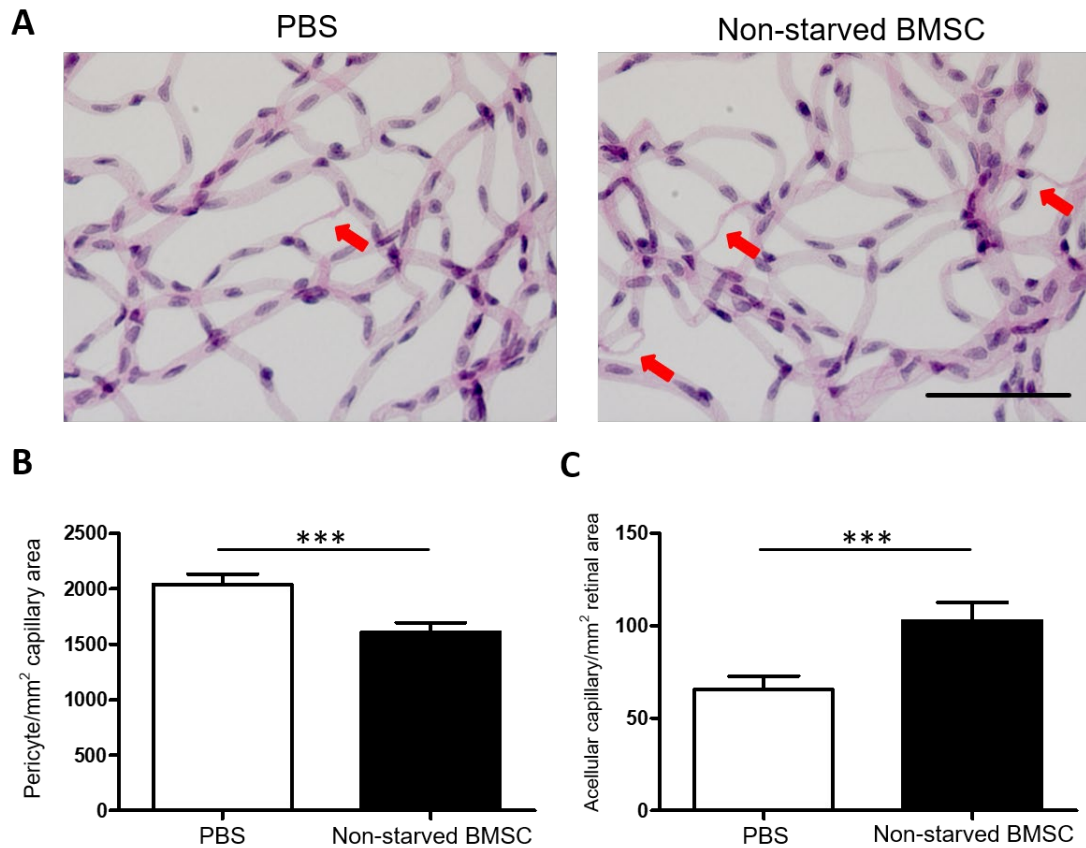


Figure 34: Intravitreal injection of non-starved BMSCs aggravates retinal vasoregression in PKD rats. PBS (left eye; 2 μL) or BMSCs (right eye; 2×10^4 in 2 μL PBS) were injected into the vitreous cavity of PKD rats at P30. A) Retinal digestion stained with PAS showed that BMSC injection significantly decreased the number of pericytes (B) and increased acellular capillary formation (C) compared that in the controls. Red arrows indicate acellular capillaries. *** $P < 0.001$. Scale bar = 50 μm . $n = 5$

3.2.5 Intravitreally injected human ASCs lead to retinal vasoregression in SD rats and aggravate retinal vasoregression in PKD rats

To investigate the effects of intravitreally injected human ASCs on retinal vasculature in SD and PKD rats, human ASCs were administrated into the vitreous cavity of 1-month-old SD rat eyes. As shown in **Fig. 35A**, the lenses (4/6) of SD rats treated with human ASCs displayed opacity, whereas the lens

in the control group remained normal. Compared to that of BMSCs, administration of human ASCs adversely affected the retina, as the lenses/vitreous usually adhered firmly to the retinas and intravitreal bleeding was not noticed frequently. Dot blot analysis demonstrated a significant increase in IL-1 β expression in the vitreous humor in SD rats (**Fig. 35B**). Compared to that in the controls, remarkable elevation (292%) in acellular capillaries and 14% loss in pericytes was observed when rats were treated with intravitreal human ASC injection (**Fig. 35C-E**). Double intravitreal injection of human ASCs at postnatal 15 days (P15) and postnatal 30 days (P30) into SD rats induced severe lens opacity, strong adherence of the lens to the retina, and retinal vascular damage (**Fig. 36**). Furthermore, we demonstrated that single intravitreal injection of human ASCs at P30 led to 50% incidence of lens opacity and increased the expression of IL-1 β in the vitreous humor of PKD rats. In terms of analysis retinal vasculature, intravitreal injection of human ASCs in the PKD rats worsened retinal vasoregression, showing an increase in pericyte loss by 16%, and formation of acellular capillaries by 103% (**Fig. 37**). These results suggest that intravitreally administrated human ASCs lead to retinal vasoregression in SD rats, aggravate retinal vascular damage in PKD rats, and upregulate vitreous IL-1 β .

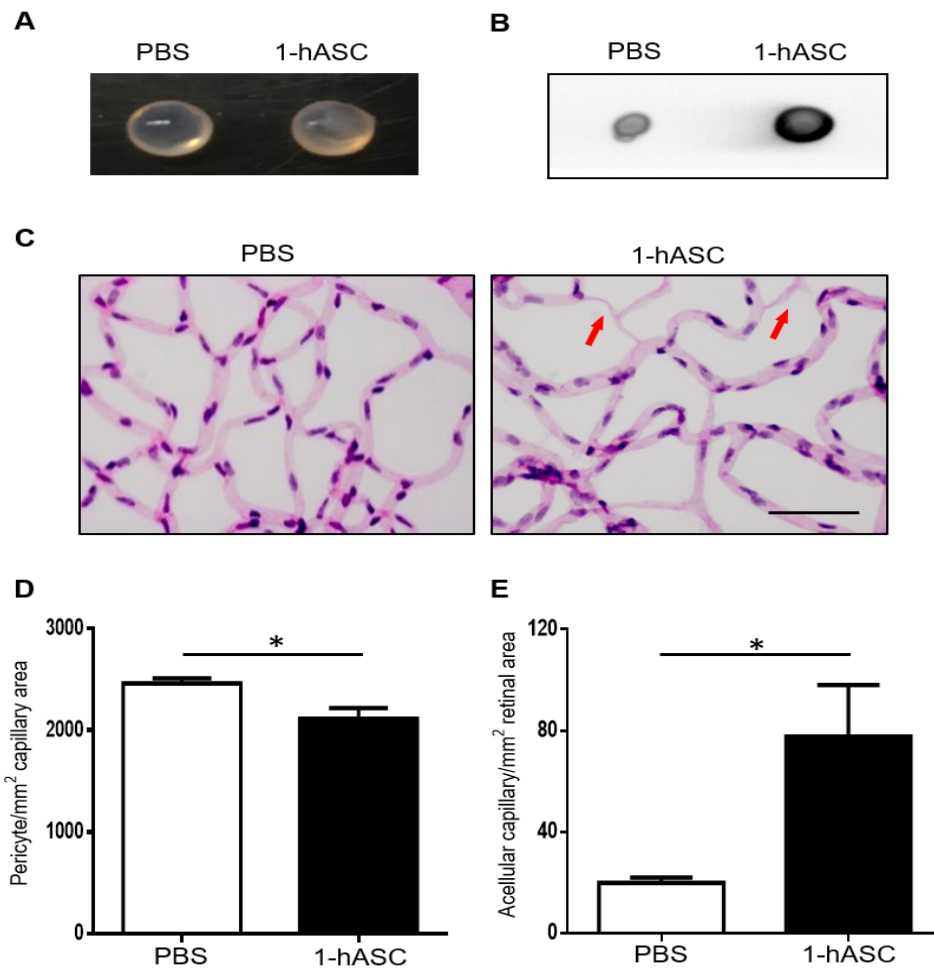


Figure 35: Intravitreally injected human ASCs lead to cataract formation and retinal vasoregression and increase IL-1 β expression in vitreous humor in SD rats. SD rats were intravitreally injected with PBS (left eye; 2 μ L) or ASCs (right eye; 2 \times 10⁴ in 2 μ L PBS) at P30. The lens morphology was analyzed 4 weeks post-injection. A) ASC injection-induced lens opacity compared to that observed after PBS injection. B) Compared to PBS injection, ASC injection increased IL-1 β expression in the vitreous humor. C-E) Retinal digestion stained with PAS (C) showed that ASC injection significantly decreased the number of pericytes (D) and increased acellular capillary formation (E) compared to that in the controls. Red arrow indicated acellular capillaries. * $P < 0.05$. 1-hASC: single intravitreal injection of human ASCs. Scale bar = 50 μ m. $n = 6$. Permission obtained from copyright © 2019 John Wiley and Sons (Huang et al., 2019b).

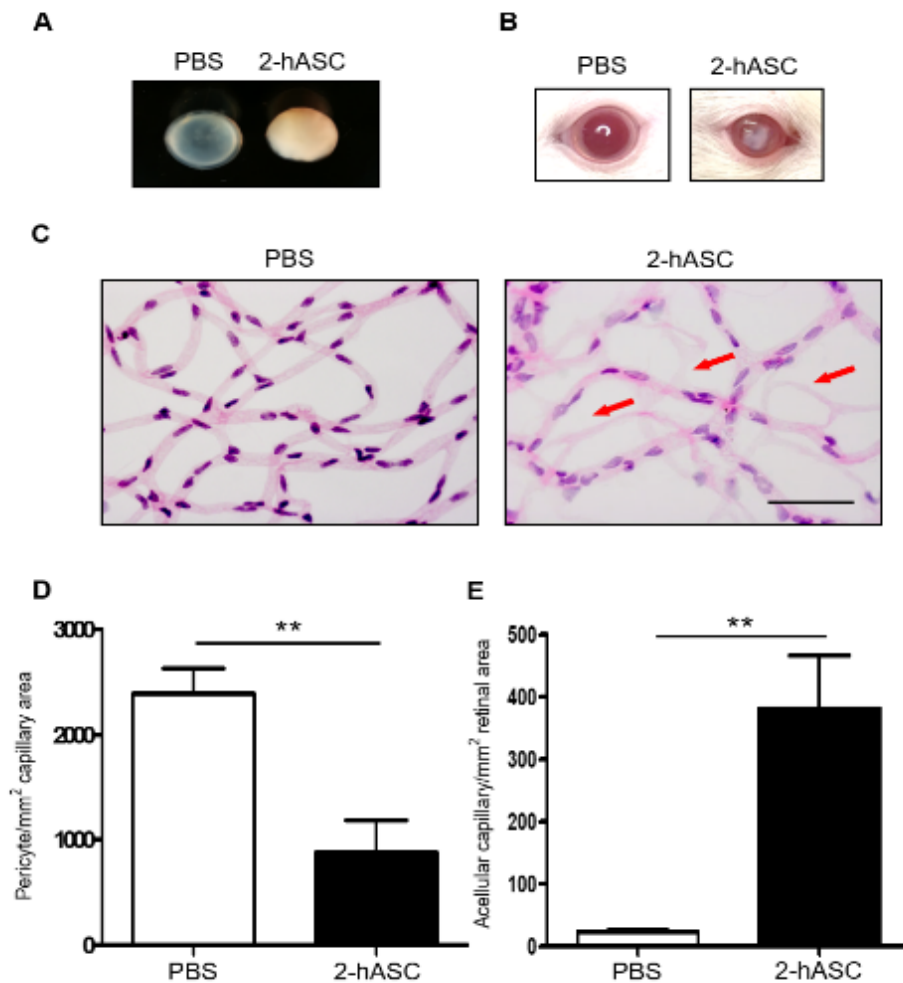


Figure 36: Double intravitreal injection of human ASCs induces severe lens opacity and retinal vasoregression in SD rats. SD rats were intravitreally injected with PBS (left eye; 2 μ L) or human ASCs (right eye; 2×10^4 in 2 μ L PBS) twice, once at P15 and again at P30. Four weeks after injection, lens morphology and pericyte coverage, as well as acellular capillary formation, were assessed. A, B) Compared to that in the controls, double ASC injection led to severe lens opacity. C-E) Double ASC injection significantly increased pericyte loss (D) and acellular capillary formation (E). Red arrow indicated acellular capillaries. ** $P < 0.01$. 2-hASC: double intravitreal injection of human ASCs. Scale = 50 μ m. $n = 5-6$. Permission obtained from copyright © 2019 John Wiley and Sons (Huang et al., 2019b).

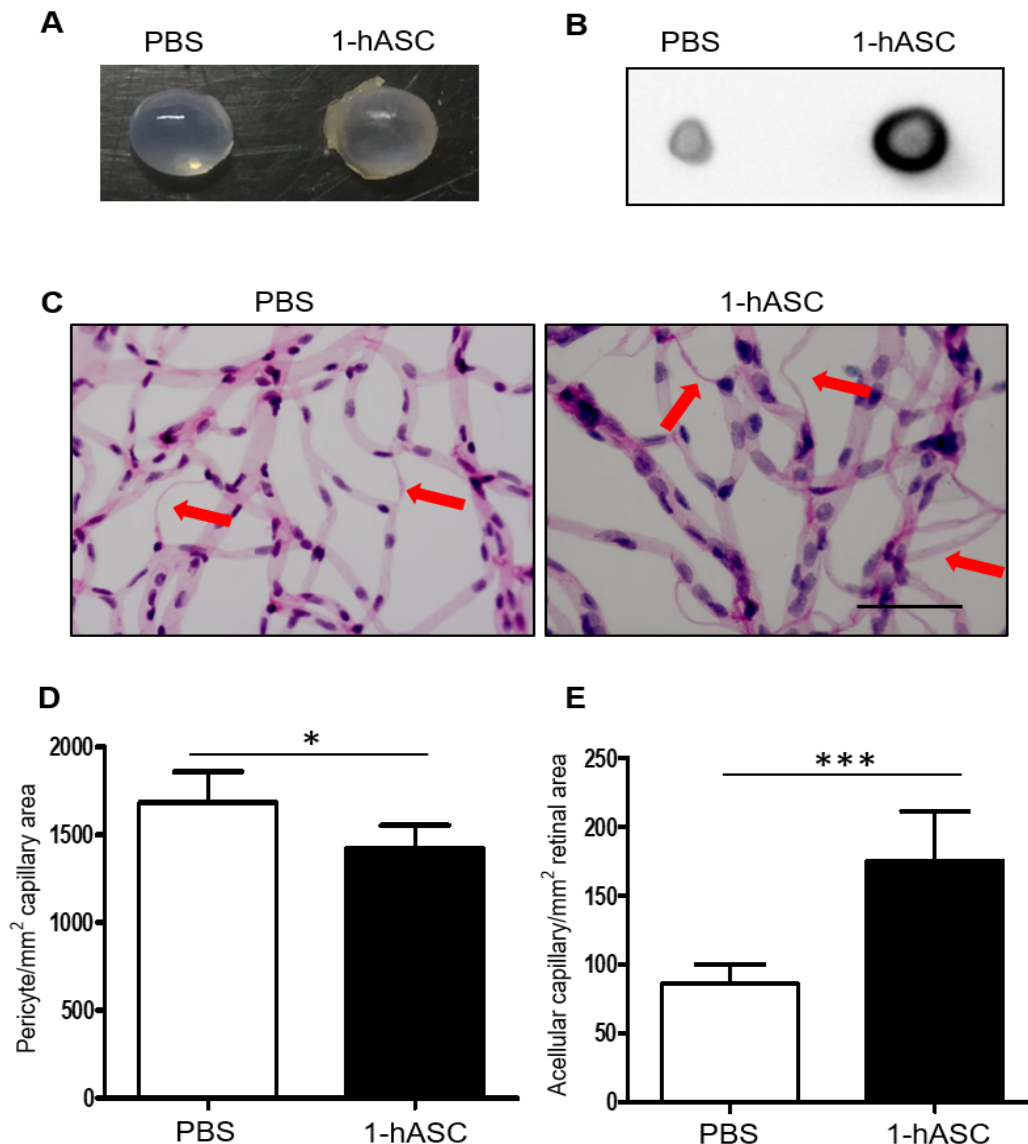


Figure 37: Intravitreally injected human ASCs lead to cataract formation and retinal vasoregression and increase IL-1 β expression in vitreous humor in PKD rats. PKD rats were intravitreally injected with PBS (left eye; 2 μ L) or ASCs (right eye; 2×10^4 in 2 μ L PBS) at P30. The lens morphology was analyzed 4 weeks post-injection. A) ASC injection-induced lens opacity compared to that observed after PBS injection. B) Compared to PBS injection, ASC injection increased IL-1 β secretion in the vitreous humor. Compared to that in the controls, retinal digestion stained with PAS (C) showed that ASC injection significantly decreased the number of pericytes (D) and increased acellular capillary formation (E). Red arrow indicated acellular capillaries. * $P < 0.05$; *** $P < 0.001$. 1-hASC: single intravitreal injection of human ASCs. Scale bar = 50 μ m. $n = 6$. Permission obtained from copyright © 2019 John Wiley and Sons (Huang et al., 2019b).

3.2.6 Intravitreal injection of HUVECs, RFPECs, and concentrated supernatant dose not cause retinal vasoregression in SD rats

To investigate whether retinal vascular damage is caused by MSC injection, we further injected either RFPECs or HUVECs (20,000 cells in 2 μ L) into vitreous space of 1-month-old SD rat eyes. No lens opacity was observed after a 4-week injection. More importantly, neither cell type was able to induce pericyte loss and formation of acellular capillaries (**Fig. 38**). These results suggest that retinal vasoregression and cataract formation might be closely related to the intravitreal administration of MSCs. To evaluate the effect of the conditioned medium of MSCs on retinal vasoregression, we intravitreally injected 2 μ L 100 \times concentrated human ASC medium into SD rats. We observed that the concentrated conditioned medium has neither beneficial nor detrimental effect on retinal vasculatures in PKD rats (**Fig. 39**). Thus, these results suggest that HUVECs, RFPECs, and concentrated medium injection cannot enhance retinal vascular damage in SD rats.

3.2.7 Intravitreally injected BMSCs do not affect the neuronal function in SD and PKD rats

The effect of BMSC injection on retinal neuronal function was evaluated using ERG, and retinal histology was evaluated using PAS staining. Compared to that observed in control eyes, we did not observe any significant difference in the amplitude of a-wave and b-wave in the BMSC-injected eyes in SD and PKD rats (**Fig. 40**). We continued to assess the thickness of the entire retina, ganglion cell layer (GCL), inner nuclear layer (INL), and outer nuclear layer (ONL) in SD rats treated with BMSCs or PBS. The thickness of the entire retina and intra-retinal layers did not show any significant change between the BMSC-injected and PBS-injected groups in SD rats (**Table 17**). In addition, statistical analysis of cell numbers in the GCL, INL, and ONL showed no significant differences in cell numbers in these three layers between BMSC-injected and control SD rats (**Table 17**). Thus, we demonstrate that intravitreally injected rat BMSCs do not affect retinal neuronal function and the cell population in retinal GCL, INL, and ONL.

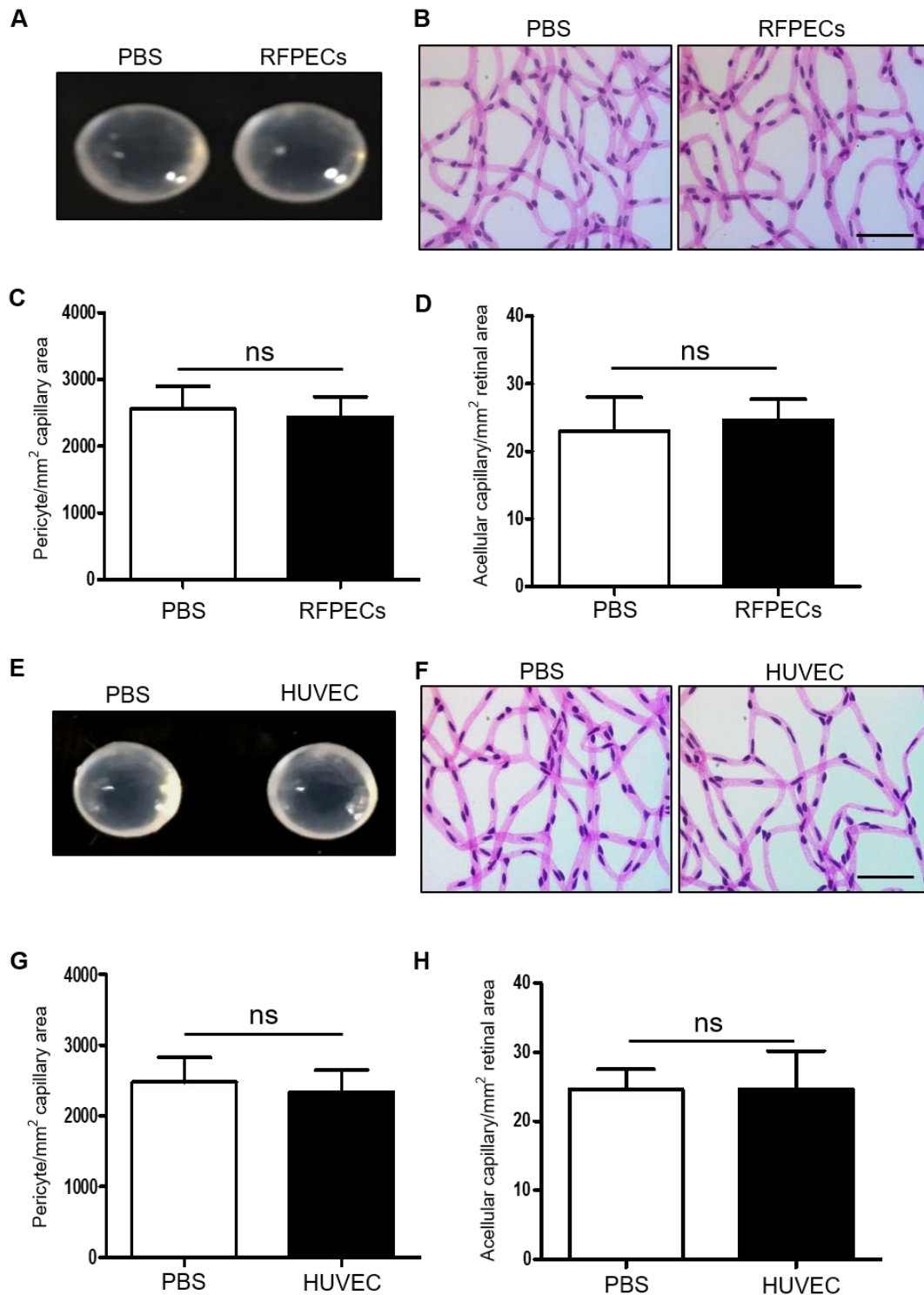


Figure 38: Intravitreal injection of either RFPECs or HUVECs does not induce lens opacity and retinal vasoregression in SD rats. PBS (left eyes; 2 μ L) or RFPECs/HUVECs (right eyes; 2×10^4 in 2 μ L PBS) were injected into the vitreous cavity of SD rats at P30. Four weeks after injection, we evaluated the lens opacity and retinal vasculature in retinal digest preparations stained with PAS. A, E) Neither RFPECs nor HUVECs were able to induce lens opacity. B-D, F-H) Pericyte number (C

and G) and acellular capillary number (D and H) in retinal digestion preparations stained with PAS (B and F) did not vary significantly between the PBS and RFPECs/HUVECs injection groups. RFPECs: rat fat pad endothelial cells; HUVECs: human umbilical vein endothelial cells. ns: not significant. Scale = 50 μ m. n = 3. Permission obtained from copyright © 2019 John Wiley and Sons (Huang et al., 2019b).

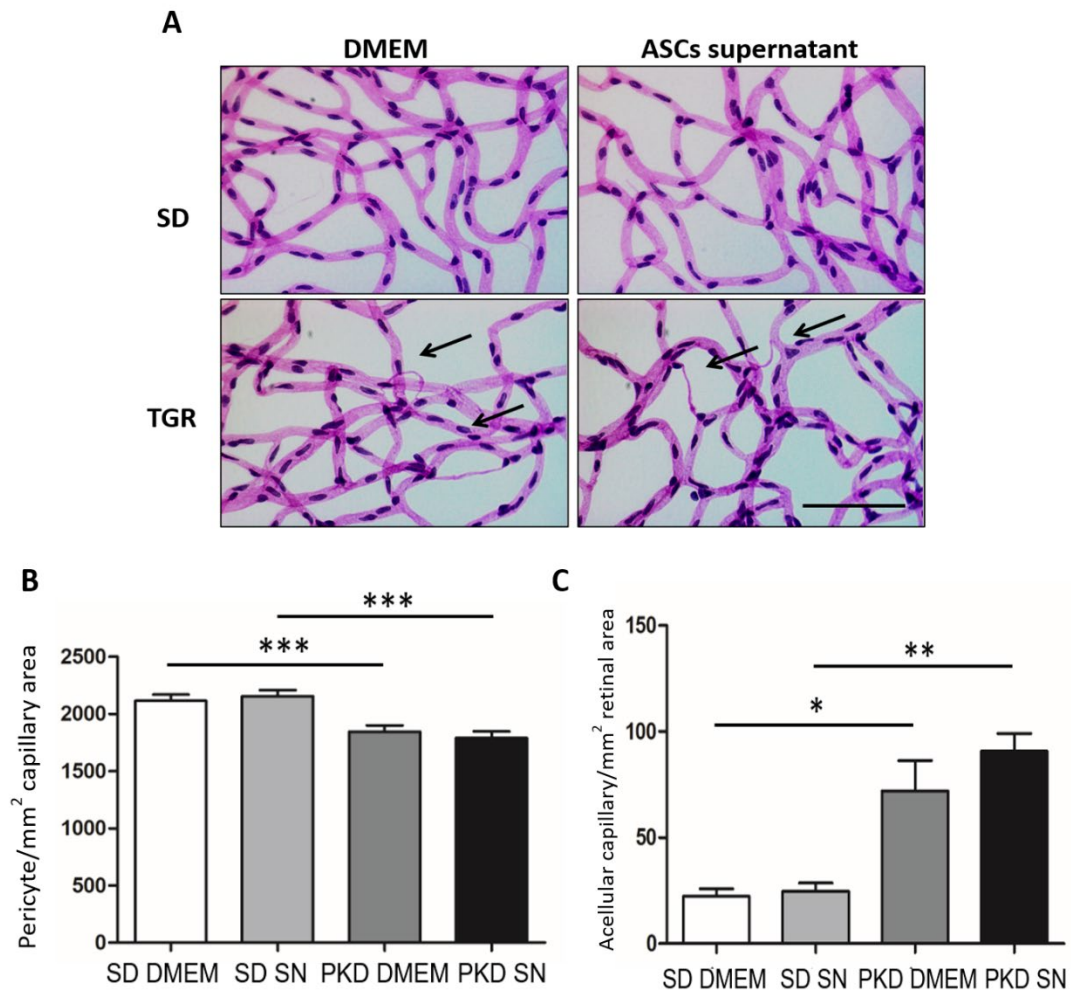


Figure 39: Intravitreal injection of conditioned media from human ASCs does not rescue retinal vasoregression in PKD rats. DMEM (left eyes; 2 μ L), or human ASCs conditioned media (right eyes; 2×10^4 in 2 μ L PBS) was injected into vitreous cavity of SD and PKD rats at P30. Four weeks after the injection, retinal vasculature was evaluated by staining retinal digest preparations with PAS. A-C) Intravitreally injected conditioned media from human ASCs were unable to induce retinal vascular damage in SD rats and did not ameliorate pericyte loss and reduce the formation of the acellular capillary. SN: supernatant, * $P < 0.05$; ** $P < 0.01$; *** $P < 0.001$. Scale = 50 μ m. n = 3.

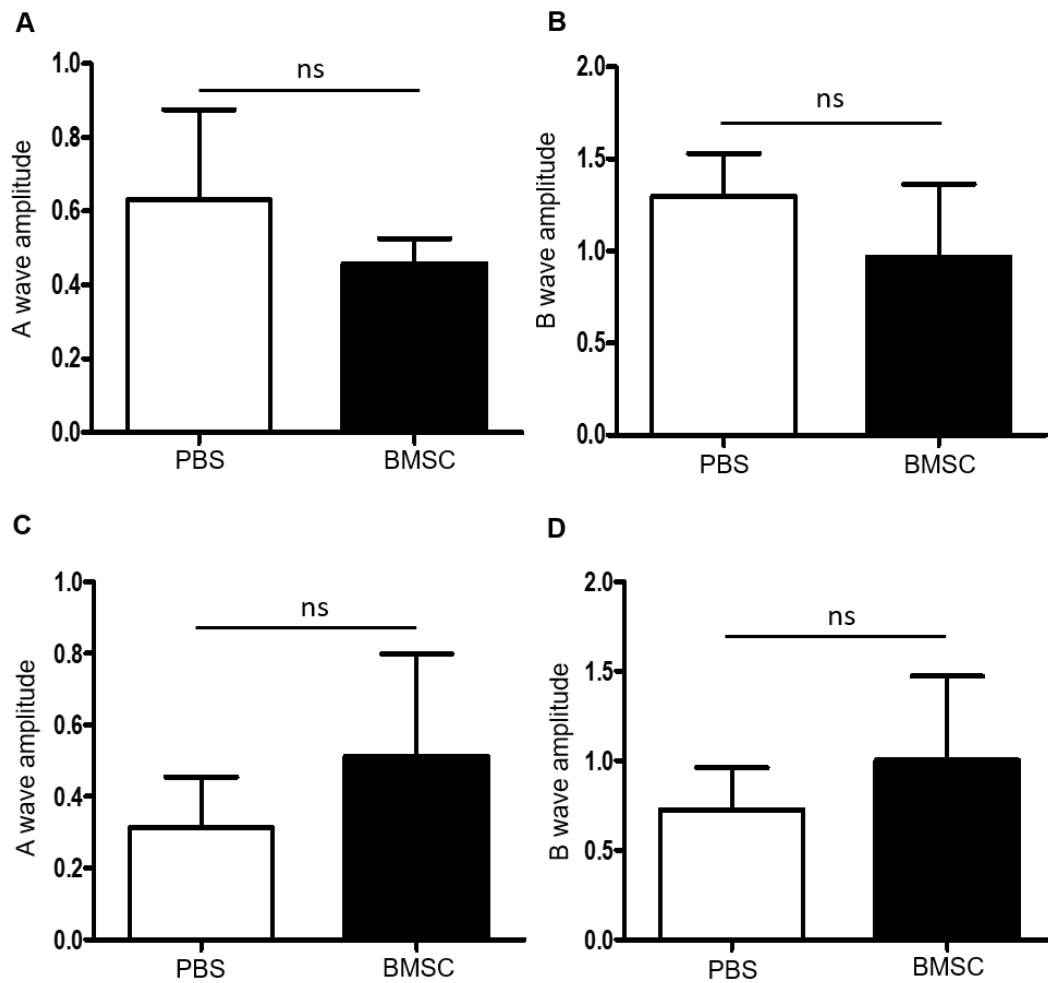


Figure 40: Intravitreally injected BMSCs do not affect neuronal functions in SD and PKD rats. SD and PKD rats were intravitreally injected with PBS (left eyes; 2 μ L) or BMSCs (right eyes; 2×10^4 in 2 μ L PBS) at P30. Four weeks after the injection, the electrical responses of the retina were measured using ERG. A, B) There were no significant differences in a wave (A) and b wave (B) amplitude between PBS and BMSC-injected SD rats. C, D) In PKD rats, no significant changes in a wave (C) and b wave amplitude (D) were observed between PBS and BMSC injected animals. ns: not significant. $n = 5-6$. Permission obtained from copyright © 2019 John Wiley and Sons (Huang et al., 2019b).

Table 17: Comparison of the thickness and cell number between PBS and BMSC-injected SD retinas.

		PBS	BMSC
Thickness	GCL	10.29 ± 0.59	10.76 ± 2.26
	INL	28.11 ± 1.92	26.28 ± 3.30
	ONL	56.08 ± 4.87	49.88 ± 7.71
	Total retina	355.62 ± 37.45	319.98 ± 48.10
Cell number	GCL	9 ± 1	8 ± 2
	INL	66 ± 9	62 ± 11
	ONL	305 ± 46	265 ± 44

The thicknesses of the entire retina, GCL, INL, and ONL were measured and the number of cells in GCL, INL and ONL were counted and expressed in 100 μm retina length for each. There were no significant differences in the thickness and cell number in retinal GCL, INL, and ONL between SD rats that received PBS and BMSC injections. GCL: ganglion cell layer; INL: inner nuclear layer; ONL: outer nuclear layer. $n = 6$. Permission obtained from copyright © 2019 John Wiley and Sons (Huang et al., 2019b).

3.2.8 Intravitreally injected BMSCs activate retinal glial cells in SD rats

Macroglial and microglial cells contribute to the course of pathological retinal vasoregression (de Hoz et al., 2016; Seitz et al., 2013). Hence, we investigated whether macroglial cells are activated in retinas after intravitreal administration of BMSCs. Western blot analysis demonstrated that the level of glial fibrillary acidic protein (GFAP), a marker for glial activation, was significantly increased in the BMSC-injected retina (**Fig. 41A and B**). Immunofluorescent data demonstrated that GFAP-positive staining was limited in astrocytes of the retinal ganglion cell layer (GCL) of PBS-injected SD rat eyes. On the contrary, BMSC-injected SD rat eyes displayed robust expression of GFAP in Müller cells, suggesting that retinal Müller cells were active when treated with BMSCs (**Fig. 41C**).

Next, we evaluated the effect of BMSC injection on the microglial cell population, Iba1-positive microglia were quantified in retina. As shown in **Fig. 41D and E**, the number of microglia increased by 130% (34 ± 11 vs. 77 ± 19 , SD + PBS vs. SD + BMSCs, $P < 0.05$) in the deep capillary layer where vasoregression had been initiated after treatment with BMSCs. Despite the increase in the number of microglia, the retinal morphology was similar in both groups. These results suggest that intravitreally injected BMSCs can induce microglial recruitment without affecting retinal morphology.

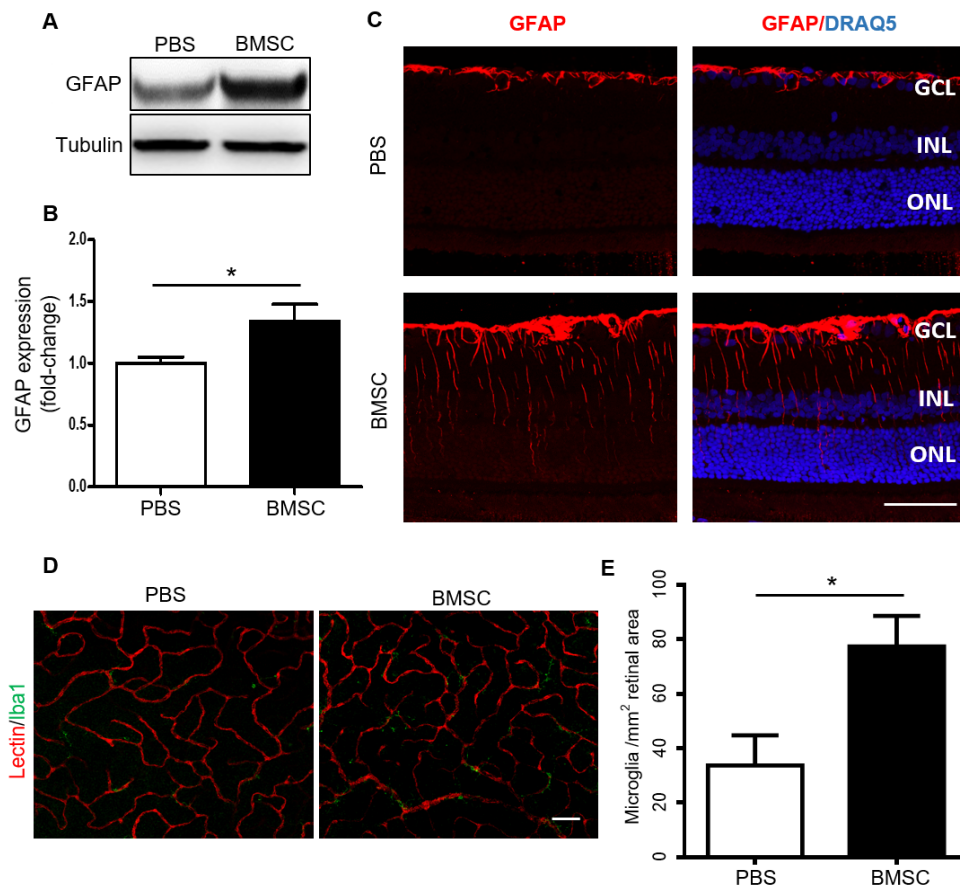


Figure 41: Intravitreally injected BMSCs activate retinal glial cells in SD rats. A) Representative image and quantification of GFAP expression using western blot analysis. B) Immunofluorescence staining of GFAP and DRAQ5. Müller cells were activated upon BMSC injection. C) Retinal whole-mount preparations stained for Iba1 (green) and Lectin (red) in SD rats injected with PBS or BMSCs. Upon BMSC injection, the number of Iba1-positive microglia increased significantly in the deep capillary layer. * $P < 0.05$. BMSC: bone marrow-derived stem cells. GFAP: glial fibrillary acidic protein, DRAQ5: nuclear staining, GCL: ganglion cell layer; INL: inner nuclear layer; ONL: outer nuclear layer; Iba1: microglial marker. Scale = 50 μm . $n=3$. Permission obtained from copyright © 2019 John Wiley and Sons (Huang et al., 2019b).

3.2.9 BMSC injection-induced retinal vasoregression is associated with immune response

To investigate the inflammatory response of the eye to the intravitreally administered BMSCs, we estimated the expression of inflammation-correlated factors in the eyes of SD rats. The results of quantitative PCR demonstrated a significant increase in IL-1 β transcription in the BMSC-treated retinas compared

to that in the control retinas. Furthermore, C3 and Arg1, the mediators in retinal inflammation and immune response, were significantly upregulated when treated with BMSCs (Fig. 42). Neuroprotective factors secreted by the active neuroglia can protect neuronal cells against insults. Therefore, we investigated the effect of intravitreally injected BMSCs on the expression of retinal neuroprotective factors. Interestingly, the expression of NGF, FGF2, CNTF, BDGF, and GDNF was comparable between PBS- and BMSC-treated retinas (Fig. 43). Taken together, intravitreal BMSC administration-induced retinal vasoregression is related to retinal immune and inflammatory response.

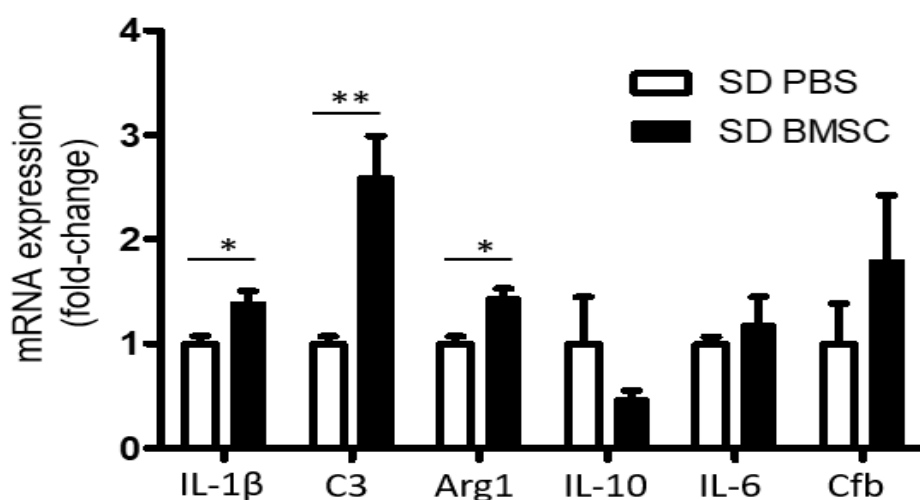


Figure 42: Intravitreally injected BMSCs trigger retinal inflammatory responses in SD rats. SD rats were intravitreally injected with PBS (left eye; 2 μ L) or BMSCs (right eye; 2×10^4 in 2 μ L PBS) at P30. Total RNA was extracted from the retinas, and inflammation-related factors were analyzed using quantitative PCR 4 weeks post-injection. BMSC injection significantly increased IL-1 β , C3, and Arg1 expression compared to that in controls. IL-1 β : Interleukin 1 beta; C3: complement component 3; Arg1: arginase 1; IL-10: interleukin 10; IL-6: interleukin 6; Cfb: complement factor b. * $P < 0.05$; ** $P < 0.01$. $n = 5$. Permission obtained from copyright © 2019 John Wiley and Sons (Huang et al., 2019b).

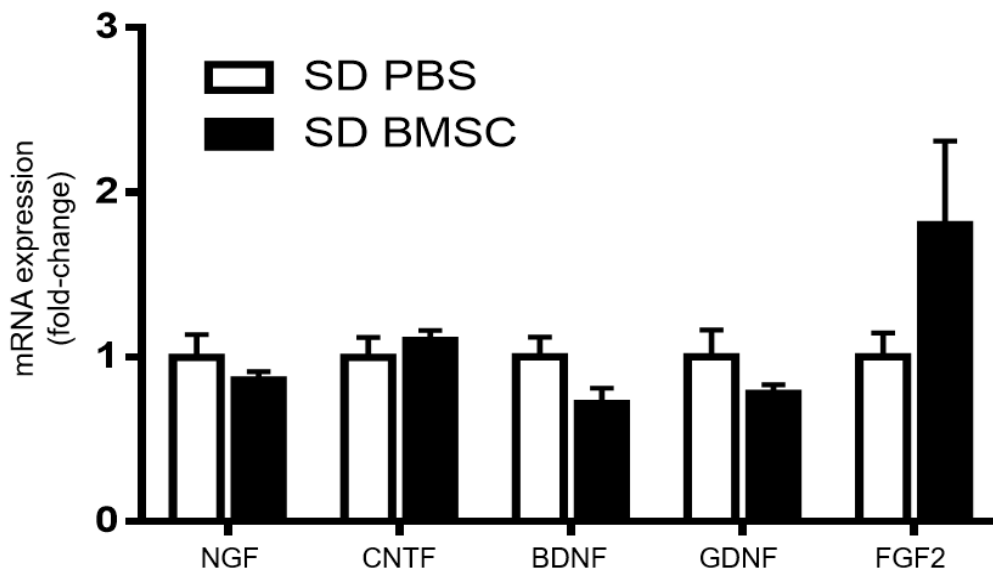


Figure 43: Intravitreally injected BMSCs do not promote the expression of retinal neurotrophic factors in SD rats. SD rats were intravitreally injected with PBS (left eyes; 2 μ L) or BMSCs (right eyes; 2×10^4 in 2 μ L PBS) at P30. Four weeks after injection, total retinal RNA was extracted from SD rats, and retinal neurotrophic factors were measured using quantitative PCR. There were no significant differences in the expression of NGF, CNTF, BDNF, GDNF, and FGF2 between the PBS and BMSC injection groups. NGF: nerve growth factor; CNTF: ciliary neurotrophic factor; BDNF: brain-derived neurotrophic factor; GDNF: glial-derived neurotrophic factor; FGF2: basic fibroblast growth factor. $n = 5$. Permission obtained from copyright © 2019 John Wiley and Sons (Huang et al., 2019b).

3.2.10 Intravitreally injected BMSCs increase retinal HSP90 expression in SD rats

HSPs play an essential role in the protection of cells from damage under pathological conditions by enhancing cytoprotective signaling against cell damage (Ikwegbue et al., 2018). Therefore, we examined the expression of HSP90 using western blot analysis. Compared to that in the controls, significant upregulation of retinal HSP90 expression was detected in BMSC-treated eyes (**Fig. 44A and B**). Immunofluorescent images demonstrated visible expression of HSP90 in the INL, IPL, and OPL, although weak expression was observed in the GCL and INL in PBS-injected SD rats. However, compared to that in the controls, intravitreally injected BMSCs induced a stronger expression of HSP90 in the GCL and, in particular, in the IPL and OPL (**Fig. 44C**). Furthermore, we verified that HSP90 upregulation is derived from macroglial cells, but not from vascular cells (**Fig. 45**). These results indicate that increased expression of

HSP90 contributes to cellular protection against BMSC injection.

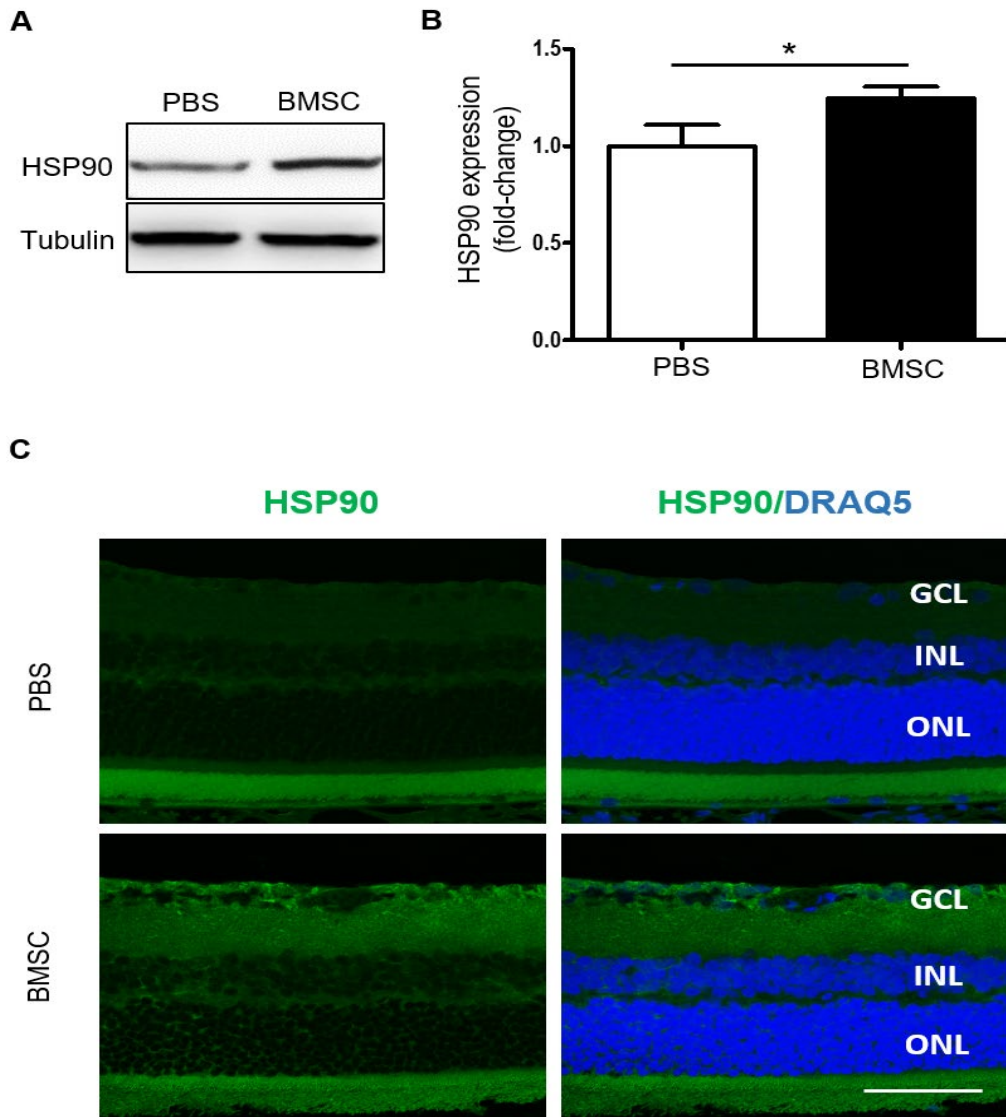


Figure 44: Intravitreally injected BMSCs elevate retinal HSP90 expression in SD rats. SD rats were intravitreally injected with PBS (left eye; 2 μ L) or BMSCs (right eye; 2×10^4 in 2 μ L PBS) at P30. Four weeks post-injection, retinal HSP90 expression was analyzed using western blot analysis and immunofluorescence staining. A) Western blot analysis showed that BMSC injection significantly increased HSP90 expression. B) Immunofluorescence staining displayed that retinal HSP90 expression (green) in BMSC-injected retinas was stronger than that in PBS-injected retinas. HSP90: Heat shock protein 90; GCL: ganglion cell layer; INL: inner nuclear layer; ONL: outer nuclear layer; DRAQ5: Nuclear staining. * $P < 0.05$. Scale = 50 μ m. $n = 3$. Permission obtained from copyright © 2019 John Wiley and Sons (Huang et al., 2019b).

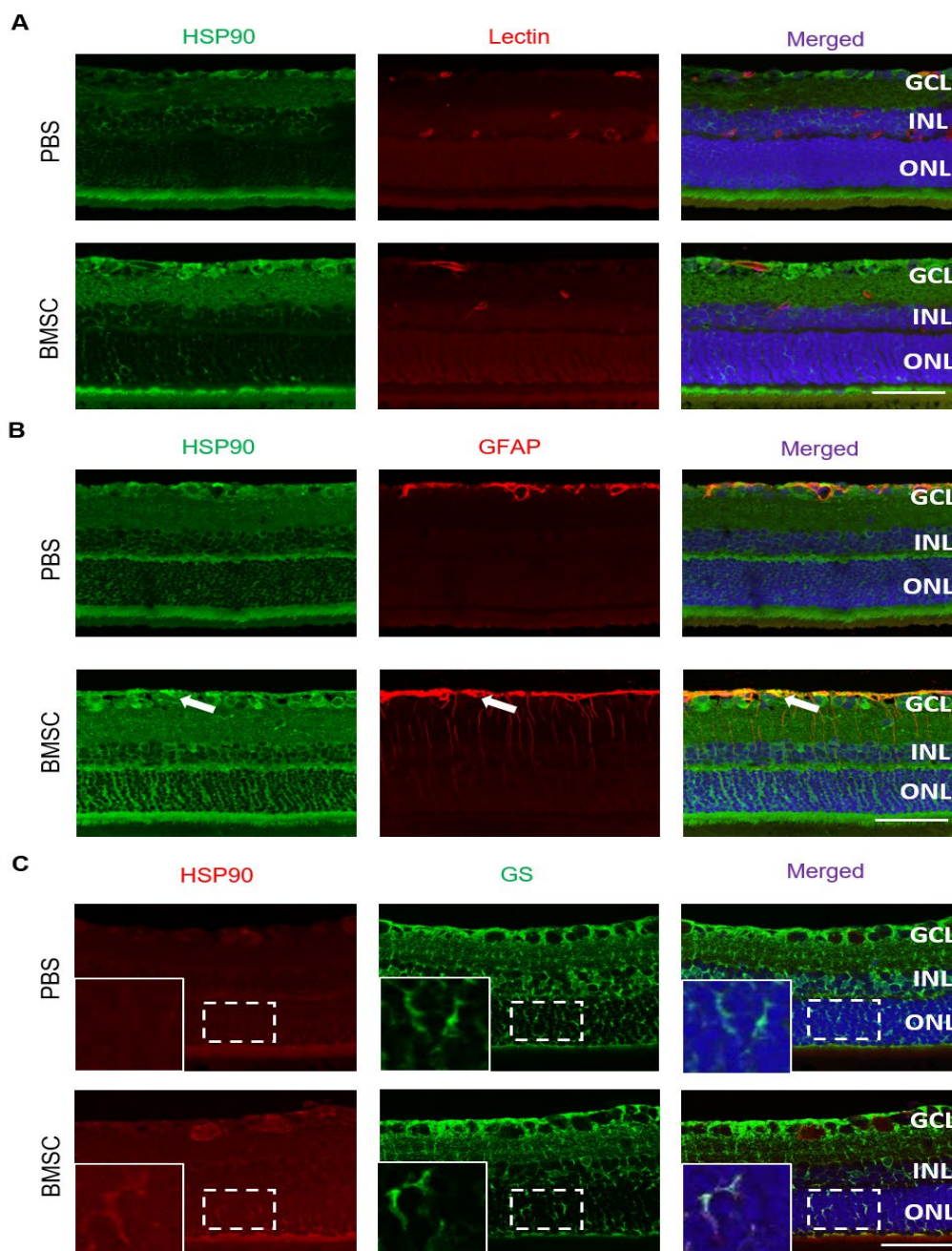


Figure 45: Colocalization of HSP90 with glial cells in the retina. Six-micrometer retinal sections were immunolabeled with anti-HSP90 antibody, anti-GFAP antibody (a marker for astrocytes and activated Muller cells), lectin antibody conjugated with TRITC (retinal vessel marker), and anti-GS antibody (a marker for Muller cells). A) Elevated HSP90 did not colocalize with lectin. B) Elevated HSP90 partially colocalized with GFAP. C) Elevated HSP90 partially colocalized with GS. The white arrow in B indicated the colocalization of HSP90 with GFAP. The insets in C with white lines are enlarged images of the area enclosed by dotted lines. GCL: ganglion cell layer; INL: inner nuclear layer; ONL: outer nuclear layer; GFAP: glial fibrillary acidic protein; HSP 90: heat shock protein 90; GS: glutamine synthetase. Scale bar = 50 μ m. n = 3. Permission obtained from copyright © 2019 John Wiley and Sons (Huang et al., 2019b).

4 Discussion

This study shows the association between endothelial VE-cadherin expression and pericyte loss in retinal vasoregression, and for the first time, provides evidence that reduced expression of retinal VE-cadherin precedes pericyte loss in three retinopathy models. VE-cadherin is essential for endothelial-pericyte interaction. Furthermore, we demonstrated that the underlying molecular mechanism of VE-cadherin degradation upon NDPK B deficiency or HG in endothelial cells involved Src kinase activation, and VE-cadherin tyrosine phosphorylation and internalization. In addition, we uncovered the harmful effects of intravitreally injected MSCs in rats; we showed that intravitreal injection of MSCs induced lens opacity, pericyte loss, glial cell activation, and retinal inflammation in rats.

4.1 Adequate expression of VE-cadherin stabilizes pericytes

Retinal pericytes and endothelial cells are the key players in retinal microvasculature homeostasis. VE-cadherin is the most studied molecule exclusively expressed in endothelial cells, which plays a crucial role in vascular integrity. It is known that pericyte loss is the earliest event in early DR (Stewart, 2016). However, in the present study, we observed reduction in the expression of retinal VE-cadherin in a hyperglycemia-dependent model and two hyperglycemia-independent models with early retinopathy, which suggested that decreased expression of VE-cadherin in retinas precedes pericyte loss and is responsible for pericyte loss. Reduction in VE-cadherin expression is a common feature of early retinal vasoregression. Furthermore, our *in vitro* data confirmed that VE-cadherin deficiency in endothelial cells leads to pericyte loss.

Indeed, VE-cadherin was essential for vascular development and stability, as VE-cadherin null mice died due to severe vascular defects in both intraembryonic and extraembryonic vasculatures (Vestweber, 2008). *In vitro* experiments demonstrated that endothelial cells deficient in VE-cadherin did not form vascular network and were maintained in a dispersed state (Vittet et al., 1997). Capillary tube formation of endothelial cells was inhibited after using anti-VE-cadherin blocking antibodies (Bach et al., 1998). The results obtained in the present study are in agreement with previous findings, showing that VE-cadherin is necessary for endothelial-pericyte stability and vascular architecture.

Nevertheless, VE-cadherin heterozygous mice appeared phenotypically normal and survived to adulthood (Gory-Fauré et al., 1999). Surprisingly, VE-cadherin heterozygous mice at postnatal day 5 displayed more pericyte coverage in lung capillaries due to increased expression of N-cadherin, which functions to increase vascular stability by recruiting pericytes (Giampietro et al., 2012). This was in agreement with the notion that VE-cadherin competed with N-cadherin expression on the endothelial plasma membrane. When VE-cadherin level was decreased, N-cadherin compensated for the reduction in endothelial contact (Gerhardt et al., 2000). Whether retinal pericyte coverage is affected in the developmental stage and adult stage of VE-cadherin heterozygous mutant mice is not clear. The precise mechanism via which VE-cadherin deficiency induces pericyte loss is not completely understood. However, we demonstrated that adequate VE-cadherin expression in endothelial cells may facilitate pericyte stability.

4.2 Endothelial cells with NDPK B deficiency or treated with HG show similarities in Src kinase activation, and VE-cadherin phosphorylation, internalization, and degradation

VE-cadherin dynamically regulates endothelial barrier function (Gory-Fauré et al., 1999). Our study also highlighted that NDPK B^{-/-} mice displayed reduced expression of retinal VE-cadherin and increased retinal vascular permeability. NDPK B deficiency activated Src kinase, induced VE-cadherin phosphorylation (Tyr685), promoted VE-cadherin internalization, and accelerated VE-cadherin degradation in endothelial cells, mimicking the impact of high glucose.

Previous studies have provided several lines of evidence indicating that HG affects endothelial cell properties and associates with the activation of multiple pathways (Davidson and Duchon, 2007; Haidari et al., 2014; Huang and Sheibani, 2008; Qiu et al., 2016). Src kinase regulates vascular permeability. Reports show that Src kinase activity increases in mice with diabetes, and that HG activates the Src signaling pathway to enhance endothelial cell migration (Schaeffer et al., 2003; Xie et al., 2013). Herein, our results were consistent with early findings showing that HG promotes Src tyrosine phosphorylation in endothelial cells. Importantly, NDPK B deficiency and HG produced similar effects on the increase in Src phosphorylation. This outcome is contrary to the observations of a previous study, which has suggested that NDPK B depletion in endothelial cells abolishes VEGF-induced Src phosphorylation (Gross et al.,

2017). Based on these results, we inferred that NDPK B may play a diverse role in the regulation of Src activity under different stimuli. However, in the present study, we did not investigate how NDPK B deficiency or HG treatment of endothelial cells increases Src activity. A possible explanation for this might be the disruption of phosphate and energy homeostasis caused by NDPK B depletion or HG treatment in endothelial cells, which might induce Src kinase tyrosine phosphorylation or alter the biological properties of Src kinase substrates.

The Src signaling pathway mediates VE-cadherin function. Src kinase activity is essential for VEGF-induced VE-cadherin phosphorylation (Tyr 685), which results in the opening of the gap between endothelial cells and increase in vascular permeability (Sidibé et al., 2014). HG also induced VE-cadherin phosphorylation (Tyr658 and Tyr731), which increased endothelial permeability (Rangasamy et al., 2011). Another study reported that endothelial cells stimulated with HG lead to VE-cadherin phosphorylation via PKC- β -dependent myosin light chain (MLC) phosphorylation. In the present study, we showed that NDPK B deficiency or HG exclusively increased VE-cadherin phosphorylation (Tyr 685) by upregulating Src kinase activity in endothelial cells.

VE-cadherin phosphorylation mediates internalization. Therefore, excessive internalized VE-cadherin leads to reduction in membranous VE-cadherin expression. Reports show that NDPK B contributes to adhesion junction integrity and plays a central role in the regulation of endocytosis (Feng et al., 2014; Snider et al., 2015). The loss of NDPK B interfered with the barrier function in the brain (Gross et al., 2017). HG enhanced horseradish peroxidase endocytosis in retinal vascular endothelial cells (Stitt et al., 1995). Our present study showed that NDPK B deficiency or HG treatment in endothelial cells promoted VE-cadherin internalization, which conversely reduced the expression of plasma membrane VE-cadherin. We further observed that internalized VE-cadherin is first captured by early endosome, and afterward is trapped into the lysosome for degradation. These results showed for the first time that NDPK B participates in the regulation of VE-cadherin endocytosis and plays a protective role in VE-cadherin degradation. The loss of NDPK B in endothelial cells mimics HG-mediated lysosomal VE-cadherin degradation.

Recent reports have demonstrated that Ras-related proteins 11 (Rab11) plays an essential role in VE-cadherin recycling. Reduced expression of Rab11

inhibited VE-cadherin recycling to the membrane, leading to increased vascular leakage in mice when treated with stimuli (Yan et al., 2015). Whether NDPK B loss or HG treatment in endothelial cells is involved in the Rab11-mediated VE-cadherin recycling pathway is still unknown. Furthermore, microRNAs also regulate VE-cadherin degradation. For example, miR-939 and miR-27a-3p target VE-cadherin and mediate the downregulation of VE-cadherin (Di Modica et al., 2017; Zhao et al., 2016). In the present study, we did not analyze the expression of microRNA, but instead analyzed the mRNA expression of VE-cadherin in NDPK B-depleted or HG-treated endothelial cells, showing that the mRNA level of junctional molecules, including VE-cadherin, is unaffected in either NDPK B deficient or HG-treated endothelial cells. These data further demonstrated that NDPK B mediates VE-cadherin expression in the post-translation modification process rather than in the transcriptional process. In addition, reduced expression of p120-catenin promotes VE-cadherin endocytosis. However, the results of this study do not support those of previous studies. We observed that the expression of p120-catenin is unaltered in NDPK B-depleted or HG-treated endothelial cells, which suggests that the reduced expression of VE-cadherin in endothelial cells caused by NDPK B deficiency or HG is independent of p120 catenin.

Studies have suggested that vascular endothelial protein tyrosine phosphatase (VE-PTP) interacts with VE-cadherin, reducing VE-cadherin tyrosine phosphorylation to maintain cell layer permeability (Nottebaum et al., 2008). Dissociation of VE-PTP and VE-cadherin weakens cellular junctions and promotes leukocyte extravasation (Broermann et al., 2011). This observation supports the hypothesis that NDPK B may facilitate the stabilization of VE-PTP and VE-cadherin, preventing VE-cadherin trafficking into the cytosol.

4.3 Evaluation of intravitreally injected MSCs in pre-clinical and clinical studies

Another key finding of the study was the unexpected induction of vasoregression upon intravitreal administration of MSCs in both healthy and diseased retinas. In addition to the vascular damage, intravitreal injection of MSCs led to cataract, activation of retinal glial cells, and elevation of inflammatory factors. This is opposite to early published results, the majority of which have reported that MSCs have beneficial vasoprotective and pro-angiogenic effects in experimental animal models of DR and other retinal

diseases (Elshaer et al., 2018; Otani et al., 2004). Mendel et al. (2013) demonstrated that intravitreal injection of MSCs prevented retinal capillary loss in mouse models of DR and hypoxia-induced proliferative retinopathy. The regenerative capacity of intravitreally administrated human ASCs in the diabetic rat retinas was also verified by Rajashekhar and colleagues (Rajashekhar et al., 2014). In addition, intravitreally injected MSCs can migrate into the retinal outer nuclear layer, differentiate into neural cells in injured rat retinas (Tomita et al., 2002), or into retinal microglia, Müller cells, and endothelial cells (Chakravarthy et al., 2016). In contrast, we observed a vasoregressive instead of a vasoprotective effect after the intravitreal injection of MSCs in healthy and diseased retinas. The vasoregressive damage typically seen in the diseased retinas was further exacerbated by MSC injection (Huang et al., 2019a).

Despite numerous encouraging and promising *in vivo* and *in vitro* results supporting MSC therapy, adverse cases have been reported by early studies, such as detrimental outcomes in stem cell therapy against eye diseases. Kuriyan et al. described complete vision loss in a patient with age-related macular degeneration after intravitreal injection with autologous stem cells (Kuriyan et al., 2017). Likewise, Satarian et al. have reported that intravitreal injection of autologous BMSCs into patients with advanced retinitis pigmentosa induced further retinal vascular deterioration, causing severe vision impairment (Satarian et al., 2017). These adverse outcomes indicated that MSC-based therapy might have bidirectional effects, protective as well as destructive, on the retinal vasculature. Determining the efficiency and safety of intravitreal stem cell injections for clinical application in DR and retinal degenerative diseases is of crucial importance.

Whether intravitreally injected MSCs can migrate into the retina and integrate with retinal vessels is still being debated (Ezquer et al., 2016). Intriguingly, our results have shown that intravitreally injected MSCs did not migrate into the retinas, supporting the observation by Johnson et al. who demonstrated that the existence of a completely developed inner limiting membrane hinders the passage of injected MSCs into the retinas (Johnson et al., 2010b). These data suggest that MSC-based therapy may be effective only in the immature retina. Some models in which therapeutic efficacy has been tested include retinopathy of prematurity (ROP) models in which vasoregression is caused by hyperoxia in immature retinal vessels (Connor et al., 2009). The retinal vascular structure is not entirely developed in those models, allowing the intravitreally injected

cells to migrate into the retina. Whether MSCs can produce beneficial effects may be dependent on the model, as immunomodulation may exert distinct effects in these models, such as the PKD model with excessive inflammatory components.

4.4 Intravitreally injected MSCs induce inflammatory responses

Interspecies MSCs have been applied in experimental studies for stem cell therapy, such as the usage of human MSCs in rodent models with retinal diseases. Preservation of retinal functions was determined after treatment of animal models with human MSCs (Wang et al., 2017; Yang et al., 2010; Zhang et al., 2017). We observed that MSCs from human sources induced more severe retinal vasoregression than allogeneic MSCs in rats. Furthermore, we demonstrated compellingly that MSCs themselves trigger vasoregression in the retina via increased inflammatory responses, in contrast to autologous or xenogeneic endothelial cells, which are inert. In contrast to mature endothelial cells, MSCs are multipotent cells that can differentiate into various cell types. As the injected MSCs did not penetrate the retinas, the induced vasoregression may not be due to the direct effect of migrated and differentiated BMSCs in the retinas. Based on the high microglia number and pro-inflammatory cytokines in the vitreous and/or retinas, we postulated that MSCs may provoke an immune-inflammatory response, indirectly causing retinal vascular damage. The key role of inflammation in the development of vascular damage in DR and retinal degeneration is evident (Rangasamy et al., 2012). Increased levels of pro-inflammatory cytokines such as IL-1 β , IL-6, and TNF have been reported in these diseases. In our study, we also detected increase in IL-1 β level in the vitreous and, to a lesser extent, in the retinas of stem cell-injected SD rats. Concurrently, C3 and Arg1 were upregulated in the retinas upon MSC injection. The results suggest a potential connection between immune-inflammatory responses and MSC treatment, supporting reports showing that pro-inflammatory cytokines mediated vascular damage. In addition, our data demonstrated that intravitreally injected MSCs induce lens opacity in both SD and PKD eyes. No cataract formation was observed in the control PKD eyes, although IL-1 β expression in the retinas was increased (Feng et al., 2011). Therefore, the increased IL-1 β level in the vitreous after BMSC injection is unlikely to be a cause of cataract, which remains to be further elucidated. Pro-inflammatory cytokines in the retina are mainly produced by activated microglial, macroglial, and endothelial cells (Altmann and Schmidt, 2018). Our results

revealed high numbers of microglial cells in the BMSC-treated retinas, suggesting that microglial cells mainly contribute to the inflammatory response when treated with stem cells in retinas. Furthermore, activation of Müller cells in the retina was observed upon MSC intravitreal injection. However, whether the inflammatory response is a critical mediator in the development of retinal vasoregression after MSC application requires further investigation.

Activated Müller cells exhibit dual functions of promoting vasoregression and protecting the retinal neuronal cells (Abcouwer, 2017; Fu et al., 2015). While vasoregression was observed in our study, no changes in neurotrophic factors or neuronal function were observed post-injection of MSCs. Our study was designed for a short-term period after MSC therapy. MSCs may have a neuroprotective effect in long-term application. MSC treatment possibly activated cytoprotective signaling pathways in our study, as the expression of HSP90 was significantly upregulated in the retina and partially in the Müller cells. HSP90 is universally expressed in the retina and plays diverse roles in retinal disorders (Kojima et al., 1996; Urbak and Vorum, 2010). HSP90 inhibitors are used in the treatment of patients with retinitis pigmentosa, AMD, and ocular oncology, indicating that the inhibition of HSP90 protects the retinal cells against cellular damage by affecting the inflammatory and angiogenic responses (Aguilà and Cheetham, 2016; Aguila et al., 2013). Elevated level of HSP90 after MSC treatment is possibly associated with the inflammation-induced cytoprotective loop in the retina to promote cell survival.

Although the eye is considered as an immune-privileged organ, low-grade inflammation may exist, especially after intravitreal injections. In one clinical study, Siqueira et al. showed that the improvement of vision-correlated life quality scores in patients at 3 months after treatment disappeared at 12 months (Siqueira et al., 2015). Most of the published animal studies were planned as short-term studies with treatment duration of months. In this study, significant aggravation of retinal vasoregression without neuronal function alteration was observed in MSC-treated eyes. We postulated that the result of persistent vasoregression will impair the retinal neuronal function in SD and PKD rats. Whether the vanishment of protective effect of MSC-based therapy at 12 months post-treatment in the clinical trials reported by Siqueira et al. is caused by MSC-induced indirect vascular damage followed by alteration of neuronal cell function is not clear.

4.5 Further studies

In this study, we have reported that reduced VE-cadherin expression in retinas precedes pericyte loss in retinopathy models. The loss of VE-cadherin in endothelial cells leads to pericyte detachment. Further research should be undertaken to investigate whether VE-cadherin heterozygote mice exhibit pericyte loss in retinas. NDPK B loss or HG treatment in endothelial cells can promote VE-cadherin internalization via increased Tyr 685 phosphorylation mediated by Src kinase activation, suggesting that Tyr 685 residue is required for VE-cadherin internalization. Despite these promising results, questions remain whether NDPK B loss or HG treatment in the endothelial cells induce VE-cadherin internalization after mutation of VE-cadherin Tyr 685.

The endocytosis pathway can be mainly classified into the clathrin-mediated pathway and the caveolae-mediated pathway. Although we already know that NDPK B loss or HG treatment of endothelial cells promotes membrane VE-cadherin internalization and lysosome-mediated degradation, the identity of the cellular endocytosis pathway involved remains unclear. NDPK B loss and HG treatment of endothelial cells might mediate VE-cadherin endocytosis via the different pathways. Furthermore, early studies had revealed that NDPK B interacts with dynamin, which is an essential regulator of endocytosis. NDPK B binding to dynamin may facilitate the homeostasis of membrane protein trafficking. NDPK B deficiency possibly leads to the dissociation of NDPK B and dynamin, which increases endocytosis. Studies have shown that NDPK B interacts with α -catenin, which is indirectly bound to the VE-cadherin complex on the membrane. Thus, the possible regulation of VE-cadherin upon NDPK B deficiency via α -catenin is not excluded.

Furthermore, how NDPK B loss or HG treatment of endothelial cells promotes internalized VE-cadherin transportation to the lysosome is still obscure. The recycling pathway may be involved, as some crucial regulators such as Rab11 and Rab7 play a vital role in the regulation of VE-cadherin recycling. NDPK B loss or HG in endothelial cells might affect the function of these molecules, which might delay the return of the internalized VE-cadherin to the plasma membrane or drive internalized VE-cadherin to the lysosome.

Contrary to expectations, this study does not show the protective roles of intravitreally injected MSCs in PKD rats; instead, it shows that intravitreally

injected MSCs induce cataract, pericyte loss, glial cell reactivation, and inflammation in rat eyes. Compared to traditional drug therapy for eye diseases, MSC-based therapy is associated with several potential risks, such as uncontrolled cellular property and unclear mechanism of action. MSCs are heterogeneous in nature and behave differently in the same environment. Thus, cell quality should be controlled and the differentiation potential and biological activity of MSCs should be elucidated prior to injection. To circumvent this problem, we propose the evaluation of cells in animal research before use in patients.

5 Summary

Pericytes and endothelial cells are the major players in maintaining retinal neurovascular unit (NVU) integrity. Pericytes contribute to vascular protection and regeneration in the retina. Previous studies have reported pericyte loss in several animal models of retinopathy with the breakdown of NVU, such as in NDPK B^{-/-} mice (5-month-old), PKD rats (2-month-old), and Ins2^{Akita} mice (3-month old). VE-cadherin is exclusively expressed in endothelial cells and preserves the endothelial barrier functions. Reduced expression of VE-cadherin leads to increased vascular permeability. However, the correlation between altered VE-cadherin expression and pericyte loss and the underlying mechanism are still not clear. From the therapeutic perspective, pericytes have been therapeutic targets for diseases with retinal vascular degeneration. Mesenchymal stem cells (MSCs) and pericytes share typical cell morphology and phenotypic characteristics. Thus, MSC-based therapy has been proposed as an alternative therapeutic approach in retinal degenerative diseases. Therefore, the study aims were to identify: 1) the link between retinal VE-cadherin expression and pericyte loss in animal models with vasoregressive retinopathy, and the underlying signal transduction; 2) the therapeutic potential of intravitreally administrated MSCs in retinopathy with vasoregression.

The following are the key observations of this study:

1. Reduced VE-cadherin expression was observed in the retinas of 4-month-old NDPK B^{-/-} mice, 1.5-month-old Ins2^{Akita} mice, and 1-month-old PKD rats prior to pericyte loss.
2. Retinal vascular permeability was increased in NDPK B^{-/-} mice. Reduced VE-cadherin expression was predominantly detected in the deep retinal capillary layer.
3. *In vitro*, either NDPK B deficiency or HG lowered VE-cadherin in the endothelial plasma membrane by promoting Src kinase activation, followed by VE-cadherin tyrosine phosphorylation (Y685), leading to internalization and degradation in a lysosome-dependent manner. Furthermore, reduced expression of VE-cadherin led to pericyte loss in endothelial cells.
4. Intravitreal administration of MSCs in both SD and PKD eyes induced or aggravated cataract, pericyte loss, and formation of acellular capillaries.
5. MSCs remained in the vitreous cavity and did not migrate into the retinas.
6. Intravitreal administration of MSCs impacted retinal neuronal function neither in SD nor PKD rats.

7. Intravitreal injection of MSCs activated retinal micro- and microglial cells in SD rats.
8. Intravitreal injection of MSCs increased the expression of inflammatory factors (IL-1 β , C3, and Arg1) and enhanced HSP90 expression in SD rats.

In conclusion, our results suggest that the alteration of retinal VE-cadherin expression precedes pericyte loss independent of hyperglycemia in different experimental animal models with early retinopathy. VE-cadherin reduction induces pericyte loss via Src kinase activation and increased VE-cadherin Y685 phosphorylation. We identify a novel signaling pathway involved in VE-cadherin-mediated pericyte loss, which provides new insights regarding therapeutic intervention in retinopathy with NVU breakdown. However, the destructive effect of MSCs in eyes indicates that intravitreal administration of MSCs is inadvisable.

6 References

- Abcouwer, S.F. (2017). Müller Cell–Microglia Cross Talk Drives Neuroinflammation in Diabetic Retinopathy. *Diabetes* 66, 261-263.
- Abcouwer, S.F., and Gardner, T.W. (2014). Diabetic retinopathy: loss of neuroretinal adaptation to the diabetic metabolic environment. *Annals of the New York Academy of Sciences* 1311, 174-190.
- Abu-Taha, I.H., Heijman, J., Feng, Y., Vettel, C., Dobrev, D., and Wieland, T. (2018). Regulation of heterotrimeric G-protein signaling by NDPK/NME proteins and caveolins: an update. *Laboratory Investigation* 98, 190.
- Adam, A.P. (2015). Regulation of endothelial adherens junctions by tyrosine phosphorylation. *Mediators of inflammation* 2015.
- Aguilà, M., and Cheetham, M.E. (2016). Hsp90 as a potential therapeutic target in retinal disease. In *Retinal Degenerative Diseases* (Springer), pp. 161-167.
- Aguila, M., Bevilacqua, D., McCulley, C., Schwarz, N., Athanasiou, D., Kanuga, N., Novoselov, S.S., Lange, C.A., Ali, R.R., and Bainbridge, J.W. (2013). Hsp90 inhibition protects against inherited retinal degeneration. *Human molecular genetics* 23, 2164-2175.
- Akagi, Y., Kador, P.F., Kuwabara, T., and Kinoshita, J.H. (1983). Aldose reductase localization in human retinal mural cells. *Invest Ophthalmol Vis Sci* 24, 1516-1519.
- Akimov, N.P., and Rentería, R.C. (2012). Spatial frequency threshold and contrast sensitivity of an optomotor behavior are impaired in the Ins2Akita mouse model of diabetes. *Behavioural brain research* 226, 601-605.
- Alcaide, P., Martinelli, R., Newton, G., Williams, M.R., Adam, A., Vincent, P.A., and Luscinckas, F.W. (2012). p120-Catenin prevents neutrophil transmigration independently of RhoA inhibition by impairing Src dependent VE-cadherin phosphorylation. *American Journal of Physiology-Cell Physiology* 303, C385-C395.
- Altmann, C., and Schmidt, M. (2018). The role of microglia in diabetic retinopathy: inflammation, microvasculature defects and neurodegeneration. *International journal of molecular sciences* 19, 110.
- Armulik, A., Genové, G., and Betsholtz, C. (2011). Pericytes: developmental, physiological, and pathological perspectives, problems, and promises. *Developmental cell* 21, 193-215.
- Association, A.D. (2010). Diagnosis and classification of diabetes mellitus. *Diabetes care* 33, S62-S69.
- Attwood, P.V., and Muimo, R. (2018). The actions of NME1/NDPK-A and NME2/NDPK-B as protein kinases. *Laboratory Investigation* 98, 283.
- Bach, T.L., Barsigian, C., Chalupowicz, D.G., Busler, D., Yaen, C.H., Grant, D.S., and Martinez, J. (1998). VE-cadherin mediates endothelial cell capillary tube formation in fibrin and collagen Gels1. *Experimental cell research* 238, 324-334.
- Baki, L., Marambaud, P., Efthimiopoulos, S., Georgakopoulos, A., Wen, P., Cui,

W., Shioi, J., Koo, E., Ozawa, M., and Friedrich, V.L. (2001). Presenilin-1 binds cytoplasmic epithelial cadherin, inhibits cadherin/p120 association, and regulates stability and function of the cadherin/catenin adhesion complex. *Proceedings of the National Academy of Sciences* **98**, 2381-2386.

Barber, A.J., Antonetti, D.A., Kern, T.S., Reiter, C.E., Soans, R.S., Krady, J.K., Levison, S.W., Gardner, T.W., and Bronson, S.K. (2005). The Ins2Akita mouse as a model of early retinal complications in diabetes. *Investigative ophthalmology & visual science* **46**, 2210-2218.

Berg, P., and Joklik, W. (1953). Transphosphorylation between nucleoside polyphosphates. *Nature* **172**, 1008-1009.

Bianco, P., Robey, P.G., and Simmons, P.J. (2008). Mesenchymal stem cells: revisiting history, concepts, and assays. *Cell stem cell* **2**, 313-319.

Boissan, M., Dabernat, S., Peuchant, E., Schlattner, U., Lascu, I., and Lacombe, M.-L. (2009). The mammalian Nm23/NDPK family: from metastasis control to cilia movement. *Molecular and cellular biochemistry* **329**, 51-62.

Broermann, A., Winderlich, M., Block, H., Frye, M., Rossaint, J., Zarbock, A., Cagna, G., Linnepe, R., Schulte, D., and Nottebaum, A.F. (2011). Dissociation of VE-PTP from VE-cadherin is required for leukocyte extravasation and for VEGF-induced vascular permeability in vivo. *Journal of Experimental Medicine* **208**, 2393-2401.

Busser, H., Najar, M., Raicevic, G., Pieters, K., Velez Pombo, R., Philippart, P., Meuleman, N., Bron, D., and Lagneaux, L. (2015). Isolation and characterization of human mesenchymal stromal cell subpopulations: comparison of bone marrow and adipose tissue. *Stem cells and development* **24**, 2142-2157.

Cadwell, C.M., Su, W., and Kowalczyk, A.P. (2016). Cadherin tales: regulation of cadherin function by endocytic membrane trafficking. *Traffic* **17**, 1262-1271.

Cao, J., and Schnittler, H. (2019). Putting VE-cadherin into JAIL for junction remodeling. *J Cell Sci* **132**, jcs222893.

Cao, Y., Feng, B., Chen, S., Chu, Y., and Chakrabarti, S. (2014). Mechanisms of endothelial to mesenchymal transition in the retina in diabetes. *Investigative ophthalmology & visual science* **55**, 7321-7331.

Caplan, A.I. (1991). Mesenchymal stem cells. *Journal of orthopaedic research* **9**, 641-650.

Castanheira, P., Torquetti, L., Nehemy, M.B., and Goes, A.M. (2008). Retinal incorporation and differentiation of mesenchymal stem cells intravitreally injected in the injured retina of rats. *Arquivos Brasileiros de Oftalmologia* **71**, 644-650.

Chakravarthy, H., Beli, E., Navitskaya, S., O'Reilly, S., Wang, Q., Kady, N., Huang, C., Grant, M.B., and Busik, J.V. (2016). Imbalances in mobilization and activation of pro-inflammatory and vascular reparative bone marrow-derived cells in diabetic retinopathy. *PloS one* **11**, e0146829.

Chichger, H., Braza, J., Duong, H., Boni, G., and Harrington, E.O. (2016). Select Rab GTPases regulate the pulmonary endothelium via endosomal

trafficking of vascular endothelial-cadherin. *American journal of respiratory cell and molecular biology* *54*, 769-781.

Chiou, S.-H., Kao, C.-L., Peng, C.-H., Chen, S.-J., Tarng, Y.-W., Ku, H.-H., Chen, Y.-C., Shyr, Y.-M., Liu, R.-S., and Hsu, C.-J. (2005). A novel in vitro retinal differentiation model by co-culturing adult human bone marrow stem cells with retinal pigmented epithelium cells. *Biochemical and biophysical research communications* *326*, 578-585.

Connor, K.M., Krah, N.M., Dennison, R.J., Aderman, C.M., Chen, J., Guerin, K.I., Sapieha, P., Stahl, A., Willett, K.L., and Smith, L.E. (2009). Quantification of oxygen-induced retinopathy in the mouse: a model of vessel loss, vessel regrowth and pathological angiogenesis. *Nature protocols* *4*, 1565.

Corada, M., Mariotti, M., Thurston, G., Smith, K., Kunkel, R., Brockhaus, M., Lampugnani, M.G., Martin-Padura, I., Stoppacciaro, A., and Ruco, L. (1999). Vascular endothelial-cadherin is an important determinant of microvascular integrity in vivo. *Proceedings of the National Academy of Sciences* *96*, 9815-9820.

Davidson, S.M., and Duchon, M.R. (2007). Endothelial mitochondria: contributing to vascular function and disease. *Circulation research* *100*, 1128-1141.

De Bari, C., Dell'Accio, F., Vandenabeele, F., Vermeesch, J.R., Raymackers, J.-M., and Luyten, F.P. (2003). Skeletal muscle repair by adult human mesenchymal stem cells from synovial membrane. *The Journal of cell biology* *160*, 909-918.

de Hoz, R., Rojas, B., Ramírez, A.I., Salazar, J.J., Gallego, B.I., Triviño, A., and Ramírez, J.M. (2016). Retinal macroglial responses in health and disease. *BioMed research international* *2016*.

Dejana, E., Orsenigo, F., and Lampugnani, M.G. (2008). The role of adherens junctions and VE-cadherin in the control of vascular permeability. *Journal of cell science* *121*, 2115-2122.

Delva, E., and Kowalczyk, A.P. (2009). Regulation of cadherin trafficking. *Traffic* *10*, 259-267.

Devi, T.S., Hosoya, K.-I., Terasaki, T., and Singh, L.P. (2013). Critical role of TXNIP in oxidative stress, DNA damage and retinal pericyte apoptosis under high glucose: implications for diabetic retinopathy. *Experimental cell research* *319*, 1001-1012.

Di Modica, M., Regondi, V., Sandri, M., Iorio, M.V., Zanetti, A., Tagliabue, E., Casalini, P., and Triulzi, T. (2017). Breast cancer-secreted miR-939 downregulates VE-cadherin and destroys the barrier function of endothelial monolayers. *Cancer letters* *384*, 94-100.

Ding, S., Kumar, S., and Mok, P. (2017). Cellular reparative mechanisms of mesenchymal stem cells for retinal diseases. *International journal of molecular sciences* *18*, 1406.

Dore-Duffy, P., and Cleary, K. (2011). Morphology and properties of pericytes. *Methods in molecular biology (Clifton, NJ)* *686*, 49-68.

Duz, B., Oztas, E., Erginay, T., Erdogan, E., and Gonul, E. (2007). The effect of moderate hypothermia in acute ischemic stroke on pericyte migration: an ultrastructural study. *Cryobiology* *55*, 279-284.

ElAli, A., Theriault, P., and Rivest, S. (2014). The role of pericytes in neurovascular unit remodeling in brain disorders. *Int J Mol Sci* *15*, 6453-6474.

Elia, L.P., Yamamoto, M., Zang, K., and Reichardt, L.F. (2006). p120 catenin regulates dendritic spine and synapse development through Rho-family GTPases and cadherins. *Neuron* *51*, 43-56.

Elshaer, S.L., Evans, W., Pentecost, M., Lenin, R., Periasamy, R., Jha, K.A., Alli, S., Gentry, J., Thomas, S.M., and Sohl, N. (2018). Adipose stem cells and their paracrine factors are therapeutic for early retinal complications of diabetes in the Ins2 Akita mouse. *Stem cell research & therapy* *9*, 322.

Enge, M., Bjarnegard, M., Gerhardt, H., Gustafsson, E., Kalen, M., Asker, N., Hammes, H.P., Shani, M., Fassler, R., and Betsholtz, C. (2002). Endothelium-specific platelet-derived growth factor-B ablation mimics diabetic retinopathy. *EMBO J* *21*, 4307-4316.

Etchevers, H.C., Vincent, C., Le Douarin, N.M., and Couly, G.F. (2001). The cephalic neural crest provides pericytes and smooth muscle cells to all blood vessels of the face and forebrain. *Development* *128*, 1059-1068.

Ezquer, M., Urzua, C.A., Montecino, S., Leal, K., Conget, P., and Ezquer, F. (2016). Intravitreal administration of multipotent mesenchymal stromal cells triggers a cytoprotective microenvironment in the retina of diabetic mice. *Stem cell research & therapy* *7*, 42.

Fan, Z., Beresford, P.J., Oh, D.Y., Zhang, D., and Lieberman, J. (2003). Tumor suppressor NM23-H1 is a granzyme A-activated DNase during CTL-mediated apoptosis, and the nucleosome assembly protein SET is its inhibitor. *Cell* *112*, 659-672.

Feng, J., Mantesso, A., and Sharpe, P.T. (2010). Perivascular cells as mesenchymal stem cells. *Expert opinion on biological therapy* *10*, 1441-1451.

Feng, Y., Gross, S., Wolf, N.M., Butenschön, V.M., Qiu, Y., Devraj, K., Liebner, S., Kroll, J., Skolnik, E.Y., and Hammes, H.-P. (2014). Nucleoside diphosphate kinase B regulates angiogenesis through modulation of vascular endothelial growth factor receptor type 2 and endothelial adherens junction proteins. *Arteriosclerosis, thrombosis, and vascular biology* *34*, 2292-2300.

Feng, Y., Pfister, F., Schreiter, K., Wang, Y., Stock, O., Vom Hagen, F., Wolburg, H., Hoffmann, S., Deutsch, U., and Hammes, H.P. (2008). Angiopoietin-2 deficiency decelerates age-dependent vascular changes in the mouse retina. *Cellular physiology and biochemistry : international journal of experimental cellular physiology, biochemistry, and pharmacology* *21*, 129-136.

Feng, Y., Wang, Y., Li, L., Wu, L., Hoffmann, S., Gretz, N., and Hammes, H.-P. (2011). Gene expression profiling of vasoregression in the retina—involvement of microglial cells. *PLoS One* *6*, e16865.

Feng, Y., Wang, Y., Stock, O., Pfister, F., Tanimoto, N., Seeliger, M.W., Hillebrands, J.-L., Hoffmann, S., Wolburg, H., and Gretz, N. (2009).

Vasoregression linked to neuronal damage in the rat with defect of polycystin-2. *PLoS One* 4, e7328.

Ferguson, S.M., and De Camilli, P. (2012). Dynamin, a membrane-remodelling GTPase. *Nature reviews Molecular cell biology* 13, 75.

Fiori, A., Terlizzi, V., Kremer, H., Gebauer, J., Hammes, H.-P., Harmsen, M.C., and Bieback, K. (2018). Mesenchymal stromal/stem cells as potential therapy in diabetic retinopathy. *Immunobiology*.

Frank, R.N., Dutta, S., and Mancini, M.A. (1987). Pericyte coverage is greater in the retinal than in the cerebral capillaries of the rat. *Invest Ophthalmol Vis Sci* 28, 1086-1091.

Frank, R.N., Turczyn, T.J., and Das, A. (1990). Pericyte coverage of retinal and cerebral capillaries. *Invest Ophthalmol Vis Sci* 31, 999-1007.

Freeman, W.M., Bixler, G.V., Brucklacher, R.M., Walsh, E., Kimball, S.R., Jefferson, L.S., and Bronson, S.K. (2009). Transcriptomic comparison of the retina in two mouse models of diabetes. *Journal of ocular biology, diseases, and informatics* 2, 202-213.

Fu, S., Dong, S., Zhu, M., Sherry, D.M., Wang, C., You, Z., Haigh, J.J., and Le, Y.-Z. (2015). Müller glia are a major cellular source of survival signals for retinal neurons in diabetes. *Diabetes* 64, 3554-3563.

Fujimoto, T., and Singer, S. (1987). Immunocytochemical studies of desmin and vimentin in pericapillary cells of chicken. *Journal of Histochemistry & Cytochemistry* 35, 1105-1115.

Fujita, Y., Krause, G., Scheffner, M., Zechner, D., Leddy, H.E.M., Behrens, J., Sommer, T., and Birchmeier, W. (2002). Hakai, a c-Cbl-like protein, ubiquitinates and induces endocytosis of the E-cadherin complex. *Nature cell biology* 4, 222.

Gallagher, A.R., Hoffmann, S., Brown, N., Cedzich, A., Meruvu, S., Podlich, D., Feng, Y., Könecke, V., De Vries, U., and Hammes, H.-P. (2006). A truncated polycystin-2 protein causes polycystic kidney disease and retinal degeneration in transgenic rats. *Journal of the American Society of Nephrology* 17, 2719-2730.

Gardner, T.W., and Davila, J.R. (2017). The neurovascular unit and the pathophysiologic basis of diabetic retinopathy. *Graefes Archive for Clinical and Experimental Ophthalmology* 255, 1-6.

Garrett, J.P., Lowery, A.M., Adam, A.P., Kowalczyk, A.P., and Vincent, P.A. (2017). Regulation of endothelial barrier function by p120-catenin- VE-cadherin interaction. *Molecular biology of the cell* 28, 85-97.

Gastinger, M.J., Kunselman, A.R., Conboy, E.E., Bronson, S.K., and Barber, A.J. (2008). Dendrite remodeling and other abnormalities in the retinal ganglion cells of Ins2Akita diabetic mice. *Investigative ophthalmology & visual science* 49, 2635-2642.

Gavard, J. (2014). Endothelial permeability and VE-cadherin: a wacky comradeship. *Cell adhesion & migration* 8, 158-164.

Gerhardt, H., and Betsholtz, C. (2003). Endothelial-pericyte interactions in

angiogenesis. *Cell and tissue research* 314, 15-23.

Gerhardt, H., Wolburg, H., and Redies, C. (2000). N - cadherin mediates pericytic - endothelial interaction during brain angiogenesis in the chicken. *Developmental dynamics: an official publication of the American Association of Anatomists* 218, 472-479.

Giampietro, C., Taddei, A., Corada, M., Sarra-Ferraris, G.M., Alcalay, M., Cavallaro, U., Orsenigo, F., Lampugnani, M.G., and Dejana, E. (2012). Overlapping and divergent signaling pathways of N-cadherin and VE-cadherin in endothelial cells. *Blood* 119, 2159-2170.

Gilles, A.-M., Presecan, E., Vonica, A., and Lascu, I. (1991). Nucleoside diphosphate kinase from human erythrocytes. Structural characterization of the two polypeptide chains responsible for heterogeneity of the hexameric enzyme. *Journal of Biological Chemistry* 266, 8784-8789.

Gilman, A.G. (1989). G proteins and regulation of adenylyl cyclase. *Jama* 262, 1819-1825.

Gory-Fauré, S., Prandini, M.-H., Pointu, H., Roullot, V., Pignot-Paintrand, I., Vernet, M., and Huber, P. (1999). Role of vascular endothelial-cadherin in vascular morphogenesis. *Development* 126, 2093-2102.

Gross, S., Devraj, K., Feng, Y., Macas, J., Liebner, S., and Wieland, T. (2017). Nucleoside diphosphate kinase B regulates angiogenic responses in the endothelium via caveolae formation and c-Src-mediated caveolin-1 phosphorylation. *Journal of Cerebral Blood Flow & Metabolism* 37, 2471-2484.

Guariguata, L., Whiting, D.R., Hambleton, I., Beagley, J., Linnenkamp, U., and Shaw, J.E. (2014a). Global estimates of diabetes prevalence for 2013 and projections for 2035. *Diabetes research and clinical practice* 103, 137-149.

Guariguata, L., Whiting, D.R., Hambleton, I., Beagley, J., Linnenkamp, U., and Shaw, J.E. (2014b). Global estimates of diabetes prevalence for 2013 and projections for 2035. *Diabetes Research & Clinical Practice* 103, 137-149.

Haidari, M., Zhang, W., Willerson, J.T., and Dixon, R.A. (2014). Disruption of endothelial adherens junctions by high glucose is mediated by protein kinase C- β -dependent vascular endothelial cadherin tyrosine phosphorylation. *Cardiovascular diabetology* 13, 105.

Halliday, M.R., Rege, S.V., Ma, Q., Zhao, Z., Miller, C.A., Winkler, E.A., and Zlokovic, B.V. (2016). Accelerated pericyte degeneration and blood-brain barrier breakdown in apolipoprotein E4 carriers with Alzheimer's disease. *Journal of Cerebral Blood Flow & Metabolism* 36, 216-227.

Hamilton, N.B., Attwell, D., and Hall, C.N. (2010). Pericyte-mediated regulation of capillary diameter: a component of neurovascular coupling in health and disease. *Frontiers in neuroenergetics* 2.

Hamm, H.E. (1998). The many faces of G protein signaling. *Journal of Biological Chemistry* 273, 669-672.

Hammes, H.-P., Feng, Y., Pfister, F., and Brownlee, M. (2011). Diabetic retinopathy: targeting vasoregression. *Diabetes* 60, 9-16.

Hammes, H.P., Lin, J., Wagner, P., Feng, Y., Vom Hagen, F., Krzizok, T., Renner,

O., Breier, G., Brownlee, M., and Deutsch, U. (2004). Angiopoietin-2 causes pericyte dropout in the normal retina: evidence for involvement in diabetic retinopathy. *Diabetes* *53*, 1104-1110.

Han, Z., Guo, J., Conley, S.M., and Naash, M.I. (2013). Retinal angiogenesis in the Ins2Akita mouse model of diabetic retinopathy. *Investigative ophthalmology & visual science* *54*, 574-584.

Hippe, H.-J., Wolf, N.M., Abu-Taha, H.I., Lutz, S., Le Lay, S., Just, S., Rottbauer, W., Katus, H.A., and Wieland, T. (2011). Nucleoside diphosphate kinase B is required for the formation of heterotrimeric G protein containing caveolae. *Naunyn-Schmiedeberg's archives of pharmacology* *384*, 461-472.

Hippe, H.-J., Wolf, N.M., Abu-Taha, I., Mehringer, R., Just, S., Lutz, S., Niroomand, F., Postel, E.H., Katus, H.A., and Rottbauer, W. (2009). The interaction of nucleoside diphosphate kinase B with G $\beta\gamma$ dimers controls heterotrimeric G protein function. *Proceedings of the National Academy of Sciences* *106*, 16269-16274.

Hirschi, K.K., and D'Amore, P.A. (1996). Pericytes in the microvasculature. *Cardiovascular research* *32*, 687-698.

Ho, K.L. (1985). Ultrastructure of cerebellar capillary hemangioblastoma. IV. Pericytes and their relationship to endothelial cells. *Acta neuropathologica* *67*, 254-264.

Hombrebueno, J.R., Chen, M., Penalva, R.G., and Xu, H. (2014). Loss of synaptic connectivity, particularly in second order neurons is a key feature of diabetic retinal neuropathy in the Ins2Akita mouse. *PloS one* *9*, e97970.

Hu, J., Dziumbila, S., Lin, J., Bibli, S.I., Zukunft, S., de Mos, J., Awwad, K., Fromel, T., Jungmann, A., Devraj, K., *et al.* (2017). Inhibition of soluble epoxide hydrolase prevents diabetic retinopathy. *Nature* *552*, 248-252.

Huang, G.-J., Gronthos, S., and Shi, S. (2009). Mesenchymal stem cells derived from dental tissues vs. those from other sources: their biology and role in regenerative medicine. *Journal of dental research* *88*, 792-806.

Huang, H., Kolibabka, M., Eshwaran, R., Chatterjee, A., Schlotterer, A., Willer, H., Bieback, K., Hammes, H.-P., and Feng, Y. (2019a). Intravitreal injection of mesenchymal stem cells evokes retinal vascular damage in rats. *The FASEB Journal* *33*, 14668-14679.

Huang, H., Kolibabka, M., Eshwaran, R., Chatterjee, A., Schlotterer, A., Willer, H., Bieback, K., Hammes, H.P., and Feng, Y. (2019b). Intravitreal injection of mesenchymal stem cells evokes retinal vascular damage in rats. *The FASEB Journal* *33*, 14668-14679.

Huang, Q., and Sheibani, N. (2008). High glucose promotes retinal endothelial cell migration through activation of Src, PI3K/Akt1/eNOS, and ERKs. *American Journal of Physiology-Cell Physiology* *295*, C1647-C1657.

Ikwegbue, P., Masamba, P., Oyinloye, B., and Kappo, A. (2018). Roles of heat shock proteins in apoptosis, oxidative stress, human inflammatory diseases, and cancer. *Pharmaceuticals* *11*, 2.

Inoue, Y., Iriyama, A., Ueno, S., Takahashi, H., Kondo, M., Tamaki, Y., Araie, M.,

and Yanagi, Y. (2007). Subretinal transplantation of bone marrow mesenchymal stem cells delays retinal degeneration in the RCS rat model of retinal degeneration. *Experimental eye research* 85, 234-241.

Janin, J., Dumas, C., Moréra, S., Xu, Y., Meyer, P., Chiadmi, M., and Cherfils, J. (2000). Three-dimensional structure of nucleoside diphosphate kinase. *Journal of bioenergetics and biomembranes* 32, 215-225.

Johnson, T.V., Bull, N.D., Hunt, D.P., Marina, N., Tomarev, S.I., and Martin, K.R. (2010a). Neuroprotective effects of intravitreal mesenchymal stem cell transplantation in experimental glaucoma. *Investigative ophthalmology & visual science* 51, 2051-2059.

Johnson, T.V., Bull, N.D., and Martin, K.R. (2010b). Identification of barriers to retinal engraftment of transplanted stem cells. *Investigative ophthalmology & visual science* 51, 960-970.

Joussen, A.M., Poulaki, V., Le, M.L., Koizumi, K., Esser, C., Janicki, H., Schraermeyer, U., Kociok, N., Fauser, S., and Kirchhof, B. (2004). A central role for inflammation in the pathogenesis of diabetic retinopathy. *The FASEB journal* 18, 1450-1452.

Kern, T.S., and Barber, A.J. (2008). Retinal ganglion cells in diabetes. *The Journal of physiology* 586, 4401-4408.

Khalaf, N., Helmy, H., Labib, H., Fahmy, I., El Hamid, M.A., and Moemen, L. (2017). Role of Angiopoietins and Tie-2 in Diabetic Retinopathy. *Electronic physician* 9, 5031-5035.

Kicic, A., Shen, W.-Y., Wilson, A.S., Constable, I.J., Robertson, T., and Rakoczy, P.E. (2003). Differentiation of marrow stromal cells into photoreceptors in the rat eye. *Journal of Neuroscience* 23, 7742-7749.

Klein, R., Klein, B.E., and Moss, S.E. (1989). The Wisconsin epidemiological study of diabetic retinopathy: a review. *Diabetes/metabolism reviews* 5, 559-570.

Kojima, M., Hoshimaru, M., Aoki, T., Takahashi, J.B., Ohtsuka, T., Asahi, M., Matsuura, N., and Kikuchi, H. (1996). Expression of heat shock proteins in the developing rat retina. *Neuroscience letters* 205, 215-217.

Kowluru, A. (2003). Defective protein histidine phosphorylation in islets from the Goto-Kakizaki diabetic rat. *American Journal of Physiology-Endocrinology and Metabolism* 285, E498-E503.

Kowluru, A., Klumpp, S., and Krieglstein, J. (2011). Protein histidine [de] phosphorylation in insulin secretion: abnormalities in models of impaired insulin secretion. *Naunyn-Schmiedeberg's archives of pharmacology* 384, 383-390.

Krebs, H., and Hems, R. (1953). Some reactions of adenosine and inosine phosphates in animal tissues. *Biochimica et biophysica acta* 12, 172-180.

Krishnan, K., Rikhy, R., Rao, S., Shivalkar, M., Mosko, M., Narayanan, R., Etter, P., Estes, P.S., and Ramaswami, M. (2001). Nucleoside diphosphate kinase, a source of GTP, is required for dynamin-dependent synaptic vesicle recycling. *Neuron* 30, 197-210.

Krymskaya, V.P., Goncharova, E.A., Ammit, A.J., Lim, P.N., Goncharov, D.A.,

Eszterhas, A., and Panettieri Jr, R.A. (2005). Src is necessary and sufficient for human airway smooth muscle cell proliferation and migration. *The FASEB journal* **19**, 428-430.

Kuriyan, A.E., Albin, T.A., Townsend, J.H., Rodriguez, M., Pandya, H.K., Leonard, R.E., Parrott, M.B., Rosenfeld, P.J., Flynn Jr, H.W., and Goldberg, J.L. (2017). Vision loss after intravitreal injection of autologous “stem cells” for AMD. *New England Journal of Medicine* **376**, 1047-1053.

Kuwabara, T., and Cogan, D.G. (1963). Retinal vascular patterns. VI. Mural cells of the retinal capillaries. *Archives of ophthalmology (Chicago, Ill : 1960)* **69**, 492-502.

Lardon, J., Romain, I., and Bouwens, L. (2002). Nestin expression in pancreatic stellate cells and angiogenic endothelial cells. *Histochemistry and cell biology* **117**, 535-540.

Laties, A.M., Rapoport, S.I., and McGlinn, A. (1979). Hypertensive breakdown of cerebral but not of retinal blood vessels in rhesus monkey. *Archives of ophthalmology (Chicago, Ill : 1960)* **97**, 1511-1514.

Leveen, P., Pekny, M., Gebre-Medhin, S., Swolin, B., Larsson, E., and Betsholtz, C. (1994). Mice deficient for PDGF B show renal, cardiovascular, and hematological abnormalities. *Genes Dev* **8**, 1875-1887.

Li, A.-F., Sato, T., Haimovici, R., Okamoto, T., and Roy, S. (2003). High glucose alters connexin 43 expression and gap junction intercellular communication activity in retinal pericytes. *Investigative ophthalmology & visual science* **44**, 5376-5382.

Li, F., Lan, Y., Wang, Y., Wang, J., Yang, G., Meng, F., Han, H., Meng, A., Wang, Y., and Yang, X. (2011). Endothelial Smad4 maintains cerebrovascular integrity by activating N-cadherin through cooperation with Notch. *Dev Cell* **20**, 291-302.

Lindahl, P., Johansson, B.R., Levéen, P., and Betsholtz, C. (1997). Pericyte loss and microaneurysm formation in PDGF-B-deficient mice. *Science* **277**, 242-245.

Liu, X., Vien, T., Duan, J., Sheu, S.-H., DeCaen, P.G., and Clapham, D.E. (2018). Polycystin-2 is an essential ion channel subunit in the primary cilium of the renal collecting duct epithelium. *Elife* **7**, e33183.

Mäurer, A., Wieland, T., Meissl, F., Niroomand, F., Mehringer, R., Krieglstein, J., and Klumpp, S. (2005). The β -subunit of G proteins is a substrate of protein histidine phosphatase. *Biochemical and biophysical research communications* **334**, 1115-1120.

Ma, Y., Zhang, H., Xiong, C., Liu, Z., Xu, Q., Feng, J., Zhang, J., Wang, Z., and Yan, X. (2018). CD146 mediates an E-cadherin-to-N-cadherin switch during TGF- β signaling-induced epithelial-mesenchymal transition. *Cancer letters* **430**, 201-214.

Mackay, A.M., Beck, S.C., Murphy, J.M., Barry, F.P., Chichester, C.O., and Pittenger, M.F. (1998). Chondrogenic differentiation of cultured human mesenchymal stem cells from marrow. *Tissue engineering* **4**, 415-428.

Maisonpierre, P.C., Suri, C., Jones, P.F., Bartunkova, S., Wiegand, S.J., Radziejewski, C., Compton, D., McClain, J., Aldrich, T.H., and Papadopoulos,

N. (1997). Angiopoietin-2, a natural antagonist for Tie2 that disrupts in vivo angiogenesis. *Science* 277, 55-60.

McLenachan, S., Chen, X., McMenamin, P.G., and Rakoczy, E.P. (2013). Absence of clinical correlates of diabetic retinopathy in the Ins2Akita retina. *Clinical & experimental ophthalmology* 41, 582-592.

Mendel, T.A., Clabough, E.B., Kao, D.S., Demidova-Rice, T.N., Durham, J.T., Zotter, B.C., Seaman, S.A., Cronk, S.M., Rakoczy, E.P., and Katz, A.J. (2013). Pericytes derived from adipose-derived stem cells protect against retinal vasculopathy. *PLOS one* 8, e65691.

Menon, M., and Schafer, D.A. (2013). Dynamin: expanding its scope to the cytoskeleton. In *International review of cell and molecular biology* (Elsevier), pp. 187-219.

Metz, S.A., Meredith, M., Vadakekalam, J., Rabaglia, M.E., and Kowluru, A. (1999). A defect late in stimulus-secretion coupling impairs insulin secretion in Goto-Kakizaki diabetic rats. *Diabetes* 48, 1754-1762.

Miyashita, Y., and Ozawa, M. (2007). Increased internalization of p120-uncoupled E-cadherin and a requirement for a dileucine motif in the cytoplasmic domain for endocytosis of the protein. *Journal of Biological Chemistry* 282, 11540-11548.

Morikawa, S., Baluk, P., Kaidoh, T., Haskell, A., Jain, R.K., and McDonald, D.M. (2002). Abnormalities in pericytes on blood vessels and endothelial sprouts in tumors. *The American journal of pathology* 160, 985-1000.

Mukherjee, S., Tessema, M., and Wandinger-Ness, A. (2006). Vesicular trafficking of tyrosine kinase receptors and associated proteins in the regulation of signaling and vascular function. *Circulation research* 98, 743-756.

Murfee, W.L., Skalak, T.C., and Peirce, S.M. (2005). Differential arterial/venous expression of NG2 proteoglycan in perivascular cells along microvessels: Identifying a venule - specific phenotype. *Microcirculation* 12, 151-160.

Na, L., Xiao-rong, L., and Jia-qin, Y. (2009). Effects of bone-marrow mesenchymal stem cells transplanted into vitreous cavity of rat injured by ischemia/reperfusion. *Graefe's Archive for Clinical and Experimental Ophthalmology* 247, 503-514.

Nadri, S., Kazemi, B., Eeslaminejad, M.B., Yazdani, S., and Soleimani, M. (2013a). High yield of cells committed to the photoreceptor-like cells from conjunctiva mesenchymal stem cells on nanofibrous scaffolds. *Molecular biology reports* 40, 3883-3890.

Nadri, S., Yazdani, S., Arefian, E., Gohari, Z., Eslaminejad, M.B., Kazemi, B., and Soleimani, M. (2013b). Mesenchymal stem cells from trabecular meshwork become photoreceptor-like cells on amniotic membrane. *Neuroscience letters* 541, 43-48.

Nagai, N., Ito, Y., and Sasaki, H. (2016). Hyperglycemia enhances the production of amyloid β 1-42 in the lenses of otsuka long-evans tokushima fatty rats, a model of human type 2 diabetes. *Investigative ophthalmology & visual science* 57, 1408-1417.

Nanes, B.A., Grimsley-Myers, C.M., Cadwell, C.M., Robinson, B.S., Lowery, A.M., Vincent, P.A., Mosunjac, M., Früh, K., and Kowalczyk, A.P. (2017). p120-catenin regulates VE-cadherin endocytosis and degradation induced by the Kaposi sarcoma-associated ubiquitin ligase K5. *Molecular biology of the cell* 28, 30-40.

Navaratna, D., McGuire, P.G., Menicucci, G., and Das, A. (2007). Proteolytic degradation of VE-cadherin alters the blood-retinal barrier in diabetes. *Diabetes* 56, 2380-2387.

Nehmé, A., and Edelman, J. (2008). Dexamethasone inhibits high glucose-, TNF- α -, and IL-1 β -induced secretion of inflammatory and angiogenic mediators from retinal microvascular pericytes. *Investigative ophthalmology & visual science* 49, 2030-2038.

Nobe, K., Miyatake, M., Sone, T., and Honda, K. (2006). High-glucose-altered endothelial cell function involves both disruption of cell-to-cell connection and enhancement of force development. *Journal of Pharmacology and Experimental Therapeutics* 318, 530-539.

Nottebaum, A.F., Cagna, G., Winderlich, M., Gamp, A.C., Linnepe, R., Polaschegg, C., Filippova, K., Lyck, R., Engelhardt, B., and Kamenyeva, O. (2008). VE-PTP maintains the endothelial barrier via plakoglobin and becomes dissociated from VE-cadherin by leukocytes and by VEGF. *Journal of experimental medicine* 205, 2929-2945.

Oas, R.G., Nanes, B.A., Esimai, C.C., Vincent, P.A., García, A.J., and Kowalczyk, A.P. (2013). p120-catenin and β -catenin differentially regulate cadherin adhesive function. *Molecular biology of the cell* 24, 704-714.

Ogata, S., Morokuma, J., Hayata, T., Kolle, G., Niehrs, C., Ueno, N., and Cho, K.W. (2007). TGF- β signaling-mediated morphogenesis: modulation of cell adhesion via cadherin endocytosis. *Genes & development* 21, 1817-1831.

Oh, M., and Nör, J.E. (2015). The perivascular niche and self-renewal of stem cells. *Frontiers in physiology* 6, 367.

Otani, A., Dorrell, M.I., Kinder, K., Moreno, S.K., Nusinowitz, S., Banin, E., Heckenlively, J., and Friedlander, M. (2004). Rescue of retinal degeneration by intravitreally injected adult bone marrow-derived lineage-negative hematopoietic stem cells. *The Journal of clinical investigation* 114, 765-774.

Owen, M., and Friedenstein, A. (1988). Stromal stem cells: marrow-derived osteogenic precursors. Paper presented at: Ciba Found Symp (Wiley Online Library).

Palacios, F., Schweitzer, J.K., Boshans, R.L., and D'Souza-Schorey, C. (2002). ARF6-GTP recruits Nm23-H1 to facilitate dynamin-mediated endocytosis during adherens junctions disassembly. *Nature cell biology* 4, 929.

Palacios, F., Tushir, J.S., Fujita, Y., and D'Souza-Schorey, C. (2005). Lysosomal targeting of E-cadherin: a unique mechanism for the down-regulation of cell-cell adhesion during epithelial to mesenchymal transitions. *Molecular and cellular biology* 25, 389-402.

Paquet-Fifield, S., Schlüter, H., Li, A., Aitken, T., Gangatirkar, P., Blashki, D.,

Koelmeyer, R., Pouliot, N., Palatsides, M., and Ellis, S. (2009). A role for pericytes as microenvironmental regulators of human skin tissue regeneration. *The Journal of clinical investigation* 119, 2795-2806.

Park, S.W., Yun, J.-H., Kim, J.H., Kim, K.-W., Cho, C.-H., and Kim, J.H. (2014). Angiopoietin 2 induces pericyte apoptosis via $\alpha 3\beta 1$ integrin signaling in diabetic retinopathy. *Diabetes* 63, 3057-3068.

Pascolini, D., and Mariotti, S.P. (2012). Global estimates of visual impairment: 2010. *British Journal of Ophthalmology* 96, 614-618.

Postel, E.H. (2003). Multiple biochemical activities of NM23/NDP kinase in gene regulation. *Journal of bioenergetics and biomembranes* 35, 31-40.

Qiu, Y., Huang, H., Chatterjee, A., Teuma, L., Baumann, F., Hammes, H.-P., Wieland, T., and Feng, Y. (2018). Mediation of FoxO1 in Activated Neuroglia Deficient for Nucleoside Diphosphate Kinase B during Vascular Degeneration. *Neuroglia* 1, 280-291.

Qiu, Y., Zhao, D., Butenschön, V.-M., Bauer, A.T., Schneider, S.W., Skolnik, E.Y., Hammes, H.-P., Wieland, T., and Feng, Y. (2016). Nucleoside diphosphate kinase B deficiency causes a diabetes-like vascular pathology via up-regulation of endothelial angiopoietin-2 in the retina. *Acta diabetologica* 53, 81-89.

Rajashekhar, G. (2014). Mesenchymal stem cells: new players in retinopathy therapy. *Frontiers in endocrinology* 5, 59.

Rajashekhar, G., Ramadan, A., Abburi, C., Callaghan, B., Traktuev, D.O., Evans-Molina, C., Maturi, R., Harris, A., Kern, T.S., and March, K.L. (2014). Regenerative therapeutic potential of adipose stromal cells in early stage diabetic retinopathy. *PloS one* 9, e84671.

Rangasamy, S., McGuire, P.G., and Das, A. (2012). Diabetic retinopathy and inflammation: novel therapeutic targets. *Middle East African journal of ophthalmology* 19, 52.

Rangasamy, S., Srinivasan, R., Maestas, J., McGuire, P.G., and Das, A. (2011). A potential role for angiopoietin 2 in the regulation of the blood–retinal barrier in diabetic retinopathy. *Investigative ophthalmology & visual science* 52, 3784-3791.

Resnikoff, S., Pascolini, D., Etya'Ale, D., Kocur, I., Pararajasegaram, R., Pokharel, G.P., and Mariotti, S.P. (2004). Global data on visual impairment in the year 2002. *Bulletin of the world health organization* 82, 844-851.

Reynolds, A.B., and Carnahan, R.H. (2004). Regulation of cadherin stability and turnover by p120ctn: implications in disease and cancer. Paper presented at: Seminars in cell & developmental biology (Elsevier).

Richardson, R., Hausman, G., and Campion, D. (1982). Response of pericytes to thermal lesion in the inguinal fat pad of 10-day-old rats. *Cells Tissues Organs* 114, 41-57.

Romeo, G., Liu, W.-H., Asnaghi, V., Kern, T.S., and Lorenzi, M. (2002). Activation of nuclear factor- κ B induced by diabetes and high glucose regulates a proapoptotic program in retinal pericytes. *Diabetes* 51, 2241-2248.

Rosengard, A.M., Krutzsch, H.C., Shearn, A., Biggs, J.R., Barker, E., Margulies,

I.M., King, C.R., Liotta, L.A., and Steeg, P.S. (1989). Reduced Nm23/Awd protein in tumour metastasis and aberrant *Drosophila* development. *Nature* **342**, 177.

Rouget, C. (1873). Memoire sur le developpment, la structure et les propietes physiologiques des capillaries senguins et lymphatiques. *Arch Physiol Norm Pathol* **5**, 603-663.

Sagare, A.P., Bell, R.D., Zhao, Z., Ma, Q., Winkler, E.A., Ramanathan, A., and Zlokovic, B.V. (2013). Pericyte loss influences Alzheimer-like neurodegeneration in mice. *Nature communications* **4**, 2932.

Santos, G., Prazeres, P., Mintz, A., and Birbrair, A. (2018). Role of pericytes in the retina. *Eye* **32**, 483-486.

Satarian, L., Nourinia, R., Safi, S., Kanavi, M.R., Jarughi, N., Daftarian, N., Arab, L., Aghdami, N., Ahmadi, H., and Baharvand, H. (2017). Intravitreal injection of bone marrow mesenchymal stem cells in patients with advanced retinitis pigmentosa; a safety study. *Journal of ophthalmic & vision research* **12**, 58.

Sato, H., and Coburn, J. (2017). *Leptospira interrogans* causes quantitative and morphological disturbances in adherens junctions and other biological groups of proteins in human endothelial cells. *PLoS neglected tropical diseases* **11**, e0005830.

Schaeffer, G., Levak-Frank, S., Spitaler, M., Fleischhacker, E., Esenabhalu, V., Wagner, A., Hecker, M., and Graier, W. (2003). Intercellular signalling within vascular cells under high D-glucose involves free radical-triggered tyrosine kinase activation. *Diabetologia* **46**, 773-783.

Seitz, R., Ohlmann, A., and Tamm, E.R. (2013). The role of Müller glia and microglia in glaucoma. *Cell and tissue research* **353**, 339-345.

Shan, S., Chatterjee, A., Qiu, Y., Hammes, H.-P., Wieland, T., and Feng, Y. (2018). O-GlcNAcylation of FoxO1 mediates nucleoside diphosphate kinase B deficiency induced endothelial damage. *Scientific reports* **8**, 10581.

Shepro, D., and Morel, N. (1993a). Pericyte physiology. *The FASEB Journal* **7**, 1031-1038.

Shepro, D., and Morel, N.M. (1993b). Pericyte physiology. *FASEB journal : official publication of the Federation of American Societies for Experimental Biology* **7**, 1031-1038.

Shih, S.-C., Ju, M., Liu, N., Mo, J.-R., Ney, J.J., and Smith, L.E. (2003). Transforming growth factor β 1 induction of vascular endothelial growth factor receptor 1: mechanism of pericyte-induced vascular survival in vivo. *Proceedings of the National Academy of Sciences* **100**, 15859-15864.

Sibov, T.T., Severino, P., Marti, L., Pavon, L., Oliveira, D., Tobo, P., Campos, A., Paes, A., Amaro, E., and Gamarra, L. (2012). Mesenchymal stem cells from umbilical cord blood: parameters for isolation, characterization and adipogenic differentiation. *Cytotechnology* **64**, 511-521.

Sidibé, A., Polena, H., Razanajatovo, J., Mannic, T., Chaumontel, N., Bama, S., Maréchal, I., Huber, P., Gulino-Debrac, D., and Bouillet, L. (2014). Dynamic phosphorylation of VE-cadherin Y685 throughout mouse estrous cycle in ovary

and uterus. *American Journal of Physiology-Heart and Circulatory Physiology* 307, H448-H454.

Siqueira, R.C., Messias, A., Messias, K., Arcieri, R.S., Ruiz, M.A., Souza, N.F., Martins, L.C., and Jorge, R. (2015). Quality of life in patients with retinitis pigmentosa submitted to intravitreal use of bone marrow-derived stem cells (Reticell-clinical trial). *Stem cell research & therapy* 6, 29.

Sivaprasad, S., Gupta, B., Crosby-Nwaobi, R., and Evans, J. (2012). Prevalence of diabetic retinopathy in various ethnic groups: a worldwide perspective. *Survey of ophthalmology* 57, 347-370.

Snider, N.T., Altshuler, P.J., and Omary, M.B. (2015). Modulation of cytoskeletal dynamics by mammalian nucleoside diphosphate kinase (NDPK) proteins. *Naunyn-Schmiedeberg's archives of pharmacology* 388, 189-197.

Spaide, R.F., Klancnik, J.M., and Cooney, M.J. (2015). Retinal vascular layers imaged by fluorescein angiography and optical coherence tomography angiography. *JAMA ophthalmology* 133, 45-50.

Steeg, P.S., Bevilacqua, G., Kopper, L., Thorgeirsson, U.P., Talmadge, J.E., Liotta, L.A., and Sobel, M.E. (1988). Evidence for a novel gene associated with low tumor metastatic potential. *JNCI: Journal of the National Cancer Institute* 80, 200-204.

Stewart, M.W. (2016). Treatment of diabetic retinopathy: recent advances and unresolved challenges. *World journal of diabetes* 7, 333.

Stitt, A., Chakravarthy, U., Archer, D., and Gardiner, T. (1995). Increased endocytosis in retinal vascular endothelial cells grown in high glucose medium is modulated by inhibitors of nonenzymatic glycosylation. *Diabetologia* 38, 1271-1275.

Stone, J., Itin, A., Alon, T., Pe'Er, J., Gnessin, H., Chan-Ling, T., and Keshet, E. (1995). Development of retinal vasculature is mediated by hypoxia-induced vascular endothelial growth factor (VEGF) expression by neuroglia. *Journal of Neuroscience* 15, 4738-4747.

Sweeney, M.D., Ayyadurai, S., and Zlokovic, B.V. (2016). Pericytes of the neurovascular unit: key functions and signaling pathways. *Nature neuroscience* 19, 771.

Tang, J., and Kern, T.S. (2011). Inflammation in diabetic retinopathy. *Progress in retinal and eye research* 30, 343-358.

Tomita, M., Adachi, Y., Yamada, H., Takahashi, K., Kiuchi, K., Oyaizu, H., Ikebukuro, K., Kaneda, H., Matsumura, M., and Ikehara, S. (2002). Bone marrow - derived stem cells can differentiate into retinal cells in injured rat retina. *Stem cells* 20, 279-283.

Trudeau, K., Molina, A.J., and Roy, S. (2011). High glucose induces mitochondrial morphology and metabolic changes in retinal pericytes. *Investigative ophthalmology & visual science* 52, 8657-8664.

Urbak, L., and Vorum, H. (2010). Heat shock proteins in the human eye. *International Journal of Proteomics* 2010, 479571.

Vellasamy, S., Sandrasaigaran, P., Vidyadaran, S., George, E., and Ramasamy,

R. (2012). Isolation and characterisation of mesenchymal stem cells derived from human placenta tissue. *World journal of stem cells* 4, 53.

Vestweber, D. (2008). VE-cadherin: the major endothelial adhesion molecule controlling cellular junctions and blood vessel formation. *Arteriosclerosis, thrombosis, and vascular biology* 28, 223-232.

Vittet, D., Buchou, T., Schweitzer, A., Dejana, E., and Huber, P. (1997). Targeted null-mutation in the vascular endothelial-cadherin gene impairs the organization of vascular-like structures in embryoid bodies. *Proceedings of the National Academy of Sciences* 94, 6273-6278.

Vogler, S., Pannicke, T., Hollborn, M., Grosche, A., Busch, S., Hoffmann, S., Wiedemann, P., Reichenbach, A., Hammes, H.-P., and Bringmann, A. (2013). Müller cell reactivity in response to photoreceptor degeneration in rats with defective polycystin-2. *PLoS One* 8, e61631.

Vogler, S., Pannicke, T., Hollborn, M., Kolibabka, M., Wiedemann, P., Reichenbach, A., Hammes, H.-P., and Bringmann, A. (2016). Impaired Purinergic Regulation of the Glial (Müller) Cell Volume in the Retina of Transgenic Rats Expressing Defective Polycystin-2. *Neurochemical research* 41, 1784-1796.

von Tell, D., Armulik, A., and Betsholtz, C. (2006). Pericytes and vascular stability. *Experimental cell research* 312, 623-629.

Vossmerbaeumer, U., Vossmerbaeumer, U., Ohnesorge, S., Kuehl, S., Haapalahti, M., Kluter, H., Jonas, J.B., Thierse, H.-J., and Bieback, K. (2009). Retinal pigment epithelial phenotype induced in human adipose tissue-derived mesenchymal stromal cells. *Cytotherapy* 11, 177-188.

Wall, M.A., Coleman, D.E., Lee, E., Iñiguez-Lluhi, J.A., Posner, B.A., Gilman, A.G., and Sprang, S.R. (1995). The structure of the G protein heterotrimer G α 1 β 1 γ 2. *Cell* 83, 1047-1058.

Wallez, Y., Cand, F., Cruzalegui, F., Wernstedt, C., Souchelnytskyi, S., Vilgrain, I., and Huber, P. (2007). Src kinase phosphorylates vascular endothelial-cadherin in response to vascular endothelial growth factor: identification of tyrosine 685 as the unique target site. *Oncogene* 26, 1067.

Wallez, Y., Vilgrain, I., and Huber, P. (2006). Angiogenesis: the VE-cadherin switch. *Trends in cardiovascular medicine* 16, 55-59.

Wang, J.D., An, Y., Zhang, J.S., Wan, X.H., Jonas, J.B., Xu, L., and Zhang, W. (2017). Human bone marrow mesenchymal stem cells for retinal vascular injury. *Acta ophthalmologica* 95, e453-e461.

Wessel, F., Winderlich, M., Holm, M., Frye, M., Rivera-Galdos, R., Vockel, M., Linnepe, R., Ipe, U., Stadtmann, A., and Zarbock, A. (2014). Leukocyte extravasation and vascular permeability are each controlled in vivo by different tyrosine residues of VE-cadherin. *Nature immunology* 15, 223.

Wieland, T. (2007). Interaction of nucleoside diphosphate kinase B with heterotrimeric G protein $\beta\gamma$ dimers: consequences on G protein activation and stability. *Naunyn-Schmiedeberg's archives of pharmacology* 374, 373-383.

Winkler, E.A., Bell, R.D., and Zlokovic, B.V. (2011). Lack of Smad or Notch

leads to a fatal game of brain pericyte hopscotch. *Dev Cell* 20, 279-280.

Wright, W.S., Yadav, A.S., McElhatten, R.M., and Harris, N.R. (2012). Retinal blood flow abnormalities following six months of hyperglycemia in the *Ins2* (Akita) mouse. *Experimental eye research* 98, 9-15.

Wu, X., Gao, Y., Xu, L., Dang, W., Yan, H., Zou, D., Zhu, Z., Luo, L., Tian, N., and Wang, X. (2017). Exosomes from high glucose-treated glomerular endothelial cells trigger the epithelial-mesenchymal transition and dysfunction of podocytes. *Scientific reports* 7, 9371.

Wu, Z., Wang, Z., Dai, F., Liu, H., Ren, W., Chang, J., and Li, B. (2016). Dephosphorylation of Y685-VE-cadherin involved in pulmonary microvascular endothelial barrier injury induced by angiotensin II. *Mediators of inflammation* 2016.

Xiao, K., Oas, R.G., Chiasson, C.M., and Kowalczyk, A.P. (2007). Role of p120-catenin in cadherin trafficking. *Biochimica et Biophysica Acta (BBA)-Molecular Cell Research* 1773, 8-16.

Xie, X., Lan, T., Chang, X., Huang, K., Huang, J., Wang, S., Chen, C., Shen, X., Liu, P., and Huang, H. (2013). Connexin43 mediates NF- κ B signalling activation induced by high glucose in GMCs: involvement of c-Src. *Cell Communication and Signaling* 11, 38.

Xu, G., Shen, J., Ishii, Y., Fukuchi, M., Dang, T., Zheng, Y., Hamashima, T., Fujimori, T., Tsuda, M., and Funa, K. (2013). Functional analysis of platelet-derived growth factor receptor- β in neural stem/progenitor cells. *Neuroscience* 238, 195-208.

Yan, Z., Wang, Z.-G., Segev, N., Hu, S., Minshall, R.D., Dull, R.O., Zhang, M., Malik, A.B., and Hu, G. (2015). Rab11a mediates vascular endothelial-cadherin recycling and controls endothelial barrier function. *Arteriosclerosis, thrombosis, and vascular biology, ATVB* 115.306549.

Yang, Z., Li, K., Yan, X., Dong, F., and Zhao, C. (2010). Amelioration of diabetic retinopathy by engrafted human adipose-derived mesenchymal stem cells in streptozotocin diabetic rats. *Graefes Archive for Clinical and Experimental Ophthalmology* 248, 1415-1422.

Yau, J.W., Rogers, S.L., Kawasaki, R., Lamoureux, E.L., Kowalski, J.W., Bek, T., Chen, S.-J., Dekker, J.M., Fletcher, A., and Grauslund, J. (2012). Global prevalence and major risk factors of diabetic retinopathy. *Diabetes care* 35, 556-564.

Yuan, H.T., Khankin, E.V., Karumanchi, S.A., and Parikh, S.M. (2009). Angiopoietin 2 is a partial agonist/antagonist of Tie2 signaling in the endothelium. *Molecular and cellular biology* 29, 2011-2022.

Zhang, W., Wang, Y., Kong, J., Dong, M., Duan, H., and Chen, S. (2017). Therapeutic efficacy of neural stem cells originating from umbilical cord-derived mesenchymal stem cells in diabetic retinopathy. *Scientific reports* 7, 408.

Zhao, N., Sun, H., Sun, B., Zhu, D., Zhao, X., Wang, Y., Gu, Q., Dong, X., Liu, F., and Zhang, Y. (2016). miR-27a-3p suppresses tumor metastasis and VM by down-regulating VE-cadherin expression and inhibiting EMT: an essential role

for Twist-1 in HCC. *Scientific reports* 6, 23091.

Zhou, S., Matsuyoshi, N., Takeuchi, T., Ohtsuki, Y., and Miyachi, Y. (2003). Reciprocal altered expression of T - cadherin and P - cadherin in psoriasis vulgaris. *British Journal of Dermatology* 149, 268-273.

Zimmermann, K.W. (1923). Der feinere bau der blutcapillaren. *Zeitschrift für Anatomie und Entwicklungsgeschichte* 68, 29-109.

Zlokovic, B.V. (2011). Neurovascular pathways to neurodegeneration in Alzheimer's disease and other disorders. *Nature Reviews Neuroscience* 12, 723.

7 Publications

1. **Huang H**, Kolibabka M, Eshwaran R, Chatterjee A, Schlotterer A, Willer H, Bieback K, Hammes HP, Feng Y. Intravitreal injection of mesenchymal stem cells evokes retinal vascular damage. *FASEB Journal*. 2019. Dec; 33 (12): 14668-14679.
2. Qiu Y*, **Huang H***, Chatterjee A, Loic T, Baumann, F, Hammes HP, Wieland T, Feng Y. Mediation of FoxO1 in Activated Neuroglia Deficient for Nucleoside Diphosphate Kinase B during Vascular Degeneration. *Neuroglia*. 2018. 1 (1): 280-291. *: co-first author
3. Kolibabka M, Acunman K, Riemann S, **Huang H**, Gretz N, Hoffmann S, Feng Y, Hammes HP. Endothelial Wnt-Pathway Activation Protects the Blood-Retinal-Barrier during Neurodegeneration-Induced Vasoregression. *Thrombosis & Haemostasis: Research*. 2018. 2 (1): 1010-1015.
4. **Huang H**, Kolibabka M, Wieland T, Hammes H-P, Feng Y. Alteration of vascular endothelial cadherin precedes pericyte loss in early retinopathy. **30th UK Cell Adhesion Society**. Annual Meeting. 2018

8 Curriculum vitae

Personnel

Family name and first name:	Huang Hongpeng
Birthday:	19/05/1988
Place of birth:	Heilongjiang, China
Marital status:	Single
Mother:	Dong runyan
Father	Huang shengcun

Education

09/2003-07/2006	Jiusan High School
09/2006-07/2011	Jilin University Bachelor of Medicine
09/2011-07/2014	Peking University Master of Science
03/2016-now	University of Heidelberg Dr. sc. hum student

9 Acknowledgments

It is an excellent time for me to study and work at the Institute of Experimental Pharmacology Mannheim (EPM) and European Center for Angioscience (ECAS) in Mannheim Medical Faculty of Heidelberg University for four years. This is a valuable and memorable experience in my life. I want to thank significantly the people who give me assistance and support throughout these four years.

Foremost, I would like to thank Prof. Dr. rer. nat. Thomas Wieland sincerely for giving me a rare opportunity to work in his laboratory. I am so grateful for his support and guidance in my doctoral researches.

Secondly, I would like to thank Prof. Dr. Hans-Peter Hammes for guiding me in my researches, inviting me to participate in his lab seminar, and revising my manuscript. I always learn a lot after each seminar.

Thirdly, my heartiest gratitude goes to my doctoral supervisor, PD. Dr. Yuxi Feng. Under her encouragement and careful instruction, I have successfully published my scientific paper on the FASEB Journal. I also cite my publication in my dissertation and thank FASEB Journal. She carefully trains me in my studies and teaches me lots of experimental techniques during these four years. Her rigorous, objective, and practical academic attitude, as well as persistent professionalism, have set an excellent example for my future work and study.

Besides advisor and supervisor, I sincerely thank my colleagues, including Shenliang Shan, Yi Qiu, Jianyuan Pan, Rachana Eshwaran, Santosh Lomada, Ulrike Kaiser, Susanne Elvers-Hornung, Nadine Dietrich, Heike Rauscher, Doris Baltus and Irene Rupprecht, etc. They are always excellent co-workers.

Most importantly, thanks to my family and my girlfriend, Ye Yuan, for their never-ending spiritual support and mental encouragement.

Thank you for all your contribution.